NUNC COGNOSCO EX PARTE

TRENT UNIVERSITY
LIBRARY

Digitized by the Internet Archive
in 2019 with funding from
Kahle/Austin Foundation

https://archive.org/details/oxygenelementary0000ardo

OXYGEN

THE PHYSICAL INORGANIC CHEMISTRY SERIES

Robert A. Plane and Michell J. Sienko, Editors

Oxygen: Elementary Forms and Hydrogen Peroxide	*M. Ardon (Hebrew University of Jerusalem)*
Inorganic Reaction Mechanisms	*J. O. Edwards (Brown)*
Metal Ions in Aqueous Solution	*J. P. Hunt (Washington State)*
Inorganic Chemistry of Nitrogen	*W. L. Jolly (Berkeley)*
The Solid-State Chemistry of Binary Metal Hydrides	*G. G. Libowitz (Kennecott Copper)*
Boron Hydrides	*W. N. Lipscomb (Harvard)*
Elements of Inorganic Chemistry	*R. A. Plane and R. E. Hester (Cornell)*
Periodic Correlations	*R. L. Rich (Bethel College)*
Physical Inorganic Chemistry	*M. J. Sienko and R. A. Plane (Cornell)*

OXYGEN

Elementary Forms
and Hydrogen Peroxide

MICHAEL ARDON
Hebrew University of Jerusalem

W. A. BENJAMIN
1965 New York Amsterdam

OXYGEN: ELEMENTARY FORMS AND HYDROGEN PEROXIDE

Copyright © 1965 by W. A. Benjamin, Inc.
All rights reserved

Library of Congress Catalog Card Number 65–11346
Manufactured in the United States of America

The manuscript was put into production on June 4, 1964;
this volume was published on June 30, 1965

W. A. BENJAMIN, INC.
New York, 10016

ONULP

Editors' Foreword

In recent years few fields of chemistry have expanded at a rate to match that of inorganic chemistry. Aside from the stimulus afforded by the demand for new materials, a primary cause for the resurgence has been the application of physics and physical chemistry concepts to inorganic problems. As a result, both researchers active in the field and students entering the field need to become as thoroughly familiar with physical concepts as with descriptive information. However, there is presently no single point of view sufficiently general to organize the entire discipline. Instead, various points of view have arisen corresponding to the most powerful methods of attack in each research area. The synthesis of these different points of view constitutes the present series of monographs. Each monograph is contributed by an inorganic chemist active in a particular research area and reflects the methods of approach characteristic to that area. The operational procedure has been to invite able scientists to write where their interests lead them.

The series fulfills several functions. Through flexible selection of several of the monographs to supplement the introductory volume, it can be used as a textbook for an advanced inorganic chemistry course that makes full use of physical chemistry prerequisites. As a series in total, it is a reference treatise of inorganic chemistry systematized by

623/6

physical principles. Finally, each monograph by itself represents a specialist's introduction to a specific research field.

It is hoped that the authors contributing to this series have succeeded in directing attention to unsolved problems and that their efforts will be repaid by continued research advances in inorganic chemistry.

M. J. Sienko
R. A. Plane

Ithaca, New York
February 1963

Preface

The chemistry of oxygen and its compounds, including simple and complex oxides, constitutes a major portion of inorganic chemisty. Nutshell presentation of this wide field was not intended. The scope of this book is limited to the allotropic forms of the element and its compounds with hydrogen. Water has been excluded, being described in other books of this series: Hunt's *Metal Ions in Aqueous Solution* and Sienko and Plane's *Physical Inorganic Chemistry.*

While no advanced textbook on oxygen exists, there are some excellent reference books on this subject, notably Gmelin's *Handbuch der anorganischen Chemie*, and Schumb's *Hydrogen Peroxide.* This volume not being intended as a miniature reference book, selection of topics was required. The mechanisms of some reactions are described in detail, others only briefly. In the description of physical properties, emphasis was laid on their interrelation and on the experimental methods used in their derivation.

The detailed presentation of *methods of formation* requires some explanation, there being a tendency in recent advanced inorganic textbooks to neglect this subject. This unfortunate trend should not be followed: the student can reach an adequate understanding of this subject only after acquiring a thorough knowledge of physical chemistry, which he does not possess at the freshman level. This knowledge is applied in the description of formation methods not less than in other sections.

The author wishes to express his thanks to Professors I. Dostrovsky and D. Samuel for a preview of the manuscript of their new book on the isotopes of oxygen (to be published by Pergamon Press), and to Doctors G. Czapski and M. L. Kremer for helpful suggestions and discussion.

MICHAEL ARDON

Jerusalem, Israel
October 1963

Contents

Editors' Foreword v

Preface vii

Chapter 1 THE ELEMENT AND ITS ATOM 1

1–1 Occurrence 2
1–2 The isotopes of oxygen 3
1–3 Electronic structure and chemical bonds 7
1–4 Formation and properties of free oxygen atoms 13
References 17

Chapter 2 O_2 19

2–1 Formation 19
2–2 Uses 27
2–3 Physical properties 27
2–4 The O_2 molecule 29
2–5 The O_4 molecule 35
2–6 Chemical properties 36
References 46

Chapter 3 OZONE 48

3–1 Occurrence 49
3–2 Formation 49
3–3 Physical properties 54
3–4 Chemical properties 58
3–5 Uses 66
References 66

Chapter 4 HYDROGEN PEROXIDE 68

4–1 Occurrence 68
4–2 Formation 69
4–3 Physical properties 76
4–4 Chemical properties 84
4–5 Uses 95
4–6 Hydrogen superoxides 95
4–7 Ionic peroxides and superoxides 97
References 101

Index 105

OXYGEN

I

The Element and Its Atom

The discovery of oxygen[1, 2]* is attributed to Joseph Priestley and Carl Wilhelm Scheele who independently prepared oxygen by thermal decomposition of oxides. Priestley used mercuric oxide for his experiments, while Scheele used potassium nitrate as well as silver carbonate, mercuric carbonate, and mercuric and other oxides. Priestley's results were first published in 1774 in his book *Experiments and Observations on Different Kinds of Air.* Scheele's findings were published in 1777 in his *Treatise on Air and Fire,* but his experimental work was carried out in the years 1771–1772.

These investigators succeeded in the preparation of relatively pure samples of the gas by collecting it over water, and they determined some of its properties. They realized that their gas was a component of air and recognized its role in respiration and combustion, but they did not realize that they had discovered a new element. Both were ardent followers of the phlogiston theory, and believed that they had prepared "dephlogisticated air." Despite the fact that Lavoisier recognized the elementary nature

* Numbers in brackets refer to references at the end of each chapter.

of oxygen soon after its discovery (1776), the two discoverers clung to their wrong notion to the end of their lives. In this connection it should be mentioned that the formation of oxygen by the decomposition of potassium nitrate was observed as early as 1678 by Ole Borch and its role in combustion was recognized in 1665 by Robert Hooke.

The fact that these early findings did not lead to the discovery of oxygen is only partly explained by inadequate experimental technique (especially in the handling of gases). The main reason for this delay was the advent of the phlogiston theory (Stahl, 1700). The discovery of oxygen is, therefore, intimately connected with the work of Lavoisier who, by overthrowing the phlogiston theory and recognizing the elementary nature of oxygen, saved the experimental results of Scheele and Priestley from the fate of those of their predecessors.

1-1 OCCURRENCE

Oxygen is the most abundant element in the solid crust of the earth, representing 46.6% of its weight, mainly in the form of oxides and silicates of metals (Al, Fe). Ocean water contains 85.8 wt % (versus 88.81 wt % in pure water), and the atmosphere contains 23.0 wt %. The combined oxygen content of the crust, hydrosphere, and atmosphere is about 50 wt %. The inner parts of the earth, especially the core, are believed to contain less oxygen, and the oxygen content of the bulk of the earth has been estimated at approximately 28 wt % [3]. This high percentage is not typical of the chemical composition of the universe, the composition of the *solar* atmosphere being more characteristic in this respect: the most abundant element there is hydrogen — 56.0 wt %(84.4% of the total number of atoms), followed by helium (40.7 wt %), neon (1.28 wt %) and oxygen (0.87 wt %). [4a].

Elementary oxygen occurs mainly in the form of O_2 molecules in the atmosphere. Its percentage (20.91 vol %, 23.0 wt %) is almost constant up to a height of 100 km, despite its high density (compared to nitrogen), due to the continuous mixing by convection and turbulence. Other forms of elementary oxygen found mainly at high altitudes are ozone (cf. Section 3–1) and

atomic oxygen, which is the major component above 100 km. Oxygen ions such as O^+ and O_2^+ are found in the ionosphere. O_2 occurs in solution in the seas: its concentration in the surface layers is almost that of a saturated solution (6.42 cm^3 $liter^{-1}$ at 10°); it decreases with depth, reaches a minimum value at a few hundred meters, and then rises again [4b]. The constant concentration of O_2 in the atmosphere is maintained by the photosynthesis-respiration cycle. It should be remembered, however, that it is a steady state and not an equilibrium concentration. The solid crust of the earth, which contains most of the terrestrial oxygen, in the combined form, is not in thermodynamic equilibrium with the atmosphere: it contains many compounds that are not saturated with O_2, such as ferrous minerals, sulfides, and organic compounds. Under equilibrium conditions, they would be oxidized and consume the atmospheric oxygen (leaving only a negligible partial pressure of free O_2). Free oxygen was probably absent from the early atmosphere and was accumulated in later geological ages by photosynthesis and photochemical decomposition of water. [3]

1-2 THE ISOTOPES OF OXYGEN [5]

Oxygen occurring in nature is a mixture of three stable isotopes: O^{16}, O^{17}, and O^{18}. Their ratio is approximately 1000: 3.7 : 20, depending to a slight extent on the origin of the sample. O^{18} and O^{17} were discovered by Giauque and Johnston [6] through their effort to interpret the "atmospheric bands" (cf. Section 2–4). These bands contain two very weak series of lines near the (O—O) band at 7596 Å, shown by Giauque and Johnston to belong to the $O^{16}O^{18}$ and $O^{16}O^{17}$ molecules. This discovery revealed a discrepancy between the accepted *chemical* scale of atomic weights which was based on the average atomic weight of atmospheric oxygen (16 amu) and the *physical* scale based on the atomic weight of O^{16} (16 amu). The average atomic weight of atmospheric oxygen became 16.004452 ± 0.000007 on the physical scale and this introduced a factor of 1.0002783 ± 0.0000005 between the two scales. This discrepancy was finally resolved in 1961 by the International Unions of Pure and Applied

Physics and Pure and Applied Chemistry, which abandoned both scales in favour of a new scale based on carbon, using C^{12} as a unit (12). According to this scale, the average atomic weight of atmospheric oxygen is now 15.9994. Mass-spectrometric analysis of the isotope ratio in different sources of oxygen revealed the fact that this ratio is not constant (Table 1–1).

Table 1-1 *Ratio Scale*

Source	Percentage O^{18}	Reference
Air	0.2039	[7]
Fresh water	0.1981	[8]
Ocean water	0.1995	[9]

Differences of up to 4% are found between different sources of the element. The origin of these differences can often be traced to the operation of a chemical or physical process of oxygen exchange between two species, characterized by an "isotope effect." Such processes will tend to enrich one species with the heavier isotope under equilibrium conditions, e.g., in the reaction

$$\tfrac{1}{2}CO_2^{16}(g) + H_2O^{18}(l) \rightleftharpoons \tfrac{1}{2}CO_2^{18}(g) + H_2O^{16}(l). \quad (1\text{–}1)$$

The equilibrium constant of (1–1)

$$K = \frac{[CO_2^{18}]^{1/2}[H_2O^{16}]}{[CO_2^{16}]^{1/2}[H_2O^{18}]}$$

is not equal to unity but to 1.0407 at 25.2° C [10]. This isotope effect explains why the isotopic ratio of $O^{18} : O^{16}$ in sedimentary rocks such as calcite is higher than in the ocean water in which they were precipitated. This isotopic ratio is not constant even in calcite rocks precipitated in different locations and ages. The reason for this variation is that the equilibrium constant of the reaction

$$\tfrac{1}{3}CaCO_3^{16}(s) + H_2O^{18}(l) \rightleftharpoons \tfrac{1}{3}CaCO_3^{18}(s) + H_2O^{16}(l) \quad (1\text{–}2)$$

is temperature-dependent, the temperature coefficient being

0.00023 per degree near room temperature [11]. By analyzing the O^{18} content of different calcite rocks, the temperature of the ocean, at the time of their precipitation, can be estimated to within 0.5° by the so-called paleotemperature scale. The difference in composition between ocean water and fresh water (obtained by condensation of water vapor from the oceans) is due to isotopic fractionation during evaporation, which tends to deplete the vapor and enrich the remaining water with O^{18}. The same effect was observed in condensation: the initial rain from a mass of moist air is "heavier" than the late rain. Atmospheric O_2 does not exchange directly with water. The noted difference in their isotopic composition may be due to indirect exchange processes, e.g., via CO_2 in the respiration-photosynthesis cycle.

Separation of Isotopes

Methods for separation of O^{18} and O^{17} from O^{16}, or their entrichment above natural concentration, depend on physical or chemical processes in which isotope fractionation occurs. In a process operating on a given isotopic mixture and separating it into two parts differing in their isotopic composition, the separation factor α is defined as

$$\alpha = \frac{\mathcal{N}}{1 - \mathcal{N}} \Big/ \frac{n}{1 - n}$$

where $\mathcal{N}$ is the atom fraction of the desired isotopic material in the enriched part, and n is its atom fraction in the depleted part. This factor is determined experimentally (by mass-spectrometric analysis) and may vary for a given process (it may, for example, be time-dependent), but if true thermodynamic equilibrium is established in the process, the separation factor is constant for a given temperature and is called the unit-process separation factor α°. Defined in this way, α is greater than one. However, for most isotopes, including those of oxygen, it is only slightly so, and often by less than 1%. It is therefore not enough, for practical

purposes, to find a process having an $\alpha > 1$; this process must in addition lend itself to repetititon (e.g., fractional distillation) so as to obtain a much higher enrichment than is possible by a single step. If $\mathcal{N}_p$ is the desired mole fraction of an isotope in the product and $\mathcal{N}_0$ its mole concentration in the starting material, then the minimum number of repetitions v of the simple process necessary to achieve $\mathcal{N}_p$ is

$$v = \frac{\ln q}{1 - \alpha}$$

where

$$q = \frac{\mathcal{N}_p}{1 - \mathcal{N}_p} \Big/ \frac{\mathcal{N}_0}{1 - \mathcal{N}_0}.$$

In order to produce H_2O^{18} of 99% purity by fractional distillation of ordinary water (containing 0.2% H_2O^{18}) the total enrichment required is $q = (0.99/0.01)/(0.998/0.002) = 49{,}500$. $\alpha°$ for the evaporation process is ~ 1.006; therefore, the minimum number of repetitions is $v = \ln 49{,}500/0.006 \sim 1800$. A distillation column of at least 1800 theoretical plates is necessary to obtain this product. A plant utilizing this process is in operation in Rehovot, Israel, and is the main supplier of oxygen isotopes. Water containing up to 97% H_2O^{18} and a few percent O^{17} is obtained. Fractional distillation of O_2, NO, or CO might also be utilized. Other easily repeatable processes are thermal diffusion and some chemical exchanges. Thermal diffusion is used in the Rehovot plant for preparation of O_2 highly enriched in O^{17}: the water produced by the distillation plant is electrolyzed and the O_2 separated by thermal diffusion to yield O^{18} of up to 99% and O^{17} of up to 60%.

O^{18} has been the most important tool in investigations of inorganic reaction mechanisms involving oxygen, especially in aqueous solution [12, 13]. Unfortunately, its concentration can be determined only by mass spectrometric analysis after separation of a sample, and it cannot therefore be used for investigation of rapid reactions. O^{17}, on the other hand, can be detected by nmr since it possesses a nuclear spin $i = \frac{5}{2}h/2$ and a magnetic moment

$\mu = -1.8928$ nuclear magnetons; [14] it has been used to investigate very rapid reactions. [12, 13]

Unstable Isotopes

The radioactive isotopes O^{14}, O^{15}, O^{19}, and O^{20} have been prepared artificially. Their half-life and methods of formation are given in Table 1–2.

Table 1-2 *Radioisotopes of Oxygen*

Isotope	Half-Life	Decay	Formation
O^{14}	70.91 sec	$\beta+, \gamma$	N^{14} (p, n) O^{14}
O^{15}	122.6 sec	$\beta+$	C^{12} (α, n) O^{15}
O^{19}	29.1 sec	$\beta-$	O^{18} (n, γ) O^{19}
O^{20}	13.6 sec	$\beta-$	O^{18} (t, p) O^{20}

All have a very short half-life, their possible use therefore being limited to rapid reactions. O^{15}, with the longest half-life, has been used for investigations of respiration in mammals [15]—the uptake of O_2 by the lungs and blood in the first few minutes after an intake was followed by using air containing O^{15}.

1-3 ELECTRONIC STRUCTURE AND CHEMICAL BONDS

The configuration $1s^2 2s^2 2p^4$ represents the most stable configuration of the 8 electrons of the oxygen atom. By promoting an electron from $2p$ to a higher orbital (e.g., $3s$, $3p$, $4s$, $3d$, etc.) a higher configuration is formed (such as $1s^2 2s^2 2p^3 3s$). In each of these electron configurations the electrons may be distributed in several ways between the available orbitals, thus giving rise to terms of different energies. In the lowest configuration, $2s^2 2p^4$, there are three possible distributions of the $2p^4$ electrons corresponding to the terms ^3P, ^1D, and ^1S. According to Hund's rules, the triplet $^3P_{2,1,0}$ (with the highest multiplicity) will have the lowest energy ($^3P_2$, with the highest J value, is the ground term). The ^1D term with highest L will come next, and the ^1S term will have the highest energy.

A confirmation of this order, as well as that of terms belonging to higher configurations, is obtained from the analysis of the atomic spectrum of oxygen (O I). Over one hundred terms with their respective energy levels were determined.[16] Some of the lower energy levels are shown in Fig. 1–1. The energy

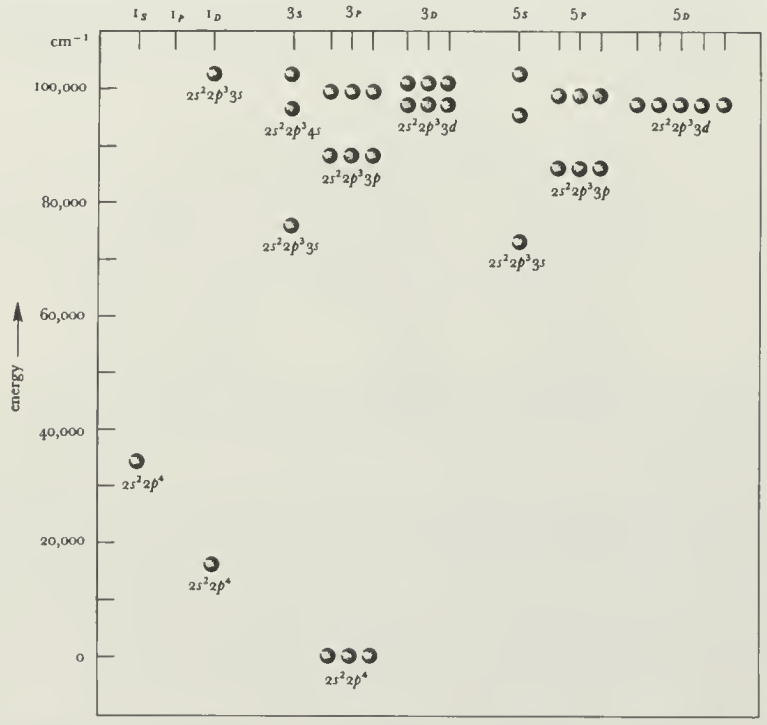

Figure 1-1 *Energy-level diagram of the neutral oxygen atom.*

levels belonging to the lowest configuration ($2s^22p^4$) are: 158.5 cm^{-1} for $^3P_1$ (above $^3P_2$, which is the ground state); 226.5 cm^{-1} for $^3P_0$; 15,867.7 cm^{-1} for $^1D_2$ and 33,792.4 cm^{-1} for $^1S_0$. They were determined from the red and green O I lines, observed in the polar aurora, which correspond to the $^3P - {}^1D$ and $^1D - {}^1S$ forbidden transitions.

Another constant determined from the O I spectrum is the *ionization potential* of the atom, necessary to produce the O^+ ion in its ground state ($^4S_{3/2}$). It is derived from the series limit at 109,836.7 cm^{-1}, equal to 13.614 volts.[16] From the line spectra of the positive oxygen ions (O II, O III, etc.) the ionization potential of successive electrons were derived[16] (in volts):

$$\underset{^3P_2}{O} \xrightarrow{13.614} \underset{^4S_{3/2}}{O^+} \xrightarrow{35.146} \underset{^3P_0}{O^{2+}} \xrightarrow{54.934} \underset{^3P_{1/2}}{O^{3+}} \xrightarrow{77.394} \underset{^1S_0}{O^{4+}} \longrightarrow$$

$$\xrightarrow{113.873} \underset{^2S_{1/2}}{O^{5+}} \xrightarrow{138.080} \underset{^1S_0}{O^{6+}} \xrightarrow{739.114} \underset{^2S_{1/2}}{O^{7+}} \xrightarrow{871.12} O^{8+}$$

The electron affinity of oxygen is less precisely known. The energy change of the reaction

$$O(g) + e^- \rightarrow O^-(g) \qquad (1\text{–}3)$$

can be determined directly from photodetachment experiments. A recent value is 1.465 eV.[17] The energy change of the reaction

$$O(g) + 2e^- \rightarrow O^{2-}(g) \qquad (1\text{–}3a)$$

was estimated indirectly from other parameters by the Born Haber cycle. It was estimated recently from lattice energies of alkaline earth oxides to be 179.8 kcal. [18] Former estimates are somewhat lower (cf. Ref. 18).

The *electronegativity* of oxygen is 3.5 according to Pauling[19] while slightly different values are quoted by other authors.[20] Some of these differences depend on improved experimental data, some on the use of alternative *definitions* of electronegativity. It is, however, agreed that only fluorine possesses a greater electronegativity (~ 4).

Oxygen forms compounds with all the elements, except some inert gases (the oxide of xenon, XeO_3, was synthesized recently.[21] The atom can accept a maximum of two electrons, by filling its $2p$ orbitals—the M-shell is too high above the L-shell to be used in formation of stable chemical bonds. The formation of an O^{2-} ion by transfer of two electrons from the oxidized atom to oxygen is realized only in the oxides of very electropositive elements (ionic oxides). In oxides of other elements, the filling of the L-shell of the atom is achieved by the formation of covalent bonds, with a varying degree of ionic character. These bonds may be two single σ bonds as in H—O—H or one double bond

as in R_2—C=O. The evidence for double-bonding is taken mainly from interatomic distances: the normal single-covalent radius of oxygen is 0.74 Å and the double-bond radius is only 0.61 Å. The π bond, in double bonds, is of the $p\pi$—$p\pi$ type in oxides of elements of the first period. It may be localized, as in ketones, or delocalized, as in NO_3^-. In oxides of elements of the second or higher periods, a $p\pi$—$d\pi$ bond sometimes occurs, as in SO_4^{2-}.[22]

The oxygen atom may have a coordination number greater than 2, in its covalent oxides, by forming coordinate bonds with its lone electron pairs. The coordination number 3 is found in oxonium ions such as H_3O^+: the shape of these compounds is pyramidal (like NH_3). Another instance is the "O*l* bridges" in complexes M – OH → M. A coordination number of 4 is encountered in compounds such as $OBe_4(OCOR)_6$, but it is doubtful whether these are true covalent bonds. The bond angles in di-covalent oxides vary between 100° and 180°, and are usually approximately 109°, as can be seen in Table 1–3.

Table 1-3 *Bond Angles in di-Covalent Oxides (Data Taken from Ref. 23)*

Oxide	Angle	Oxide	Angle
H_2O	104.5	$(C_6H_5)_2O$	124
F_2O	103.2	α Quartz	142
Cl_2O	110.8	$(Cl_5Ru)_2O$	180
$(CH_3)_2O$	110	$[TiCl_2(C_5H_5)]_2O$	180

When the two available orbitals p_y and p_z of the normal oxygen atom ($2s^2 2p_x^2 2p_y 2p_z$) are used in the formation of two single σ bonds with the two other atoms, the angle of 90° is expected. The fact that the observed angle is always greater than that was explained by assuming that the bonds are not pure $p\sigma$ bonds, and that sp hybrid orbitals take part in bond formation. An sp^3 hybridization would lead to a tetrahedral angle of 109°, which is close to the bond angle of many oxides. An sp^2 hybridization would account for angles near 120°, and sp hybridization for 180°. The deviations from these angles are explained by a varying degree of sp hybridization.

A different approach to this problem[23] considers the steric arrangement of electron pairs (bonding pairs and lone pairs) favored by Pauli's exclusion principle, which tends to keep electrons with parallel spins as far removed from each other as possible. These "Pauli forces" favor a tetrahedral arrangement of the four electron pairs if they are equivalent. If the four pairs are not equivalent as, for example, in the case of the di-covalent molecules of oxides, in which two electron pairs are bonding electrons, and two are lone pairs, the shapes of the orbitals are no longer identical, and therefore the degree of mutual repulsion will be affected: the bonding orbitals become more "compressed" along the bond direction, as a result of attraction to the second nucleus, and therefore will repulse each other less than the lone pairs. The angle will subsequently become smaller than 109°. This is the case of H_2O and F_2O. The smaller angle in F_2O is a result of the greater electronegativity of fluorine, which tends to concentrate the bonding orbitals of oxygen more than the hydrogen atom. When the bonds are formed with atoms of the second or higher period, the lone pairs of oxygen can partly delocalize into their partly vacant outer shell. A similar situation exists in oxides of aromatic ring compounds. This delocalization decreases the repulsion between the lone pairs and, as a result, the bond angle is expected to increase, and angles greater than 109° are expected (cf. Table 1–3).

Ionic Oxides

The formation of an ionic oxide by oxidation of an active metal with molecular oxygen is an exothermic reaction, because of the high lattice energy of the crystal. The endothermic steps of ionization (formation of M^{n+} and O^{2-} from the gaseous atoms-equal to the ionization potential of the metal + the electron affinity of oxygen), dissociation of O_2 into atoms, and sublimation of the metal are compensated by the highly exothermic reaction of the formation of the lattice from the gaseous ions. A list of standard heats of formation of the alkaline earth oxides is given in Table 1–4, together with the respective lattice energies.

The presumed existence of discrete O^{2-} ions in hese crystals is supported by X-ray data: there is no evidence for tany localized

Table 1-4 *Standard Heats of Formation and Lattice Energies of Alkaline Earth Oxides*

Oxide	ΔH_f[24]	Lattice Energy[18]
BeO	− 146.0	− 1097 ± 10
MgO	− 143.84	− 942 ± 10
CaO	− 151.9	− 853 ± 10
SrO	− 141.1	− 806 + 10
BaO	− 133.4	− 766 ± 10
RaO	− 125.0	− 751 ± 10

covalent bond between the oxygen atom and some of its neighbors in the crystal (which would be revealed by the interatomic distances). The radius of O^{2-} in these oxides is almost constant (1.40 Å), whereas in covalent oxides it is smaller, 0.74 Å being the radius in pure covalent bonds (such as in $[O—O]^{2-}$); it is some what larger, however, in covalent bonds having a considerable ionic character. The distinction between covalent and ionic oxides is not clear-cut in every case, especially in oxides of heavy metals, where it is not always easy to distinguish between a true ionic crystal and a covalent crystal possessing delocalized bonds between the oxygen atom and its neighbors. One way of distinguishing between these alternatives is by investigation of the electric conductivity of the oxides in their liquid state[25] ("oxide melts"). Ionic oxides are expected to conduct electricity in their melts, but not every conducting melt is necessarily ionic. Ionic melts conduct electricity by an ionic mechanism (ionic transport of charge) whereas other conducting melts, such as semiconductors, are *electronic* conductors. These two conductance types differ mainly in two properties: (1) ionic conductance is accompanied by electrochemical decomposition of the melt, in accordance with Faraday's laws, (2) ionic crystals do not conduct, appreciably, in the solid state, and their conductivity rises sharply at the melting point (Fig. 1–2). Semiconductors are not decomposed electrochemically. Their conductivity rises with temperature, but this rise is gradual (and does not change steeply at the melting point) from a very low to a high value (Fig. 1–2). Oxide melts constituting ionic conductors are evidently ionic oxides (if abrupt change of the nature of their chemical bond at the melting point is not assumed), but no clear conclusion can be

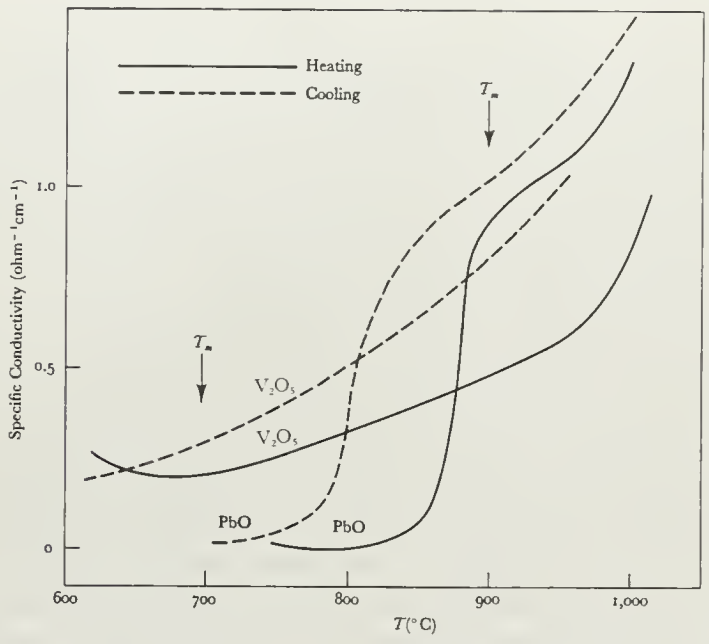

Figure 1-2 *Specific conductivity of* V_2O_5 (*semiconductor*) *and* PbO (*ionic conductor*).

drawn in the case of semiconductors, where ionic conductance may be overlooked if a much higher electronic conductance takes place.

1-4 FORMATION AND PROPERTIES OF FREE OXYGEN ATOMS

Free oxygen atoms take part in many complex reactions, such as combustion, thermal and photochemical decomposition of oxides, etc. Evidence for their participation has mainly been derived from kinetic investigations of the over-all processes (cf., e.g., Section 2–6), and needed confirmation by direct investigation of the steps involving oxygen atoms, i.e., by determining the chemical properties of free oxygen atoms. In addition, outer space exploration has increased the interest in the chemical reactions occuring in the upper atmosphere, and given a new impact to the investigation of the properties of oxygen atoms, which are a major component of the atmosphere above 100 km.

Most atomic oxygen reactions, including their recombination to form O_2 molecules, are very rapid, and are therefore usually investigated by the use of flow methods. A stream of gas containing

atomic oxygen is led through a glass tube, and the second reagent is added to this stream by injection from a jet opening into the tube (Fig. 1–3). The rate at which the oxygen atoms react is determined by measuring their concentration downstream of the point of mixing, at several points along the tube; $-d[O]/dt$ is is calculated from these concentrations, the distance from the point of mixing, and the known flow rate.

The main problems that needed solving before a systematic investigation of atomic oxygen reactions became practical were: (1) preparation of a stream of normal (^3P) oxygen atoms free from other active froms of oxygen (ozone, excited atoms, etc.), (2) identification and separation of the reaction products (this is especially important in reactions with organic and other polyatomic molecules which often yield several products simultaneously) (3) measuring the concentration of oxygen atoms for the determination of rate laws and activation energies by kinetic methods.

The partial dissociation of a stream of O_2 molecules into atoms can be achieved by passage through a silent electric discharge (glow-discharge or electrodeless discharge) under a total pressure of approximately 1 mm Hg. Over 10% of the O_2 molecules can be dissociated in this way. When higher pressures are used (e.g., atmospheric pressure) the main product of the discharge will be ozone (cf. Section 3–2):

$$O + O_2 + M \rightarrow O_3 + M \qquad (1\text{–}4)$$

but at a pressure of 1 mm Hg its concentration will be negligible compared to that of the free oxygen atoms: ozone is formed by a three-body collision in Reaction 1–4 and is decomposed by a bimolecular reaction:

$$O_3 + O \rightarrow 2O_2 \qquad (1\text{–}5)$$

As the pressure drops, the frequency of the three-body collision decreases much faster than that of Reaction 1–5, and as a result the steady state concentration of ozone decreases with decrease of pressure. It was shown experimentally that at 1 mm Hg the concentration is negligible. [26]

The pioneering work of Harteck and Kopsch on reactions of atomic oxygen with several compounds (H_2, CO, H_2O, HCl, HBr, H_2S, HCN, and some simple organic molecules) revealed that some molecules react quantitatively (HBr, H_2S), others react with lower yields (HCl, NH_3), and some do not react appreciably (H_2, CO). This does not mean, of course, that molecules such as H_2 are unable to react with oxygen atoms, but only that the rate of recombination of atomic oxygen is much faster.

A precise analytical method for determinung the O-atom concentration was required, before a more quantitative investigation could be carried out. This concentration was formerly estimated in flow systems by means of the "catalytic probe" method, which measured the heat evolved when atoms recombined quantitatively on the surface of an active catalyst (silver). This method is not specific for oxygen atoms, because excited molecules are also deactivated efficiently by the catalyst and increase the amount of heat evolved. Recent advances in this field are due to the development of two specific methods—the "air afterglow" and the "NO_2 titration." [27]

The air afterglow is created by the radiative recombination reaction (greenish yellow light is emitted)

$$NO + O \rightarrow NO_2 + h\nu \qquad (1\text{–}6)$$

The rate of Reaction 1–6 is very slow compared to atom recombination. The light intensity I is proportional to the rate of Reaction 1–6

$$I = k'[O]\,[NO]$$

If a very small amount of NO is added to the stream of atomic oxygen, the concentration of NO will remain constant along the reaction tube, as any NO_2 formed by Reaction 1–6 will be reduced to NO by the very rapid reaction

$$NO_2 + O \rightarrow NO + O_2 \qquad (1\text{–}7)$$

Thus I will be proportional to [O] only, and its decrease downstream is a direct measure of the decrease of the oxygen atom concentration. The "NO_2 titration" utilizes Reactions 1–7 and 1–6: a measured stream of NO_2 is added, with increasing flow rate, to the atomic oxygen. The air afterglow, at the point of entry, is created by Reaction 1–6 by the NO formed in Reaction 1–7. It will reach a maximum intensity I_{max} when $[NO_2] = \frac{1}{2}[O]$ and will be extinguished completely just as $[NO_2] = [O]$.

The recombination reaction of oxygen atoms has been investigated by these methods and it was established that the reaction takes place both heterogeneously (on the walls) and homogeneously. The heterogeneous reaction was measured on different surfaces and temperatures in an apparatus shown in Fig. 1–3. It

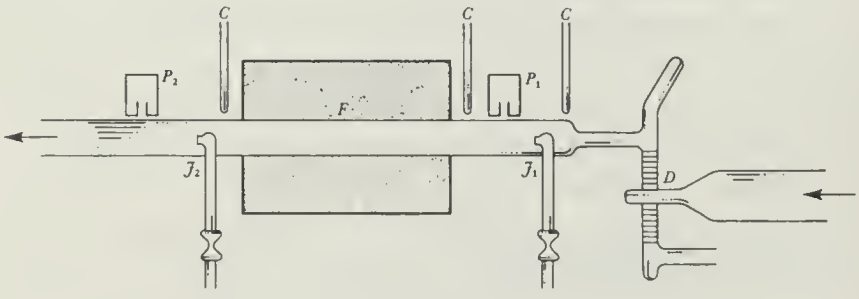

D, Discharge exciter and quartz discharge tube
J_1, J_2, Jets for added gases
P_1, P_2, Photomultipliers
F, Furnace
C, Cooling air jets

Figure 1-3 *Fast-flow apparatus for atomic oxygen reactions.*

was established that pyrex, silica, and alkali halides are not very reactive, while transition metals are very efficient catalysts for recombination. The homogeneous reaction proceeds by two different mechanisms: (1) the ozone mechanism, consisting of Reactions 1–4 and 1–5, (2) the direct recombination by

$$O + O + M \rightarrow O_2 + M \qquad (1\text{–}8)$$

The over-all rate of the homogeneous recombination is given by

$$-\frac{d[O]}{dt} = k_8[O]^2[M] + 2k_4[O]\,[O_2]\,[M]$$

According to a recent estimate[28] $k_8 = 10(\pm 3)10^8 l^2$ mole^{-2} sec^{-1} and $k_4 = 0.4(\pm 0.1)10^8 l^2$mole^{-2} sec^{-1} for the case $[M] = [O_2]$ (no inert gases are added) at room temperature. Other atomic oxygen reactions measured in recent years are with NO, NO_2 [27], *n*-butane, ethylene[29] and, H_2S. [30]

The reaction of oxygen atoms with paraffins, olefins, and other organic compounds was investigated by a different method, especially suitable for isolation of the reaction products. When nitrous oxide (containing Hg vapor) is irradiated with ultraviolet light of the mercury resonance line (2537 Å), a mercury sensitized photodecomposition of N_2O takes place[31]:

$$Hg(^3P_1) + N_2O \rightarrow N_2(^1\Sigma) + O(^3P) + Hg(^1S_0) \quad (1\text{–}9)$$

The normal oxygen atoms produced by this reaction are not mixed with O_2 molecules. When a hydrocarbon is added to this mixture (prior to irradiation) the oxygen atoms will react with it directly, and the relatively high yields of the reaction products can be separated and analyzed. In reactions with olefins, the oxygen atoms were shown to attack the double bond and form epoxides and carbonyl compounds.[31] With paraffins, alcohols, and aldehydes, their most important reaction is hydrogen abstraction.[31] Although absolute reaction rates cannot be obtained by this method, it can be used to obtain relative rates of reaction of various substrates with atomic oxygen by adding their mixture to the nitrous oxide and determining the concentration ratio of the products obtained by irradiation. These data can be converted to absolute rates by measuring the reaction rate of *one* substance in a flow system.

REFERENCES

1. Gmelin, *Handbuch der Anorganischen Chemie*, Auflage 8, "Sauerstoff," System No. 3, pp. 1–82 (1953–1960).
2. M. E. Weeks, "Discovery of the Elements," *J. Chem. Educ.*, 5th ed., pp. 89–105 (1948).

3. B. Mason, *Principles of Geochemistry*, p. 51, Wiley (1958).
4a. Gmelin, p. 91.
4b. Gmelin, p. 113.
5. I. Dostrovsky and D. Samuel, *Isotopes of Oxygen*, Pergamon Press (in press).
6. F. W. Giauque and H. L. Johnston, *Nature*, **123**, 831 (1929); *J. Am. Chem. Soc.*, **51**, 3528 (1929).
7. A. O. Nier, *Phys. Rev.*, **77**, 789 (1950).
8. W. Dansgaard, *Geochim. et Cosmochim. Acta*, **6**, 241 (1954).
9. S. Epstein and T. Mayeda, *Geochim. et Cosmochim. Acta*, **4**, 213 (1953).
10. W. Compston and S. Epstein, *Abstracts of the American Geophysical Union Meeting* (1 58).
11. R. N. Clayton, *J. Chem. Phys.*, **30**, 1246 (1959).
12. J. P. Hunt, *Metal Ions in Aqueous Solution*, Benjamin, p. 85 (1963).
13. D. Samuel and F. Steckel, *Bibliography of the Stable Isotopes of Oxygen*, Pergamon Press (1959); Supplement, *Intern. J. Appl. Radiation and Isotopes*, **11**, 190 (1961).
14. Gmelin, p. 319.
15. C. T. Dollery and J. B. West, *Nature*, **187**, 1121 (1960).
16. C. E. Moore, "Atomic Energy Levels", *Circ. Bur. Stand.*, No. 467, pp. 45–49 (1949).
17. L. M. Branscomb *et al.*, *Phys. Rev.*, **111**, 504 (1958).
18. M. F. C. Ladd and W. H. Lee, *Acta Cryst.*, **13**, 959 (1960).
19. L. Pauling, *Nature of the Chemical Bond.*, 3rd ed., p. 93 (1960).
20. R. T. Sanderson, *Chemical Periodicity*, Reinhold (1960).
21. D. H. Templeton *et al.*, *J. Am. Chem. Soc.*, **85**, 817 (1963).
22. G. W. Chantry and R. A. Plane, *J. Chem. Phys.* **32**, 319 (1960).
23. R. J. Gillespie, *J. Am. Chem. Soc.*, **82**, 5978 (1960).
24. F. D. Rossini *et al.*, *Circ. Bur. Stand.*, No. 500 (1952).
25. J. D. Mackenzie, *Advances in Inorganic Chemistry and Radiochemistry*, **4**, 293, Academic Press (1962).
26. P. Harteck and U. Kopsch, *Z. Phys. Chem.*, **B12**, 327 (1931).
27. F. Kaufman, "Reactions of Oxygen Atoms," *Progress in Reaction Kinetics*, Vol. 1, Pergamon Press (1961).
28. F. Kaufman, *C. A.* **57**, 1906a (1962).
29. L. Elias and H. I. Schiff, *Canad. J. Chemistry*, **38**, 1657 (1960).
30. G. Liuti, S. Dondes, and P. Harteck, 145*th Meeting of the Am. Chem. Soc.* (1963), *Abstracts* T. 40.
31. R. J. Cvetanovic, *J. Chem. Phys.*, **23**, 1203, 1208, 1375 (1955); *ibid.*, **25**, 376 (1956); *ibid.*, **30**, 19 (1959); *Canad. J. Chem.*, **33**, 1684 (1955); *ibid.*, **34**, 775 (1956); *ibid.*, **36**, 623 (1958).

2

O_2

2-1 FORMATION

Laboratory Methods

The methods of preparation used by Priestley and Scheele demonstrate the use of simple (HgO) and complex (KNO_3) oxides for O_2 formation. Many oxides decomposing near red-heat temperatures may serve as a source for O_2 in the laboratory, where they are often preferred to O_2 derived from liquid air, especially if high purity is desired. The choice of the oxide will therefore depend primarily on the purity of the product obtained — and neither HgO nor KNO_3 is suitable. The decomposition of KNO_3 is a reversible reaction.

$$KNO_3 \rightleftharpoons KNO_2 + \tfrac{1}{2}\ O_2 \qquad (2\text{–}1)$$

Decomposition attains a measurable rate above 500° C. Below 600°, equilibrium favors the nitrate, but shifts toward the nitrite between 600° and 800°. At this temperature nitrite also undergoes

slow decomposition into K_2O, O_2, NO, and N_2. [1] The O_2 produced in this way is, therefore, contaminated with nitrogen and its oxides. O_2 obtained by decomposition of $KClO_3$ is contaminated by small amounts of Cl_2 and HCl. A high grade of purity is obtained by catalytic decomposition of H_2O_2 (cf. Section 4–4), but thermal decomposition of $KMnO_4$ is the most commonly practiced method of preparing pure O_2. The decomposition yields O_2, potassium manganate, and manganese dioxide:

$$2\,KMnO_4 \rightarrow K_2MnO_4 + MnO_2 + O_2 \qquad (2\text{–}2)$$

Decomposition begins above 200°C and is complete as in Reaction 2–2 at 240°. In order to obtain maximum purity, the pure permanganate is degassed from occluded air at 160° to 175° under vacuum, prior to decomposition. [2]

Separation from Air

Air is the main source for large-scale oxygen production. Although water and most minerals have a higher oxygen content than air, their use as a source of O_2 is of minor importance because of the energy required to oxidize the oxygen to the elementary state.

The minimum energy required to separate O_2 from air is only 0.73 kwh /m^3 of O_2 (at 20° C). The enthalpy change of this process is very small ($\Delta H = 0$ for a mixture of ideal gases), and the free energy requirements are mainly those necessary to overcome the entropy of mixing: $\Delta F \sim T\Delta S_{mix}$. The energy required by practical processes is much greater than this minimum (by a factor of 6 in the best processes), but it is still much smaller than in any decomposition process.

Fractional distillation of liquid air is the only industrial process used for large-scale oxygen separation from air, which liquefies at normal pressure by cooling below − 191° C. Liquefaction is carried out by expansion of compressed air. In the first process of liquefaction, elaborated by C. Linde, air is compressed isothermally and then expanded through an orifice. This form of expansion (without performing work) causes a drop in tem-

perature due to the Joule-Thompson effect, because the JT coefficient for air is positive at ordinary temperatures:

$$\left[\frac{\partial T}{\partial P}\right]_H > 0$$

In the *Claude Process*, the gas is made to perform work against the external pressure by moving a piston or a turbine. In this way, a lower temperature is produced than by the JT effect, as seen in Fig. 2–1: the JT expansion is essentially isenthalpic ($\Delta H = 0$) and the drop in temperature (to point C) is accompanied by an

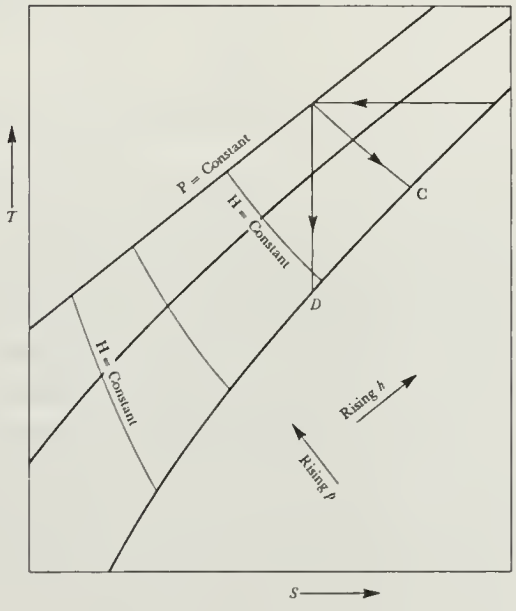

Figure 2-1 *Isothermal compression, isenthalpic expansion, and isentropic expansion on (T, S) diagram.*

increase in entropy. The second expansion is nearly isentropic ($\Delta S = 0$ in the ideal case that the process is carried out reversibly) and the temperature drops to point D. Water vapor and carbon dioxide must be removed from air before cooling, as they freeze and clog the valves and moving parts of the machinery. Removal is effected chemically or by condensation through precooling of air. The boiling point difference between O_2 and N_2 is almost 13°.

Liquid air may be fractionated to yield pure nitrogen and pure oxygen, since they do not form azeotropes (Fig. 2–2). The vapor

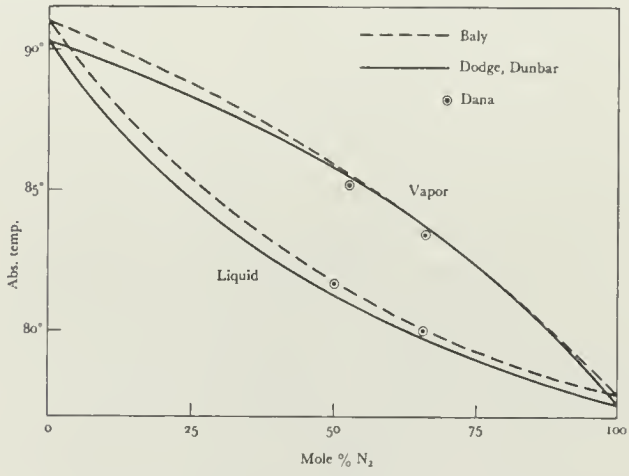

Figure 2-2 *Concentration dependence of the normal boiling point of liquid air.*

in equilibrium with liquid air contains 93% nitrogen and 7% oxygen. By feeding liquid air into the top of a fractionating column, the down-flowing liquid becomes progressively richer in oxygen, which can be obtained at any desired purity by using an appropriate number of plates. Six theoretical plates are sufficient to obtain O_2 over 98% pure. The gaseous mixture will contain, besides nitrogen, at least 7% oxygen and as a result, some 20% of the total oxygen is wasted, and no pure nitrogen will be produced. These shortcomings could be overcome by introducing the liquid air in the middle of the column, rather than at the top (Fig. 2–3), thereby fractionating not only the liquid but also the gaseous phase, so that pure nitrogen will condense at the top of the column. This arrangement, however, necessitates the cooling of the upper half of the column to a temperature below that of liquid air (even below that of liquid nitrogen at the top), and these temperatures are not readily available in this system. Linde's solution for this problem, still in use, is that of a double column consisting of a high pressure and a low pressure fractionating column. The high pressure column operates at about 5 atm and the low pressure column at normal pressure. Under 5 atm the boiling point of pure nitrogen is 94° K—higher than that of

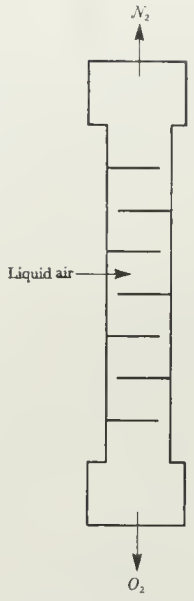

Figure 2-3 *Column for distillation of liquid air.*

pure oxygen at normal pressure (90°K). Pure liquid oxygen, accumulating at the bottom of the low pressure column, can therefore serve to cool the upper half of the high pressure column and to condense pure nitrogen in it (Fig. 2–4). Liquid air is first produced by expansion of precooled compressed air to 5 atm and introduced at the middle of the high pressure column. The products of fractionation (enriched liquid oxygen and liquid + gaseous nitrogen) are then fed into the low pressure column (after expansion to 1 atm), pure gaseous nitrogen being removed at the top and pure liquid oxygen at the bottom. The liquid O_2 serves as a heat remover from the high pressure nitrogen. The outcoming cold products serve to cool the incoming compressed air. This heat exchange is a source of inefficiency in the process. Other losses occur in irreversible steps within the column, and during the air compression which is not isothermal, but nearly adiabatic. Even when only 95% pure oxygen is produced (so-called "tonnage oxygen"), the minimum energy needed for separation of 1 cubic meter of O_2 is over 4 kwh.

Separation by Other Physical Processes. Many physical processes have been suggested for separation of air, e.g., centrifugation [3], diffusion through membranes of Kauchuk rubber [4] and silver [5]

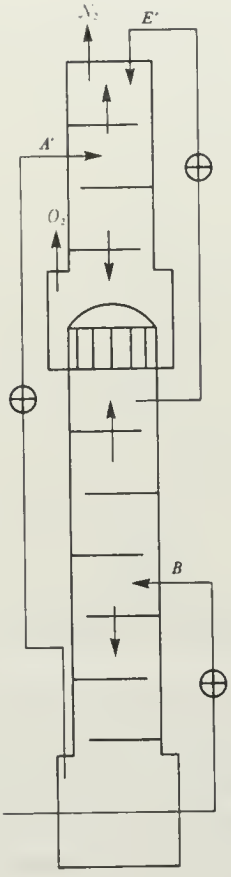

Figure 2-4 *The double column.*

(at 600°), selective absorption, and even magnetic separation [6]—making use of the paramagnetism of oxygen. All these processes have only small separation factors, and the energy losses in irreversible steps are too high to be of practical use.

Separation by Chemical Processes. The Brin process utilizes the equilibrium

$$2BaO + O_2 \rightleftharpoons 2\,BaO_2 \qquad (2\text{–}3)$$

and was in use before the introduction of Linde's liquid air process. BaO is converted to the peroxide by heating to 500° to 600° in air, and BaO_2 is then decomposed by heating to 800°; alternatively, the process can be carried out at constant temperature (700°) with variation of pressure (alternating high pressure

and partial vacuum). Another reaction suggested for O_2 separation is the decomposition of sodium manganate by superheated steam at 450° to yield manganic oxide and sodium hydroxide. This reaction is reversible by heating in air:

$$2\,Na_2MnO_4 + 2\,H_2O \rightleftharpoons Mn_2O_3 + 4\,NaOH + 1\tfrac{1}{2}\,O_2 \quad (2\text{–}4)$$

Although this cycle continues to attract the attention of some investigators [7], it is not economical, as are all other chemical processes. The basic weakness of these processes (in contrast to liquefaction) lies in the fact that the irreversible steps involve chemical energy changes (of the order of chemical energies) that are usually above 10 kcal $mole^{-1}$, which increases the energy requirements of these processes.

Investigation of the biochemical separation of air by means of the weak molecular complex of hemoglobin with oxygen initiated efforts to synthesize more stable, reversible oxygen "carriers" such as "Salcomin" and "Ethomin," which are chelates of Co^{II}, with bis-salicylaldehyde-imine and its derivatives (cf. Section 2–6). These "carriers" were used on a pilot plant scale on ships during World War II, but are not suitable for large-scale production. [8]

Electrolysis of Water

Water is electrolyzed commercially for hydrogen and oxygen production: cells usually contain 20% to 30% NaOH or KOH as electrolyte, steel cathodes, nickel plated steel anodes, and asbestos diaphragms. Very pure products are obtained. The limited use of this process for oxygen production (about 3% of world production is due to electrolysis) is owing to the high energy requirements—a factor which outweighs the low capital costs and simplicity of operation. For the production of 1 $meter^3$ oxygen and 2 $meter^3$ hydrogen at 20° C, about 10 kwh are required. This process is therefore economical only when O_2 is a by-product in H_2 production. The theoretically required energy is considerably lower. An electrolytic cell in which the reversible reaction:

$$2\ H_2O \rightarrow 2\ H_2 + O_2 \qquad (2\text{–}5)$$

takes place requires only 1.23 V, but in practice the voltage is around 2V, the difference being mainly due to the anodic overvoltage and, to a lesser extent, to cathodic overvoltage.

Electrolysis under high pressure ($\sim$ 200 atm) can be carried out by closing the outlets of the cell until the required pressure is built up by the evolving gases. This process has the advantage of direct feeding of the gases into high pressure cylinders without use of compressors. The *theoretical* decomposition voltage of the reversible high-pressure cell is of course higher than at normal pressure (because of the energy needed for compression of the gases) but the practical cell voltage is, surprisingly, lower in these cells, as shown in Fig. 2–5. This effect is probably due to the

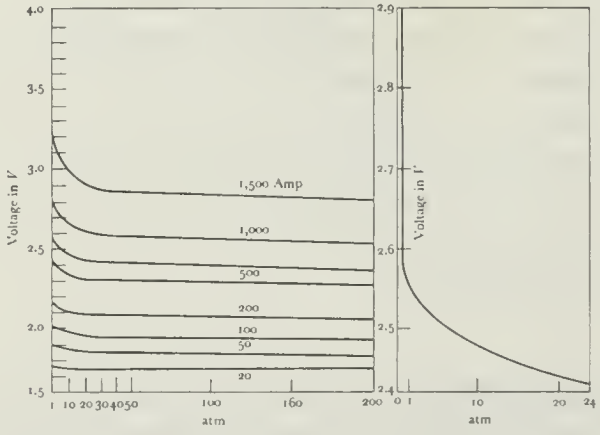

Figure 2-5 *Cell voltage variation with pressure.*

reduction of polarization overvoltage, outweighing the rise in the theoretical decomposition voltage. [9]

An interesting variation of the electrolytic method, aiming at doubling the yield of O_2 for a given quantity of electricity, by eliminating the simultaneous evolution of hydrogen, uses a conventional cell in which the cathode is made of activated carbon. [10] Air is used to oxidize the cathodic H_2 to H_2O_2 (cf. Section 4–2), which is decomposed to yield H_2O and another equivalent of oxygen. As no water is consumed in this process, it may be termed an electrochemical method of air separation.

2-2 USES

The early uses of oxygen were confined to welding and cutting of steel by the oxyacetylene torch and to medical purposes (oxygen tents in hospitals, breathing apparatus). Today, the greatest consumer is the steel industry, followed by the chemical and missile industries. The major use in the steel industry is replacement of air in burners and hearths, which eliminates the wasteful heating of inert nitrogen, and results in reducing the time necessary to reach operating temperatures (e.g., in the open hearth furnace) as well as in fuel saving. In the production of town gas the elimination of nitrogen from the product results in much higher calorific value.

In the chemical industry, the main consumption is in the production of ammonia, where N_2 is used for NH_3 synthesis and O_2 for production of hydrogen from natural gas or fuel gas ("synthesis gas"). Other important uses are the manufacture of acetylene (from natural gas), ethylene oxide, sodium peroxide, hydrogen peroxide (cf. Section 4–2), etc. For all these purposes, medium purity oxygen ($\sim 95\%$) or "tonnage oxygen" is used.

Oxygen can be produced economically only in high-capacity plants (100 to 1000 tons per day). Transportation costs are therefore the main obstacle to widespread use. High pressure steel cylinders are gradually being replaced by shipments of liquid oxygen. In 1961, world production-capacity was estimated at 72,475 tons per day. [11]

2-3 PHYSICAL PROPERTIES

Oxygen, a colorless, odorless gas at ordinary temperatures, condenses upon cooling to a bluish liquid which freezes to solid γ oxygen. This modification undergoes a transition to the β modification at lower temperatures, and finally to the α modification. The transition temperatures between the various phases are given in Table 2–1 together with the enthalpies of the transitions.

The structures of the α and β modifications are not known. It is, however, noteworthy that they are probably very similar to each other and antiferromagnetic [15] (magnetic susceptibility increases with temperature) whereas the γ modification is para-

Table 2-1 *Transition Temperatures and Enthalpies*

Transition	Temperature		Heat of transition	
	°K	Ref.	cal mole^{-1}	Ref.
α–β	23.876	[12]	22.42	[13a]
β–γ	43.818	[12]	177.6	[13a]
Melting point[a] (triple point)	54.376	[12]	106.3	[13b]
Normal boiling point	90.190	[14]	1630.0	[13c]

a) The mp at 1 atm is unknown.

magnetic, like liquid and gaseous O_2. The γ modification has a cubic structure: the cell length is a = 6.83 Å and contains 8 molecules. These molecules are arranged in pairs (evidence for O_4 molecules) and the centers of these pairs are arranged in a face-centered structure of closest packing. [16]

Liquid O_2 is made up of polymeric O_4 molecules, in equilibrium with simple O_2 molecules (cf. Section 2–5). Its density is 1.476 (at 88.94° K); the surface tension is 13.2 dyn cm^{-1} at the normal boiling point. The viscosity is $187.9 \cdot 10^{-5}$ dyn sec cm^{-2}, and the specific heat is 12.51 cal mole^{-1} degree^{-1} at 72.8° K.

A strong inhomogeneous magnetic field causes a slight change in many physical constants because of the paramagnetism of the liquid. The boiling point, for example, is elevated by 0.6° in a field of 28,800 gauss. [17]

Some of the more important properties of gaseous O_2 are summed up in Table 2–2.

Table 2-2 *Properties of Gaseous* O_2

Specific gravity (at NTP)	1.42895 g liter^{-1}
Viscosity (17 °C)	$2.0105 \cdot 10^{-4}$ dyn sec cm^{-2}
Molal magnetic susceptibility χ_m	$0.997/T$ emu
JT coefficient	0.31 degree atm^{-1}
Boyle's temperature $(\partial T/\partial P)_H$	150 °C
Critical temperature	154.78 °K
Critical pressure	50.14 atm
Critical density	0.430
Heat capacity (C_p) at 25 °C	7.02 cal mole^{-1} deg^{-1}
C_p/C_v at 25 °C	1.401
Molal entropy $S°_T$ at 25 °C	49.01 cal mole^{-1} deg^{-1}

The specific heat below room temperature is almost constant and very close to the values of $5/2R = 4.97$ and $7/2R = 6.95$ cal mole^{-1} deg^{-1} for C_v and C_p, respectively, the reason being that nearly all molecules are in their lowest vibrational state, so that only the translational and rotational degrees of freedom count. Near room temperature, the increasing population of higher vibrational states begins to affect C_p, e.g., at 1000° K $C_p = 8.34$ cal mole^{-1} deg^{-1}. At still higher temperatures the *electronic transition* $^3\Sigma_g^- \rightarrow {}^1\Delta_g$ has to be considered as well (cf. Section 2–4).

O_2 is slightly soluble in water: 34.3 cm^3 dissolve in 1 liter of water at 15° C and atmospheric pressure. It is considerably more soluble in alcohols—226 cm^3 liter^{-1} in ethanol at 10°C. Spectrophotometric studies of O_2 solutions in water and other solvents reveal a uv absorption at wavelengths in which neither gaseous O_2 nor H_2O absorbs. This absorption was interpreted [18] as evidence for the existence of solvates such as $O_2 \cdot H_2O$, $O_2 \cdot 2H_2O$, but it is more likely to be due to a contact charge transfer of an electron from solvent to solute. [19]

An O_2 hydrate was shown to exist in concentrated aqueous solution [20] (under high O_2 pressure) with a dissociation pressure of 120 atm at 0° C.

2-4 THE O_2 MOLECULE

The fact that gaseous oxygen is attracted to a magnet was observed by M. Faraday (1848). Liquid and solid O_2 possess the same property: when liquid O_2 is poured between the poles of a magnet it is attracted by the pole pieces (moves in the direction of increasing magnetic field strength). This behavior is due to the existence of a permanent magnetic dipole in the O_2 molecule. At moderate and low pressures gaseous O_2 obeys Curie's law: $\chi_m = \text{constant}/T$ (χ_m is the molar susceptibility). The magnitude of the constant as determined experimentally is 0.997 emu. Almost the same value (0.994 emu) is expected theoretically for a molecule with two unpaired electrons having parallel spins and the orbital quantum numbers 1 and -1, respectively. In this case, $L = 0$, and only the combined spins ($S = 1$) will determine the elementary magnetic moment of the molecule:

$$\mu_0 = 2\sqrt{S(S+1)}\, he/4\pi mc.$$

Since $\mathcal{J} = S = 1$ ($^3\Sigma$ state), and Landé's factor is $g = 2$, χ_m will be equal to

$$\chi_m = \frac{\mu_0^2 N^2 \mathcal{J}(\mathcal{J}+1)g^2}{3RT} = \frac{0.994}{T}$$

At high pressure and in liquid O_2, deviations from Curie's law were observed and are accounted for by assuming the formation of diamagnetic O_4 molecules (cf. Section 2–5).

The Lewis formula for the double-bonded oxygen molecule

$$:\ddot{O} = O:$$

I

should have only spin-paired electrons, according to the valence bond approach, and hence cannot account for the observed paramagnetism. Structures such as II,

$$:\dot{O}:\dot{O}:$$

II

besides violating the octet rule, are not reconcilable with the interatomic distance and decomposition energy, which require a double bond. In order to explain the paramagnetism in terms of the valence bond theory, Pauling [21] suggested the structure III,

$$:O\overset{\cdot\cdot\cdot}{\underset{\cdot\cdot\cdot}{---}}O:$$

III

consisting of a single bond and two 3-electron bonds. This structure is expected to have about the same stability as structure I, since each 3-electron bond has approximately half the energy of

a single bond. Each 3-electron bond has an unpaired electron and they could interact to form either a singlet (by pairing) or a triplet (by staying parallel). Wheland [22] estimated that the triplet state is more stable than the singlet, and so may be more stable than the double bond of structure I. In this way, the valence bond theory accounts for the paramagnetism of the oxygen molecule.

The *molecular orbital* approach leads to the $^3\Sigma$ ground state of oxygen in a straightforward way. When the available molecular orbitals of O_2 are filled with the L-shell electrons of two oxygen atoms, according to the Aufbau principle, the following lowest energy configuration is obtained:

$$2\,O(1s^2 2s^2 2p^4) \rightarrow \tag{2-6}$$

$$\rightarrow O_2[KK(\sigma 2s)^2\,(\sigma^* 2s)^2\,(\sigma 2p)^2\,(\pi 2p)^4\,(\pi^* 2p)^2]$$

The correlation diagram is given in Fig. 2–6. The antibonding

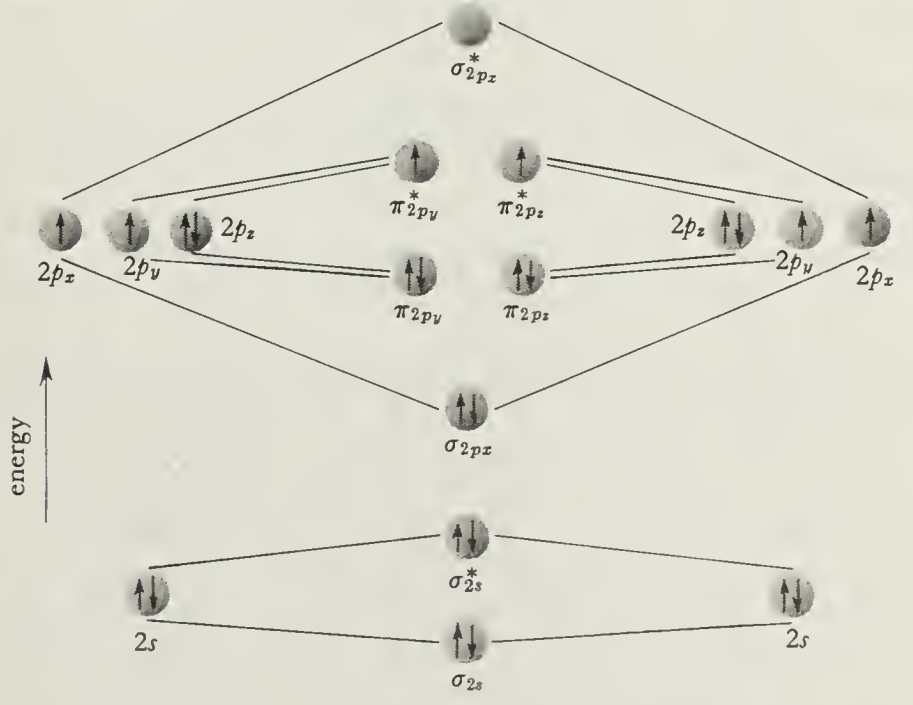

Figure 2-6 *Correlation diagram for* O_2.

orbitals π^*2p_y and π^*2p_z are of equal energy (degenerate). They accomodate only 2 electrons, which will attain the most stable configuration if each occupies a different orbital (to minimize coulombic repulsion) and their spins are parallel. This arrangement gives the $^3\Sigma_g^-$ ground state. The bond order will be that of a double bond: there are 8 bonding electrons: $(\sigma 2s)^2$, $(\sigma 2p)^2$, $(\pi 2p_y)^2$, $(\pi 2p_z)^2$ and 4 antibonding electrons: $(\sigma^*2s)^2$, (π^*2p_y), (π^*2p_z), so that the bond order is $(8-4)/2 = 2$. Since the π^*2p orbitals are antibonding an increase in bond strength is to be expected if one of their electrons is removed, which is indeed the case: the dissociation energy of the O_2^+ ion is 6.48 eV and of the O_2 molecules only 5.114 eV.

The significance of the molecular orbital description of the O_2 molecule is revealed even more in the field of molecular spectroscopy. It was a valuable aid in the investigation and analysis of numerous bands (mainly absorption bands) observed in the uv, visible, and ir regions, and these in turn yielded the most precise data for the molecular constants (interatomic distance, force constant, dissociation energy, etc.).

All known absorption bands, at ordinary temperature, originate in the absorption of radiation by the ground state $^3\Sigma_g^-$, and therefore this triplet state is the lower term in all transitions.

Transitions within the Lowest Electron Configuration

The lowest configuration of O_2 is given by Fig. 2–6. This configuration can exist in three states: $^3\Sigma_g^-$, $^1\Delta_g$, and $^1\Sigma_g^+$ (Fig. 2–7). By applying Hund's rules [23], we expect the state of

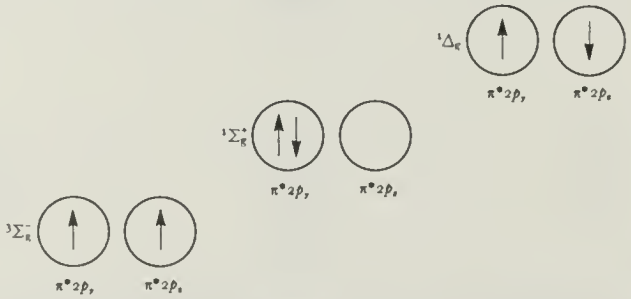

Figure 2-7 *Possible arrangement of electrons in π^*2p orbitals in the lowest electron configuration of O_2.*

highest multiplicity $^3\Sigma_g^-$ to be the lowest state. Of the remaining two terms with equal multiplicity (singlets), that with the highest orbital number $^1\Delta_g$ is expected to be lower than $^1\Sigma_g^+$. Analysis of the so-called "atmospheric bands" of O_2 in the visible region (observed in the red part of the solar spectrum) revealed that they originate in the $^3\Sigma_g^- \rightarrow {}^1\Sigma_g^+$ transition, and placed this state 1.62 eV. above the ground state. This suggests that the lower state $^1\Delta_g$ may cause absorption bands in the near ir region by the transition $^3\Sigma_g^- \rightarrow {}^1\Delta_g$. The existence of these bands was thus predicted by Mulliken [24] (1928), and they were later detected by Herzberg [25] (1934) in the ir region of the solar spectrum. The $^1\Delta_g$ state was thereby found to be 0.97 eV above the ground state. The two transitions just mentioned are forbidden, and this explains their very low intensity (O_2 is colorless). They are observed only in the solar spectrum since the whole height of the atmosphere serves as an absorption path in this case. Analysis of the vibrational and rotational fine structure of these bands yielded the best data for the interatomic distance and force constant of the O_2 molecule.

Transitions Involving Higher Electronic Configurations

The first excited electron configuration is formed from the lowest by transfer of one electron from a $\pi 2p$ to a $\pi^* 2p$ orbital:

$$O_2[KK(\sigma 2s)^2(\sigma^* 2s)^2(\sigma 2p)^2(\pi 2p)^3(\pi^* 2p)^3]$$

In this configuration six states may exist: $^1\Sigma_u^+$, $^1\Sigma_u^-$, $^3\Delta_u$, $^3\Sigma_u^+$ $^3\Sigma_u^-$, $^1\Delta_u$. The allowed transition $^3\Sigma_g^- \rightleftharpoons {}^3\Sigma_u^-$ is responsible for the strong Schumann-Runge absorption bands [26] in the uv, between 2000 Å and 1751 Å. At 1751 Å the bands converge, and a continuum begins. It is the high absorption of these bands, and the continuum, that prevent solar radiation below 2000 Å from penetrating the atmosphere. The search for the other five predicted states of this configuration was hindered by the fact that such states would undergo only forbidden transitions to the ground state. The resulting weak bands could not be detected easily in the solar radiation, as they are expected to be in the uv region,

below 3000 Å, which is effectively absorbed by atmospheric ozone (cf. Section 3–1). The use of a long absorption path (25 meters) led to the detection of the Herzberg bands [27] between 2400 Å and 2700Å. They belong to the transition $^3\Sigma_g^- \rightarrow {}^3\Sigma_u^+$ and are 10^{-6} times weaker than the Schumann bands. The use of specially constructed cells with an absorption path of 800 meters led to the discovery of two very faint bands [28], in the same region, that belong to the transition $^3\Sigma_g^- \rightarrow {}^1\Sigma_u^-$ and $^3\Sigma_g^- \rightarrow {}^3\Delta_u$.

The potential curve for the observed states of O_2 is reproduced in Fig. 2–8. It does not include the $^3\Delta_u$ and $^1\Sigma_u^-$ states which lie

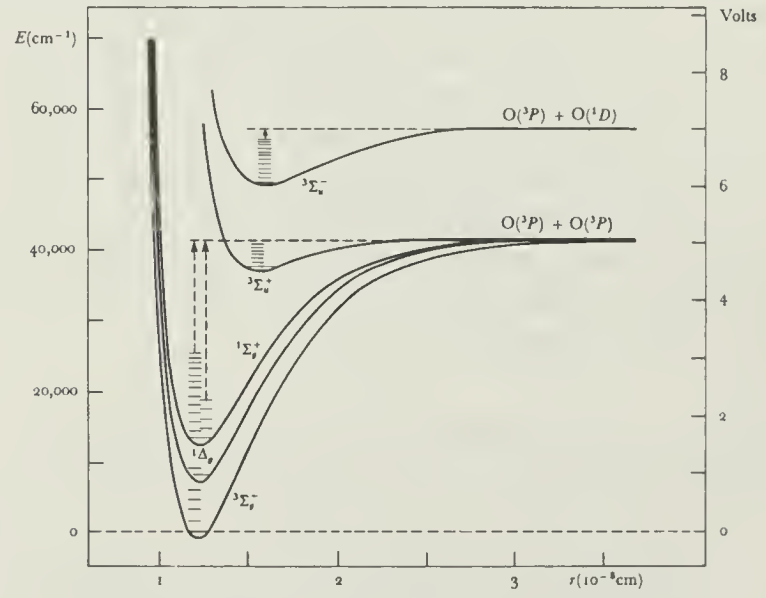

Figure 2-8 *Potential curve for* O_2 *molecule.*

near that of $^3\Sigma_u^+$. [29] Note that, while the dissociation of the $^3\Sigma_u^-$ molecule leads to the formation of one normal oxygen atom (^3P) and one excited atom (^1D), all the other states in Fig. 2–8 dissociate into two normal ^3P atoms.

The dissociation energy of the normal ($^3\Sigma_g^-$) oxygen molecule was determined from the precisely known value of the convergence limit of the Schumann-Runge bands, $57{,}128 \pm 5\ cm^{-1}$. [30] This limit, and the onset of the continuum, is the dissociation energy of the reaction:

$$O_2(^3\Sigma_g^-) \rightarrow O(^3P) + O(^1D) \qquad (2\text{–}7)$$

If the excitation energy of the ^1D atom (15,867.7 cm^{-1}) is subtracted from this value, we obtain 41,260 $\pm$ 5 cm^{-1} or 5.114 eV or 117.96 kcal $mole^{-1}$. This value coincides with the less precise value of 41,259 cm^{-1} obtained from the convergence limit of the Herzberg bands.

Vibrational and Rotational Transitions

The absence of a vibrational spectrum of O_2 in the ir region is expected from the symmetry of this diatomic molecule. O_2 does not possess a permanent electric dipole to interact with radiation. A very faint absorption is observed in highly compressed O_2 and also in the liquid state, probably due to momentary dipoles produced by collision. The polarizability of the molecule changes during vibrational transitions, and therefore a Raman spectrum is observed.

In the microwave region, a very faint absorption is observed at a wavelength of 2 cm. It is due to interaction of radiation with the *magnetic* dipole of the molecule, rather than with a (nonexistent) electric dipole. This interaction effects transitions within the triplet level of the ground state $^3\Sigma_g^-$ by changing the orientation of the electron-spin momentum with respect to the angular momentum of the rotating molecule. Some of the molecular constants derived from spectroscopic data are given in Table 2–3.

Table 2-3 *Molecular Constants*

Constant		Source
Interatomic distance	1.207404 Å	Atmospheric bands [31]
Interatomic distance	1.20741 Å	Microwaves [32]
Moment of inertia I_e	19.3589 · 10^{-40}g cm^2	Atmospheric bands [31]
Dissociation energy	117.96 kcal $mole^{-1}$	Schumann-Runge bands [30]
Force constant k	11.409 · 10^{-5} dyn cm^{-1}	Atmospheric bands [31]
Ionization potential	12.075 eV	Photoionization [33]

2-5 THE O_4 MOLECULE

The magnetic susceptibility of liquid O_2 does not obey Curie's law. The experimental data fit into $\chi_m = 7.309 \cdot 10^{-2} T^{1/2}$. In solutions of O_2 in liquid nitrogen, χ_m increases with dilution

and reaches the value calculated for gaseous O_2 at infinite dilution. This behavior was explained by assuming the formation of a diamagnetic O_4 molecule consisting of a pair of normal O_2 molecules bound together by the weak interaction of their electronic spins. The equilibrium constant K_p of the reaction

$$2\ O_2 \rightleftharpoons O_4 \qquad (2\text{–}8)$$

in solutions of O_2 in liquid nitrogen was calculated by Lewis [34] from the change of χ_m with concentration. From the change of K_p with *temperature*, the enthalpy change of the reaction was found to be approximately 130 cal mole^{-1}.

The deviations from Curie's law occurring in highly compressed oxygen are likewise explained by the increase in the concentration of the diamagnetic O_4 molecule. Under normal conditions the concentration of O_4 is negligible. The appearance of new absorption bands in the ultraviolet, visible, and infrared regions in highly compressed oxygen is attributed to the O_4 molecule. [35] The same bands are found in liquid O_2.

2-6 CHEMICAL PROPERTIES

Thermal Dissociation

At ordinary temperatures the equilibrium constant $K_P = (P_O)^2/P_{O_2}$ of the reaction

$$O_2 \rightleftharpoons 2\ O \qquad (2\text{–}9)$$

is so small that even at 500° K the odds are against finding a single free atom in a liter of the gas. The value of K_p at different temperatures is given in Table 2–4, together with the degree of dissociation α at atmospheric pressure. These values were calculated from the known thermodynamic functions of atomic and molecular oxygen (derived from spectroscopic data).

The rate of dissociation can be estimated from the known rate of recombination (cf. Section 1–4) and K_p values. This disso-

Table 2-4[a] *K_p Values*

$T°K$	$\log K_p$	α (1 atm)
300	− 80.668	$2.3 \cdot 10^{-41}$
500	− 45.876	$5.9 \cdot 10^{-24}$
1000	− 19.612	$7.8 \cdot 10^{-11}$
2000	− 6.356	$3.3 \cdot 10^{-4}$
3000	− 1.896	$5.6 \cdot 10^{-2}$
4000[b]	+ 0.373	$0 \cdot 61$
5000[b]	+ 1.712	$0 \cdot 964$

[a] Calculated from data given by D. R. Stull and G. C. Sinke, *Thermodynamic Properties of the Elements*, A. C. S. **18**, 144 (1956).
[b] Taken from H. Zeise, *Thermodynamik*, **3**, 121, Hirzel, Leipzig (1954).

ciation reaction may be an intermediate step in reactions of O_2 at very high temperatures (in flames), but it is too slow to account for homogeneous gas phase reactions taking place at ordinary or red-heat temperatures. Some nonthermal dissociation reactions are described in Chapter 3.

The Reaction with Hydrogen

Thermal reaction. [36] The highly exothermal reaction

$$2\ H_2 + O_2 \rightarrow 2\ H_2O \qquad (2\text{–}10)$$

does not proceed at a measurable rate at ambient temperatures, because of the high activation energy needed to break the O—O and H—H bonds. Even at temperatures at which the reaction is very rapid (explosive), e.g., at 500°, the known rates of the homogeneous dissociation of H_2 and O_2 are too slow to account for the observed reactivity. At 500° C the reaction may proceed at a measurable rate, e.g., at a pressure of 300 mm Hg and a H_2/O_2 ratio of 2 : 1. The same mixture will explode spontaneously at the same temperature if the pressure is 5 mm Hg. The change of explosion limits of this mixture with temperature and pressure is shown in Fig. 2–9 for a given reaction vessel (the dimensions and material of the vessel affect the rates of the heterogeneous steps in the over-all mechanism). It can be seen that, raising the

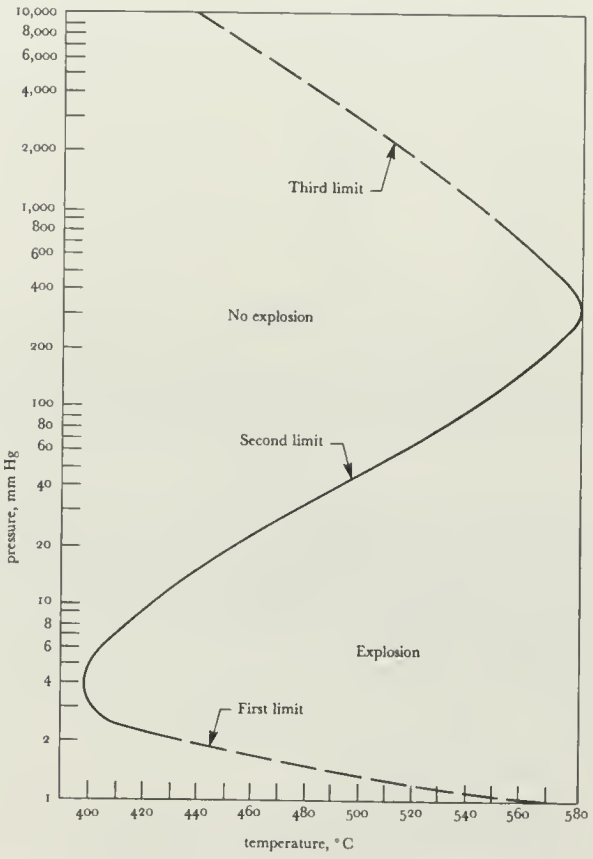

Figure 2-9 *Explosion limits of a stoichiometric hydrogen-oxygen mixture in a spherical* KCl*-coated vessel of 7.4 cm diameter.*

temperature of the gases to 500° C, no explosion occurs if the pressure is between 50 mm Hg and 3000 mm Hg (the reaction will proceed at a measurable rate). If the pressure is gradually reduced by isothermal expansion, the observed rate will first decrease, but when the second explosion limit is reached (50 mm Hg), it will suddenly increase to explosive rate. If the gases are compressed isothermally, the rate will increase and at the third explosion limit (3000 mm Hg), explosion will occur again. At very low pressure (< 1 mm Hg), the gases will react very slowly (at 500°) but when the pressure is increased to about 1 mm Hg the mixture will explode (first explosion limit).

The existence of a second explosion limit is the most significant experimental fact characterizing the mechanism of this

reaction as a branched chain reaction. The existence of a (first) explosion limit is common to all explosive reactions—thermal explosions and branched chain explosions alike—but the occurrence of a *second* or upper explosion limit proves the operation of a branched chain mechanism. At very low pressures (below 1 mm Hg) the chains are initiated by surface reactions such as

$$H_2 + \text{wall} \rightarrow \text{wall} + H + H \qquad (2\text{–}11)$$

and propagated by

$$H + O_2 \rightarrow OH\cdot + O - 15 \quad \text{kcal} \qquad (2\text{–}12)$$

$$O + H_2 \rightarrow OH\cdot + H + 1 \quad \text{kcal} \qquad (2\text{–}13)$$

$$OH\cdot + H_2 \rightarrow H_2O + H + 13.8 \quad \text{kcal} \qquad (2\text{–}14)$$

Note that in Reactions 2–12 and 2–13 two radicals are formed by each reacting radical, and that therefore these reactions are chain branching steps. At room temperature, Reaction 2–12 is very slow because this endothermic reaction has a high activation energy, and nearly all the free radicals are destroyed by chain termination steps at the wall, such as:

$$2\ H \xrightarrow{\text{wall}} H_2 \qquad (2\text{–}15)$$

$$2\ O \xrightarrow{\text{wall}} O_2 \qquad (2\text{–}16)$$

For this reason the $H_2 + O_2$ mixture is not reactive at room temperature. At higher temperatures ($\sim 500°$ C) Reactions 2–12 and 2–13 compete with 2–15 and 2–16. At very low pressure their rate is very small because of the scarcity of collisions, but as the pressure increases this rate increases, while the rate of termination remains unchanged, until the first explosion limit is reached ($\sim$ 1 mm, depending on surface/volume ratio and wall material). This occurs when the rate of chain branching equals the rate of chain breaking, or $\alpha \geqq \beta$ in

$$\frac{dn}{dt} = n_0 - (\beta - \alpha)n$$

where n is the chain carriers' concentration, n_0 is the rate of chain initiating reactions, and α and β are coefficients of chain branching and chain breaking, respectively.

At still higher pressures, a new three-body reaction becomes important:

$$H + O_2 + M \rightarrow HO_2^{\cdot} + M \qquad (2\text{–}17)$$

This is an effective chain terminating reaction, as it is followed by diffusion of the $HO_2^{\cdot}$ radicals to the wall where they are destroyed:

$$HO_2^{\cdot} \xrightarrow{\text{wall}} \text{stable species} \qquad (2\text{–}18)$$

These stable species may be $H_2O_2 + O_2$, and H_2O_2 is in turn decomposed catalytically at the walls:

$$2\ H_2O_2 \xrightarrow{\text{wall}} 2\ H_2O + O_2 \qquad (2\text{–}19)$$

The termination reaction (2–17) competes with the branching reactions (2–12 and 2–13). The rate of Reaction 2–12 is equal to $k_{12}[H]\ [O_2]$ and the rate of radical formation is twice that rate (because Reaction 2–13 follows Reaction 2–12). The rate of Reaction 2–17 is equal to $k_{17}[H]\ [O_2]\ [M]$, where [M] is the concentration of the third body (O_2, H_2, or H_2O). At low pressure $2k_{12} > k_{17}[M]$, and explosion will occur, but as the pressure increases, the second explosion limit will be reached when $2k_{12} = k_{17}[M]$, and above it the over-all reaction becomes very slow ($\sim$ 50 mm Hg at 500°).

The occurence of a third explosion limit is explained by the fact that not all $HO_2^{\cdot}$ radicals formed by Reaction 2–17 are destroyed at the walls. At higher pressure the reaction

$$HO_2^{\cdot} + H_2 \rightarrow H_2O_2 + H \qquad (2\text{–}20)$$

becomes appreciable and competes with Reaction 2–18, which means that not all H atoms reacting in Reaction 2–17 are destroyed permanently, but only a fraction:

$$\frac{k_{18}}{k_{20}[H_2] + k_{18}}$$

Only at low pressure (second explosion limit) can $k_{20}[H_2]$ be neglected, since it is much smaller than k_{18}. The condition $\alpha = \beta$ (explosion limit) is therefore realized when

$$2k_{12} = \frac{k_{17}k_{18}}{k_{20}[H_2] + k_{18}}[M]$$

This equation is of the second order with respect to pressure and its two roots are the second and third explosion limits. It is noteworthy that H_2O_2 formed in the homogeneous gas phase, Reaction 2–20, is not stable under the conditions of the reaction (cf. Section 4–4), but decomposes by

$$H_2O_2 + M \rightarrow 2\ OH\cdot + M \qquad (2\text{–}21)$$

It is therefore a homogeneous chain initiator. Thus, at high pressure a completely homogeneous mechanism for the combination of hydrogen and oxygen becomes the most prominent reaction path, whereas at low pressure, the nature of the wall surface is a controlling factor.

Photochemical Reaction

Reaction 2–10 is possible at room temperature if chain initiators are available. They may be supplied by adding O atoms or H atoms, formed in an electric discharge, or by producing them within the mixture, e.g., by photochemical methods.

Ultraviolet radiation cannot be used directly to decompose H_2 molecules into atoms, as they do not absorb it. The considerable absorption of ultraviolet in the Schumann-Runge bands, and especially below its convergence limit (1751 Å), may be utilized

to form O atoms (^3P as well as ^1D), and thereby to initiate Reactions 2–13, 2–14, and 2–12. When Hg vapor is added to the gases, the Hg resonance line of 2537 Å can be used to produce H atoms (cf. Section 4–2), which in turn react by Reaction 2–12. The rate of the photochemical reaction increases with the intensity of the radiation, but no explosion will occur at ordinary temperatures, as the branched chain mechanism cannot operate.

Reactions in Aqueous Solution

Many reducing agents are spontaneously oxidized by oxygen at room temperature (autoxidation). The occurence of autoxidation in aqueous solution is confined to reducing agents with a more positive oxidation potential than the H_2O/O_2 couple:

$$2H_2O \rightarrow O_2 + 4H^+ + 4e^- \quad {}^*E^\circ_H = -1.229\ V \qquad (2\text{–}22)$$

A review of the list of redox potentials** reveals the great number of autoxidation reactions that are possible thermodynamically. Only very few of these proceed rapidly, e.g., the reactions with Cr^{2+}, Ti^{3+}, V^{2+}, alkaline pyrogallate, and ammoniacal cuprous chloride, some of which are used for quantitative absorption and determination of O_2 in gas analysis. It was shown that Cr^{2+} reacts much faster than the other reagents. [37]

Other reducing agents react only slowly with O_2, e.g., Fe^{2+}, I^-, and H_2SO_3, and many show no measurable reaction at all. A weaker oxidizing agent such as bromine (Br^-/Br_2, -1.07 V) oxidizes more reducing agents in solution than O_2. This slow oxidation rate of O_2 is due to the high activation energies of its reactions. The four-equivalent oxidation Reaction 2–22 requires the breaking of the strong double bond in the molecule—hence the high activation energy. It is noteworthy that no truly reversible oxygen electrode exists, at which the reversible

---

* This is the oxidation potential of O_2 under atmospheric pressure in an acid solution of pH = O. In a neutral solution (pH = 7) the potential is -0.815 V and in a basic solution of pH = 14 it is -0.401 V.

** M. J. Sienko and R. A. Plane, *Physical Inorganic Chemistry*, W. A. Benjamin (1963), p. 136.

Reaction 2–22 may take place. The E_H° of Reaction 2–22 was indirectly derived from the free energy of formation of water.

The activation energy can be changed by an oxidation process occurring stepwise: if the π bonds of O_2 are severed first, in a two-equivalent oxidation leading to H_2O_2, the activation energy will in many cases be lower than in Reaction 2–22, but the oxidation potential will become less negative in this case:

$$H_2O_2 \rightarrow O_2 + 2H^+ + 2e^- \quad E_H^\circ = -0.682 \text{ V}^* \qquad (2\text{–}23)$$

If H_2O_2 is formed in this way during autoxidation, it will usually react with the substrate much faster than O_2, and be reduced to H_2O(cf. Section 4–4).

This mechanism explains the inertness towards O_2 of most reducing agents with a more negative potential than that of Reaction 2–23. In many autoxidation reactions the intermediate formation of H_2O_2 was proven, e.g., in the autoxidation of metals and of organic compounds. Some of these reactions are used industrially for H_2O_2 production (cf. Section 4–2). In some reactions H_2O_2 may be formed, but escapes detection by specific reagents because of its rapid reaction with the reductant—this situation is demonstrated by the autoxidation of Ti^{3+} to TiO^{2+}. The purple color of Ti^{3+} is first bleached by oxidation to the colorless TiO^{2+}, but just before it vanishes the solution turns orange-yellow as a result of the formation of peroxytitanyl ion (a test for H_2O_2). This behavior is explained by the following steps [39]:

$$2Ti^{3+} + O_2 + 2H_2O \rightarrow 2TiO^{2+} + H_2O_2 + 2H^+ \textit{(slow)} \qquad (2\text{–}24)$$

$$2Ti^{3+} + H_2O_2 \rightarrow 2TiO^{2+} + 2H^+ \qquad \textit{(rapid)} \qquad (2\text{–}25)$$

$$TiO^{2+} + H_2O_2 \rightleftharpoons TiO_2^{2+} + H_2O \qquad \textit{(rapid, reversible)} \qquad (2\text{–}26)$$

---

* A reversible O_2 electrode at which Reaction 2–23 occurs in acid solution is unknown, but in alkaline solution containing H_2O_2 such an electrode has been prepared from porous carbon through which O_2 is injected into the solution. [38]

H_2O_2 is consumed by Reaction 2–25 as soon as it is produced by Reaction 2–24, and only towards the end of the reaction can Reaction 2–26 take place.

It should not be concluded, however, that the peroxide mechanism operates in all autoxidation reactions. In those cases where the peroxide mechanism does operate, we are still faced with the problem of the detailed mechanism of Reaction 2–23. The fact that many reducing agents with a much more positive potential than Reaction 2–23 are very slow to react with O_2 (e.g., ferrocyanide: $Fe(CN)_4^{4-}/Fe(CN)_6^{3-}$, − 0.36 V) shows that many reactions involving Reaction 2–23 still have a high activation energy. The reaction may occur in more than one step. In some cases, a radical mechanism with the following steps is believed to operate [40]:

$$O_2 + e^- \rightarrow [O_2^-] \overset{H^+}{\rightleftharpoons} HO_2 \quad E_H^\circ = -0.74 \text{ V} \qquad (2\text{–}27)$$

$$HO_2 + e^- \rightarrow [HO_2^-] \overset{H^+}{\rightleftharpoons} H_2O_2 \quad E_H^\circ = +2.11 \text{ V} \qquad (2\text{–}28)$$

Similar one-equivalent steps may occur in the subsequent reduction of H_2O_2 (cf. Section 4–4). In the autoxidation of Fe^{2+} to Fe^{3+} in acid solution, it was shown that the above scheme contradicts the kinetic data [41] (the reaction is of the second order with respect to Fe^{2+}). A two-equivalent oxidation mechanism was suggested for this reaction. The O_2 may form a weak labile complex with Fe^{2+}, in which it is activated and reduced by another ferrous ion:

$$Fe^{2+} + O_2 \rightleftharpoons FeO_2^{2+} \qquad (2\text{–}29)$$

$$2H^+ + FeO_2^{2+} + Fe^{2+} \rightarrow 2Fe^{3+} + H_2O_2 \qquad (2\text{–}30)$$

An alternative mechanism, also involving a two-equivalent oxidation, assumes the participation of an unstable higher oxidation state of the reductant (Fe^{IV} in this reaction). This may be the case in Cr^{+2} autoxidation. [42].

Complexes that combine with O_2 reversibly as in Reaction

2–29 are known to exist in nature—they are the oxygen-carrying chelates, hemoglobins and hemocyanins. A growing number of artificial oxygen carriers have been synthesized in recent years. The best known are Co^{II} chelates of the type:

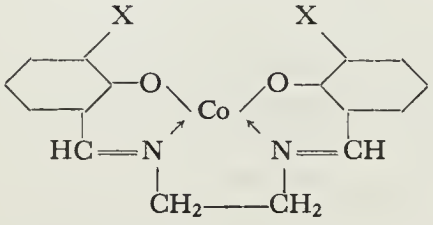

X = H: Salcomin

X = F: Huomin

X = OC_2H_5: Ethomin

IV

but some chelates of Ni, Fe, and Mn are also known. [43]

Many organic autoxidation reactions proceed by a chain mechanism [44], e.g., the autoxidation of olefins. This mechanism is found also in inorganic reactions such as the Cu^{2+}-catalyzed autoxidation of sulfite. [44] These reactions are initiated by a radical-forming step which does not always involve oxygen, as in the sulfite reaction:

$$Cu^{2+} + SO_3^{2-} \rightarrow Cu^{+} + SO_3^{-} \cdot \qquad (2\text{–}31)$$

The propagation reaction consists of the combination of O_2 with an active radical to produce a peroxy radical:

$$R \cdot + O_2 \rightarrow RO_2^{\cdot} \qquad (2\text{–}32)$$

Intimately linked with autoxidation is the phenomenon of induced oxidation [45], known in organic as well as inorganic chemistry. Many substances not autoxidized in the pure state will be oxidized in the presence of another reducing agent: arsenous acid, stable in aqueous solution, will be oxidized in the presence of Cr^{2+} or SO_3^{2-}. From the above discussion, it is clear that this phenomenon can be accounted for by different mechanisms, e.g., by the action of H_2O_2 or $HO_2^{\cdot}$ or other labile intermediates formed during the autoxidation of the activating substances.

The Oxidation of O_2 to O_2^+

Positive oxidation states of oxygen in its covalent compounds with fluorine are well known, but the very high ionization potential of O_2 (12.1 eV) makes the oxidation of O_2 to the O_2^+ ion by a chemical reaction seem unlikely. This feat was nevertheless recently accomplished by Bartlett [46] by means of platinum hexafluoride. The vapor of this compound combines with O_2 at room temperature, to yield dioxygenyl-hexafluoroplatinate V.

$$O_2 + PtF_6 \rightarrow O_2^+ PtF_6^- \qquad (2\text{–}33)$$

The success of this oxidation led to the formation of the first compound of an inert gas [47], $Xe^+ PtF_6^-$ (the ionization potential of Xe is about the same as that of O_2).

REFERENCES

1. E. S. Freeman, *J. Am. Chem. Soc.*, **79**, 838 (1957).
2. Gmelin, p. 304–305.
3. U. S. Patent No. 2422882 (1947).
4. French Patent No. 838040 (1939).
5. Gmelin, p. 198.
6. French Patent No. 643823 (1928).
7. R. C. Brasted, *Comprehensive Inorganic Chemistry*, **8**, 255, Van Nostrand (1961).
8. R. F. Stewart *et al.*, *U. S. Bur. Mines Inform. Circ.*, No. 7906 (1959).
9. C. L. Mantell, *Industrial Electrochemistry*, McGraw-Hill (1950); p. 469.
10. N. Jones, U. S. Patent No. 2390591 (1945).
11. M. Sittig, *Chem. & Eng. News*, **39**, 92 Nov. 27 (1961).
12. M. P. Orlova, *Izmeritel Tekh.*, **2**, 21 (1961), *C. A.* **55**, 19412b (1961).

13a Gmelin, p. 416; 13b *ibid.*, p. 415; 13c *ibid.*, p. 413.

14. D. R. Stull and G. C. Sinke, *Thermodynamic Properties of the Elements*, A.C.S. 18 (1956), p. 25.
15. A. S. Borovic-Romanov *et al.*, *Doklady Akad. Nauk SSSR*, **99**, 699 (1954).
16. L. Vegard, *Nature*, **136**, 720 (1935).
17. A. Dupre *et al.*, *Physica*, **28**, 353 (1962). P. Kapitza *et al.*, *J. Sci. Inst.*, **14**, 201 (1937).
18. L. J. Heidt and A. M. Johnson, *J. Am. Chem. Soc.*, **79**, 5587 (1957).
19. J. Jortner and O. Sokolov, *J. Phys. Chem.*, **65**, 1633 (1961).
20. A. Van Cleff and G. A. M. Diepen, *Rec. Trav. Chim.*, **79**, 582 (1960).
21. L. Pauling, *J. Am. Chem. Soc.*, **53**, 3225(1931).
22. G. W. Wheland, *Trans. Faraday Soc.*, **33**, 1499 (1937).

23. M. J. Sienko and R. A. Plane, *Physical Inorganic Chemistry*, W. A. Benjamin (1963), p. 19.
24. R. S. Mulliken, *Phys. Rev.* [2] **32**, 880 (1928).
25. G. Herzberg, *Nature*, **133**, 759 (1934).
26. V. Schumann, *Smithsonian Contrib. Knowledge*, **29**, No. 1413 (1903).
27. G. Herzberg, *Naturwiss.*, **20**, 577 (1932).
28. G. Herzberg, *Canad. J. Phys.*, **31**, 657 (1953).
29. J. T. Vanderslice *et al. J., Chem. Phys.*, **32**, 515 (1960).
30. P. Brix and G. Herzberg, *Canad. J. Phys.*, **32**, 110 (1954).
31. H. D. Babcock and L. Herzberg, *Astrophys. J.*, **108**, 167 (1948).
32. M. Tinkham *et al.*, *Phys. Rev.*, **97**, 951 (1955).
33. K. Wantabe, *J. Chem. Phys.*, **26**, 542 (1957).
34. G. N. Lewis, *J. Am. Chem. Soc.*, **46**, 2027 (1924).
35. H. Salow and W. Steiner, *Z. Phys.*, **99**, 137 (1936).
36. B. Lewis and G. Von Elbe, *Combustion, Flames and Explosions of Gases*, Academic Press (1951).
37. H. W. Stone, *J. Am. Chem. Soc.*, **58**, 2591 (1936); *A.C.S.*, 142*nd Meeting, Abstracts*, 37N (1962).
38. W. G. Berl, *Trans. Electrochem. Soc.*, **83**, 253 (1943).
39. D. M. Yost and H. Russel, *Systematic Inorganic Chemistry*, Prentice Hall (1946), p. 368.
40. Review by P. George and J. S. Griffith, *The Enzymes*, Academic Press (1959), **1**, 374.
41. P. George, *J. Chem. Soc.*, 4349 (1954).
42. M. Ardon and R. A. Plane, *J. Am. Chem. Soc.*, **81**, 3197 (1959).
43. H. M. Feigenbaum and S. E. Wiberley, *Chem. Rev.*, **63**, 269 (1963).
44. N. Uri, *Autoxidation and Anti-oxidants*, Interscience (1961), **1**, 55.
45. W. P. Jorissen, *Induced Oxidation*, Elsevier (1959).
46. N. Bartlett *et al.*, *Proc. Chem. Soc.* (1962), 115.
47. N. Bartlett *et al.*, *Proc. Chem. Soc.* (1962), 218.

3

Ozone

The smell of ozone, noticed during thunderstorms, has been known since ancient times (Homer's *Iliad* and *Odyssey* mention it). Van Marum produced ozone by passing electric sparks through oxygen, noting a decrease in the volume of the gas (1786), and Cruickshank noted its "chlorine-like" smell during electrolysis of sulfuric acid (1801); but its discovery is unquestionably due to Schönbein. He realized that the preparative methods used by Van Marum and Cruickshank produced one and the same product —an elementary gas, which he named "ozone" (from the Greek *οζειν*, to smell). The true nature of ozone was not determined for several years after its discovery, and even Schönbein was led to the erroneous conclusion that it was a higher oxide of hydrogen (1845–1849). Delarive and Marignac upheld the view that ozone was an allotropic modification of oxygen, based on the formation of ozone from pure, dry oxygen. This view was soon generally accepted, but not until twenty years later was the correct triatomic formulation of O_3 established. The difficulty lay in the fact that ozone was available only in a diluted form (in oxygen)—

a situation that delayed the precise determination of its molecular weight.

3-1 OCCURRENCE

Ozone is a minor constituent of the atmosphere. Its concentration depends on the season, time of day, altitude, and local conditions, and is usually below $2 \cdot 10^{-8}$ vol per vol of air, or 0.002 cm km^{-1} (a frequently used unit expressing the thickness of a layer of pure ozone at STP, in centimeters, contained in an air layer of 1 kilometer). Much higher concentrations occur in smog-infected regions, such as the Los Angeles area, where up to $100 \cdot 10^{-8}$ vol per vol_{air} (100 p.p.h.m.) has been recorded.

The ozone concentration rises appreciably with altitude, both relatively and absolutely, and reaches a maximum of over 0.02 cm km^{-1} at approximately 25 km. This concentrated ozone layer is an efficient absorber of solar short-wave ultraviolet radiation (< 300 mμ) and thus protects life on earth from its harmful effects.

Atmospheric ozone is formed mainly by high-altitude photochemical synthesis, from molecular oxygen, which occurs by absorption of solar radiation (< 200 mμ). Some ozone is formed at low altitudes, especially in polluted air that contains precursors which make possible photochemical synthesis by radiation of longer wavelength.

The concentrated ozone layer at 25 km is a warm layer, due to the heat generated by light absorption and by the exothermic decomposition of ozone. This layer plays an important part in temperature regulation of the lower atmosphere.

3-2 FORMATION

Equilibrium Methods

The reaction $1\frac{1}{2}\ O_2 \rightarrow O_3$ is accompanied by an enthalpy change of $\Delta H^{\circ}_{298^{\circ}K} = +\ 34.0$ kcal $mole^{-1}$ (at atmospheric pressure). The free energy change is $\Delta F^{\circ}_{298^{\circ}K} = +\ 39.0$ kcal $mole^{-1}$. From these data it is evident that equilibrium conditions for ozone formation are highly unfavorable at room temperature.

The expected favorable shift toward ozone at higher temperatures cannot be utilized, not only because of the high temperatures required, but because both ozone and oxygen dissociate into atoms at higher temperatures (both are endothermic processes). Therefore the equilibrium concentration of ozone reaches a maximum (at 3400° K) and then falls off again at higher temperatures. The maximum partial pressure of ozone is 10^{-6} atm (at 1 atm total pressure at 3400° K); thus, there is no set of temperatures and pressures which might be practically used for ozone production by equilibrium methods. Small concentrations of ozone can be produced by heating oxygen to high temperatures, followed by rapid cooling (to minimize decomposition), e.g., by an incandescent platinum wire immersed in liquid oxygen. The formation of ozone traces in several flames is due to a smiliar mechanism.

Electrolytic Methods

The reversible uptake by O_2 of the free energy of ozone formation (39.0 kcal $mole^{-1}$) would yield 1058 g of pure ozone per kwh of electrical energy; however, no efficient anodic oxidation process of oxygen is known to date. All practical electrolytic processes use water as a source of ozone, so that another 170 kcal are needed for the formation of $1\frac{1}{2}$ moles of O_2, and the theoretical yield for ozone production drops to 198 g per kwh in a reversible process.

The highest yields so far obtained are 24 g per kwh, the average practical yield being still lower. For this reason, electrochemical processes cannot compete economically with silent electric discharge methods of ozone production. One noteworthy feature of the electrolytic method is that it can furnish higher concentrations of ozone than any other method (up to 58 wt %).

Aqueous sulfuric acid and perchloric acid solutions are the most suitable electrolytes. Current and energy efficiencies decrease markedly with increase of temperature—electrolysis is best carried out at $-50°$ to $-60°$C, and near eutectic solutions are employed (40% $HClO_4$) in order to prevent freezing at these temperatures.

Photochemical Methods

Ozone is formed from oxygen by irradiation with ultraviolet light of wavelength shorter than 2100 Å. In this region, the quantum yield is approximately 2 (two ozone molecules formed per photon absorbed).

The mechanism of this reaction is still unknown. Warburg [1] believed that O_2 is dissociated photochemically into two normal (^3P) atoms, which in turn combine with two O_2 molecules to form two ozone molecules:

$$O_2 \xrightarrow{h\nu} 2\,O \qquad (3\text{–}1)$$

$$O + O_2 \longrightarrow O_3 \qquad (3\text{–}2)$$

Although this mechanism accounts for the quantum yield, it is erroneous: the dissociation of O_2 into two normal (^3P) atoms requireds 117 kcal mole^{-1}, corresponding to a wavelength of 2427 Å, but in this range no O_3 formation is observed. The decomposition of O_2 into one normal (^3P) and one activated (^1D) atom requires 163.8 kcal or 1750 Å. This wavelength indeed coincides with the convergence limit of the Schumann-Runge band. If this step constitutes the primary photochemical reaction, the synthetic activity of wavelengths shorter than 1750 Å and the quantum yield of 2 are explained--but it cannot account for the activity of the equally efficient range between 1750 Å and 2100 Å. It was suggested [2] that the activated O_2 molecule in the $^3\Sigma_u^-$ state formed in the Schumann band (1751 to 2000 Å) is also effective in ozone formation:

$$O_2 + h\nu \rightarrow O_2^* \qquad (3\text{–}3)$$

$$O_2^* + O_2 \rightarrow O_3 + O \qquad (3\text{–}4)$$

$$O + O_2 \rightarrow O_3 \qquad (3\text{–}5)$$

In this mechanism the quantum yield of 2 is expected. Other mechanisms were suggested for this spectral region, e.g., the participation of the double oxygen molecule $(O_2)_2$. [3]

The photochemical synthesis which is responsible for the formation of atmospheric ozone is of little practical value, since it cannot compete with the electric discharge process. The highest yield obtained by this method is approximately 3 g per kwh (using liquid oxygen). This lower yield is mainly due to the low efficiency of converting electrical energy to ultraviolet radiation of wavelength shorter than 2100 Å in the mercury vapor lamp, and also to the thermal and photochemical decomposition of ozone occuring during the process.

Silent Electric Discharge Method

Synthesis of ozone from molecular oxygen by silent electrical discharge is the only method used for production on an industrial scale, because it is the most economical process. The reaction is carried out in an ozonizer in which the electric discharge takes place between electrodes connected to a high-voltage source (5000 to 30,000 volts). They are separated by a dielectric layer (glass) and an air gap. The dielectric layer acts as a stabilizing resistance, counteracting any increase or localization of the density of the high voltage discharge. A current of oxygen (or air) is passed through the air gap and is enriched with ozone.

The basic features of the ozonizer were developed by Siemens (1857). The gases pass between two concentric glass tubes—the inner coated on the inside, and the outer on the outside, with metal foil, serving as electrodes. In an improved arrangement, the inner tube is made of metal and serves as one electrode, and the outer tube, made of glass, dips into cooling water that serves as the second electrode (Fig. 3–1).

The silent discharge is more efficient than spark or arc discharges because the large area of the electrodes, in the former, makes possible efficient cooling of the gases, thus minimizing thermal decomposition of ozone. Yields of about 150 g per kwh are realized in industry (using pure O_2). Up to 300 g per kwh have been produced from liquid oxygen. If air is used, both yield and concentration are lowered, and oxides of nitrogen are formed along with ozone.

There is a similarity between the mechanism of photo-

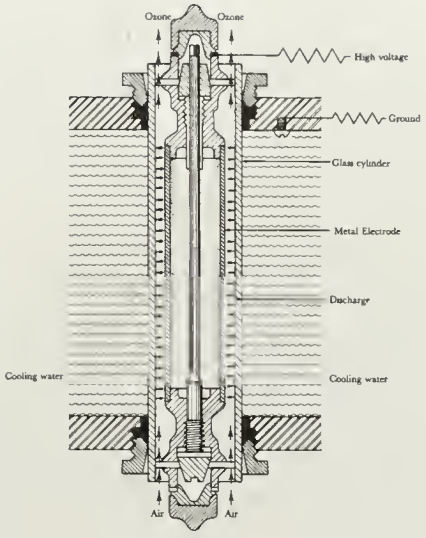

Figure 3-1 *Ozonizer.*

chemical synthesis and the silent discharge method. Both proceed via oxygen atoms and excited molecules produced by the impact of photons or electrons, but the latter is more complex. Electron impact will effect both allowed transitions (e.g., $^3\Sigma_g^- \rightarrow {}^3\Sigma_u^-$) and disallowed transitions (e.g., $^3\Sigma_g^- \rightarrow {}^3\Sigma_u^+$), whereas photons will mainly produce allowed transitions. In the electric discharge, as in the photochemical method, the synthetic reactions are accompanied by decomposition reactions. The concentration of ozone in the outflowing gases depends on the geometry of the ozonizer, the flow rate, the electron (or photon) flux, etc. This is a steady state condition and should not be mistaken for a chemical equilibrium depending solely on temperature and pressure.

Chemical Methods

A great number of chemical reactions have been claimed to lead to ozone formation: the autoxidation of white phosphorus, the thermal decomposition of many oxides and of oxygen-acids and their salts, the decomposition of peroxides, peroxy acids, and superoxides in acid solutions, the decomposition of water by fluorine, etc. [4] Many of the reactions cited in the literature as ozone-producing were later shown not to produce any. The most common error of many authors was the use of faulty analytical methods. [5] Some reactions do lead to ozone formation (such

as the decomposition of peroxydisulfates by strong acids [6], but many others have to be carefully reinvestigated in order to confirm their positive results.

Separation of O_3 from O_2

The oxygen emerging from the ozonator contains 2% to 5% ozone. After liquefying the mixture, O_2 can be pumped off owing to its much higher vapor pressure. Liquid ozone is highly explosive, and special safety devices have to be used for handling it. On an industrial scale this method is impractical. Ozone is separated from O_2 by absorption on silica gel: the O_2 is recycled to the ozonizer and O_3 is desorbed by nitrogen or argon.

3-3 PHYSICAL PROPERTIES

Ozone is a blue gas, liquid ozone is dark blue, and the solid is dark purple. It possesses a characteristic odor and is highly explosive.

The hazards encountered in handling ozone may partly account for the unusual situation that many important physical properties of this substance were not measured accurately for a period of one hundred years following its discovery, and some are still uncertain today. Recent interest in ozone for rocket propulsion, high altitude exploration, and other practical uses initiated a number of basic research projects that have supplied new data and improved previous knowledge during the last decade.

The Ozone Molecule

The ozone molecule is angular. Its shape has been accurately determined by microwave spectrum investigations [7] (Fig. 3–2).

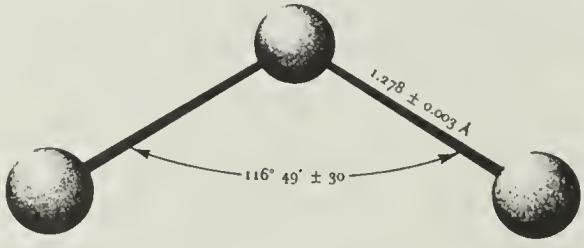

Figure 3-2 *Configuration of the ozone molecule.*

These investigations as well as infrared studies supplied improved data for other molecular properties. Force constants [8] (in 10^{-5} dyn cm^{-1}): $f_d = 5.707$; $f_\alpha = 1.2847$; $f_{d\alpha} = 0.3324$; $f_{dd} = 1.5233$. Moments of inertia [7] (in 10^{-40} g cm^2): $\mathcal{J}_A = 7.8749$; $\mathcal{J}_B = 62.844$; $\mathcal{J}_C = 70.888$. The dipole moment is 0.58 ± 0.05 Debye units (D). [9]

The fact that the ozone molecule is angular became evident thirty years ago from ir spectrum analysis and dipole moment determinations, which ruled out a linear or ring structure. The angle was first believed to be acute (Gerhard, 1932), but reinterpretation of the ir data showed it to be obtuse (Badger and Bonner, 1933). Electron diffraction measurements [10] assigned a length of 1.26 ± 0.02 Å to the O—O bond, and an angle of $127 \pm 5°$ between the central and outer atoms. The bond length was correct (within the experimental error), but the angle was some 10° too wide, as shown by the microwave investigation mentioned above. [7] The bond length (1.28 Å) is shorter than the single O—O bond (1.49 Å in H—O—O—H) and longer than in the O_2 molecule (1.21 Å); thus, it is evident that this O—O bond in ozone must have a considerable double bond character. The binding may be considered as consisting of two σ bonds between the central and the outer atoms, and a delocalized π orbital spread over the whole molecule. According to the valence bond approach, the ozone molecule is described as a resonance hybrid of structures I and II.

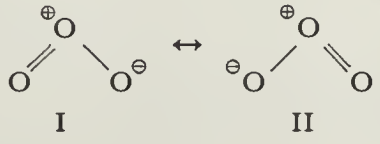

I II

This hybrid structure would have a higher dipole moment than determined experimentally (1.62 instead of 0.58 ± 0.05 D). The discrepancy might be explained by the contribution of two additional resonance structures III and IV, which cancel each other's polarity and decrease the resultant dipole of the hybrid [10], but a considerable contribution of III and IV will result

III IV

in a greater bond length than 1.28 Å. The smaller than expected dipole can be accounted for by assuming the σ bonds of the molecule to be formed by sp^2 hybridization of the central O atom, leaving 2 electrons in the third sp^2 atomic orbital, directed upwards, and producing a negative center, opposing the dipole of structures I and II. Another explanation is offered by assuming the molecule to be a hybrid of I and II with the structures V and VI. [11]

V VI

A detailed theoretical investigation of the electronic structure of ozone was conducted by the molecular orbitals derived by the LCAO [12] method. Three different approximations were used: in the simplest case, only the $2p\pi$ electrons were considered. A better agreement with experimental data was achieved by considering all $2p$ electrons, and the best results were obtained by considering all $2s$ and $2p$ electrons. The values of ionization potential, dissociation energy, dipole moment, and energy levels calculated by this refined treatment are in good agreement with the experimental data.

Thermal and Mechanical Properties

The normal boiling point of liquid ozone is − 111.9°; the critical temperature is − 12.1° and the critical pressure 54.6 atm. [13] The melting point of pure ozone determined by Riesenfeld and Schwab (1922) was − 250° C, but this was recently found to be some 60° lower than the correct value which is − 192.5°. [14] It seems likely that the stability of ozone in the supercooled form caused the investigators to overlook the delayed freezing altogether, so that they were misled into investigating the tempe-

rature region of boiling hydrogen (instead of that of liquid air). The transition they measured was probably a solid phase transition. [14] Surface tension is 38.1 dyn cm^{-1} at $-182.7°$, and the density is 1.5727 g cm^{-3} at $-182.9°$. Viscosity is 1.56 centipoises at $-183°$ and 4.14 at $-195.6°$ (supercooled liquid). [14]

The specific heat of liquid ozone is 0.434 cal g^{-1} at $-176.6°$ [15], and of gaseous ozone 0.197 cal g^{-1} at 25° and 1 atm. [16]

The heat of formation is $\Delta H_f^0 = 34.0$ kcal $mole^{-1}$, and the free energy of formation $\Delta F_f^0 = 39.06$ kcal $mole^{-1}$ both at 1 atm and 25° C. [17]

The heat of vaporization of liquid ozone is 2.59 kcal $mole^{-1}$, and the entropy of vaporization 15.92 cal $mole^{-1}$ $degree^{-1}$, both at the normal boiling point.

Solubility: Above $-180°$ liquid oxygen and ozone are miscible in all proportions but below that temperature two liquid phases appear over a certain range of concentrations. [18] The solubility in water is higher than that of oxygen: 0.52 liter will dissolve in 1 liter of water at 0° C and 1 atm. [19] Ozone is appreciably soluble in $CHCl_3$, CCl_4, CF_2Cl_2, CF_3Cl, and other organic solvents.

The dielectric constant of the gas is $\varepsilon = 1.0019$ at 0° and 1 atm [20] and in liquid ozone $\varepsilon = 4.75$ (at $-183°$). [21]

Absorption Spectrum

Ozone possesses numerous absorption bands extending from the infrared through the visible to the short-wave ultraviolet. In the infrared several bands are known, starting with the 14.2 μ band. In the visible region, 13 maxima exist between 7392 Å and 4069 Å with the highest at 6019 Å. In the ultraviolet there are bands between 3650 Å and 3400 Å (Chalonge-Lefebvre band), at 3400–3050 Å (Huggins band), and at 3000–2200 Å (Hartley band). The most intense is the Hartley band with a maximum at 2550 Å: this wavelength is used for analytical purposes in the gas phase and in solution. The ionization potential is 12.8 eV or 13.15 eV, if molecular oxygen is assumed as an impurity in the mass-spectrometry experiments used. [21a]

3-4 CHEMICAL PROPERTIES

Decomposition

The decomposition of ozone to oxygen is a spontaneous process at all temperatures; the thermal decomposition of pure ozone is, however, a slow reaction at room temperature. It is accelerated by many homogeneous and heterogeneous catalysts. Ozone is also decomposed photochemically and by an electric discharge.

Thermal Decomposition. The thermal decomposition in the gas phase was believed to proceed by a chain mechanism [22], but this view is rejected by recent investigators. [23] The reaction probably proceeds by the following mechanism:

$$M + O_3 \underset{2}{\overset{1}{\rightleftharpoons}} M + O_2 + O \qquad (3\text{–}6)$$

$$O + O_3 \xrightarrow{3} 2\,O_2 \qquad (3\text{–}7)$$

M is an inert molecule (O_2, O_3, CO_2, N_2, etc.) that activates O_3 by collision. Concentrated and liquid ozone are highly explosive. The explosion is not a result of a chain mechanism, but of a temperature rise within the reaction medium. It is noteworthy, in this respect, that ultraviolet radiation does not initiate explosion [24] (as might be expected by some chain mechanisms).

Small amounts of impurities (e.g., hydrocarbons, H_2, Br_2, etc.) can sensitize explosion of ozone. These same sensitizers are also efficient catalysts of the slow thermal decomposition and operate by a chain mechanism. [23] Chlorine, for example, will accelerate the decomposition; reaction chains are initiated by steps such as:

$$Cl_2 + O_3 \rightarrow OCl + Cl + O_2 \qquad (3\text{–}8)$$

or

$$O_3 + Cl_2 \rightarrow OCl + ClO_2 \qquad (3\text{–}9)$$

propagated by

$$OCl + O_3 \rightarrow Cl + 2\,O_2 \qquad (3\text{–}10)$$

or

$$Cl + O_3 \rightarrow OCl + O_2 \qquad (3\text{–}11)$$

and terminated by

$$OCl + OCl \rightarrow Cl_2 + O_2 \qquad (3\text{–}12)$$

or

$$Cl + Cl + M \rightarrow Cl_2 + M \qquad (3\text{–}13)$$

Bromine reacts similarly, and is more efficient. This is not the only available path: higher oxides of the halogens are formed in the reaction and may play an important part (Cl_2O_6, Br_3O_8, Cl_2O_7, etc.). [25]

The activity of N_2O_5 was explained by the reaction

$$2N_2O_5 \rightarrow 4NO_2 + O_2$$

followed by

$$2NO_2 + O_3 \rightarrow N_2O_5 + O_2,$$

but this mechanism would make the slow thermal decomposition of N_2O_5 the rate-determining step, and is not compatible with the fact that the catalytic decomposition is much faster. A mechanism involving NO_3 is probably operating in this case. [26]

Heterogeneous catalysis: Many solid substances are catalytically active; coal, metals (Fe, Pt group), many oxides (e.g., P_2O_5), peroxides (BaO_2), and hydroxides. A comparative kinetic study of a number of oxides [27] links the decrease of activation energy with an increase of basic properties (electron pair donation) of the oxides. It was suggested that this reaction proceeds by an O atom association with the catalyst [27]:

$$O_3 + \text{catalyst} \rightarrow O_2 + O \text{ catalyst} \qquad (3\text{–}14)$$

Decomposition in aqueous solution: Acidified aqueous solutions are relatively stable (a $1.6 \cdot 10^{-3}$ *M* solution in 0.2 *M* $HClO_4$ lost 5% of its oxidizing power after 20 hours at 0° C [5]).

The reaction is accelerated by OH^- ions. Conflicting experimental results of different authors make mechanistic interpretations highly speculative. [28] Free radicals such as $OH\cdot$ and HO_2^- probably take part in the reaction.

Photochemical Decomposition. Pure ozone is photochemically decomposed by absorption of visible or ultraviolet light. With red light the quantum yield is approximately 2, but in the ultraviolet, yields of 6.7 were recorded. [29] The red light is believed to decompose O_3 into O_2 and a normal O atom

$$O_3 + h\nu \rightarrow O_2 + O(^3P)\cdot \qquad (3\text{–}15)$$

This O atom (at the ground state ^3P) will attack another ozone molecule:

$$O + O_3 \rightarrow O_2 + O_2 \qquad (3\text{–}16)$$

The quantum yield is 2 and no chain reaction takes place. [23] The energy-rich ultraviolet will produce an activated O atom:

$$O_3 + h\nu \rightarrow O_2 + O(^1D) \qquad (3\text{–}17)$$

This $O(^1D)$ atom can initiate a chain mechanism [30] by producing a vibrationally excited O_2 molecule, $O_2^*(^3\Sigma_g^-)$, in Reaction 3–16 which will react with a normal O_3 molecule to reproduce $O(^1D)$ (if its excitation energy is greater than 69 kcal). The chain is terminated by one of the following:

$$O + O + M \rightarrow O_2 + M;$$

$$O + O_2 + M \rightarrow O_3 + M;$$

$$O_2^* + M \rightarrow O_2 + M$$

(M is an inert gas molecule).

The effect of impurities on the photolysis is remarkable: water vapor will not affect the quantum yield with red light [31] but will increase it from 6.7 to 130 in the ultraviolet. [32] The

reason for this effect is that the activated ^1D atom produced in Reaction 3–17 will readily react with water to form OH· radicals:

$$O(^1D) + H_2O \rightarrow 2\ OH\cdot \qquad (3\text{–}18)$$

The OH· radical, which was detected in flash photolysis of wet ozone [30], is a more efficient chain carrier than the excited $O_2^*(^3\Sigma_g^-)$ molecule:

$$OH\cdot + O_3 \rightarrow HO_2^{\cdot} + O_2 \qquad (3\text{–}19)$$

$$HO_2^{\cdot} + O_3 \rightarrow OH\cdot + 2\ O_2 \qquad (3\text{–}20)$$

Chlorine and bromine are also catalytically active. The principal reactions in this case are [30]:

$$Cl_2 + h\nu \rightarrow Cl(^2P_{3/2}) + Cl(^2P_{1/2}) \qquad (3\text{–}21)$$

$$Cl + O_3 \rightarrow ClO^* + O_2 \qquad (3\text{–}22)$$

$$ClO + O_3 \rightarrow Cl + 2\ O_2 \qquad (3\text{–}23)$$

The same holds for Br_2.

In aqueous solutions ozone is decomposed by ultraviolet but not by red light. [33]

$$O_3 + H_2O \xrightarrow{h\nu} O_2 + H_2O_2 \qquad (3\text{–}24)$$

In this case, as in the vapor phase, the activated $O(^1D)$ atom initiates the reaction by attacking the H_2O molecule.

Oxidation Reactions

The redox potential [34] of the ozone-oxygen couple in acid solution is

$$O_2 + H_2O \rightarrow O_3 + 2H^+ + 2e^- \quad -2.07\ V \qquad (3\text{–}25)$$

and in basic solution

$$O_2 + 2OH^- \rightarrow O_3 + H_2O + 2e^- \quad -1.24\ V \qquad (3\text{–}26)$$

This makes ozone the strongest oxidizing agent after F_2 (and fluorine oxides), not counting short-lived free radicals and atoms. When an excess of ozone is used, it will oxidize most elements and compounds to the highest oxidation state. In most oxidation reactions only one O atom is used, and O_2 is formed along with the oxidation product, e. g.

$$2\ H^+ + 2\ Co^{2+} + O_3 \rightarrow 2\ Co^{3+} + H_2O + O_2 \qquad (3\text{–}27)$$

because the reduction to H_2O furnishes a much lower potential.

In a few reactions all three atoms are combined with the reducing agent, e.g.,

$$3\ SO_2 + O_3 \rightarrow 3\ SO_3 \qquad (3\text{–}28)$$

Most metal surfaces are converted to their highest oxidation states (especially if traces of the vapor are present): Pb to PbO_2, Ag to AgO and Ag_2O_3, Hg to HgO, etc.

Many reactions of O_3 with elements and compounds in the gaseous phase have been investigated kinetically, and some of the more important will be mentioned:

Halogens — act as catalysts for thermal and photochemical decomposition of ozone. During the reaction, oxides such as $I(IO_3)_3$ [35], Br_2O_5, $(Br_3O_8)_n$ [36] (the last may be identical with BrO_3), ClO_2, Cl_2O_7 [25] are formed and have been isolated.

N_2 — this inert molecule is reactive at unusually low temperature. It reacts according to $N_2 + O_3 \rightarrow N_2O + O_2$, the reaction being complete within one minute at 295°, but the yield is small since most of the O_3 is decomposed catalytically. [37]

NO — reacts in a very fast reaction: $NO + O_3 \rightarrow NO_2 + O_2$ with a small activation energy of 2.5 kcal. This reaction is believed to be elementary bimolecular. [38]

NO_2 — reacts rapidly to form N_2O_5 during the catalytic decomposition of ozone. The reaction proceeds in two steps:

$$NO_2 + O_3 \rightarrow NO_3 + O_2 \qquad (3\text{-}29)$$

$$NO_2 + NO_3 \rightarrow N_2O_5 \qquad (3\text{-}30)$$

NH_3 — is oxidized to NH_4NO_3.

CO — reacts surprisingly slowly at 100°, and has a high activation energy (> 30 kcal). [39]

Of the many oxidation reactions in aqueous solutions, only a few will be mentioned: ions in highly unstable oxidation states (which are reduced by water) are obtained with ozone, such as Ag^{II} and Ag^{III} (from Ag^+ in concentrated nitric acid) or the Co^{3+} ion mentioned above. Mn^{2+} is oxidized to MnO_4^- (in acid solution), lead^{II} acetate to PbO_2, Tl^+ to Tl^{3+}, and As^{III} to As^V. The last two reactions are useful for O_3 analysis (only one O atom participates). H_2O_2 reacts with ozone in acid solution, both as a reducing agent and as a catalyst for decomposition:

$$H_2O_2 + O_3 \rightarrow H_2O + 2\,O_2 \qquad (3\text{-}31)$$

$$2\,O_3 \rightarrow 3\,O_2 \qquad (3\text{-}32)$$

At high H_2O_2 concentration, Reaction 3-31 predominates, but at very dilute peroxide concentrations, catalytic decomposition is the main reaction.

These reactions were shown to proceed by a chain mechanism [5]:

$$H_2O_2 + O_3 \rightarrow OH\cdot + HO_2^{\cdot} + O_2 \qquad (3\text{-}33)$$

$$HO_2^{\cdot} + O_3 \rightarrow OH\cdot + 2\,O_2 \qquad (3\text{–}34)$$

$$OH\cdot + O_3 \rightarrow HO_2^{\cdot} + O_2 \qquad (3\text{–}35)$$

$$OH\cdot + H_2O_2 \rightarrow HO_2^{\cdot} + H_2O \qquad (3\text{–}36)$$

Reaction 3–33 is chain-initiating. Reactions 3–34 + 3–35 yield Reaction 3–32, while Reactions 3–34 + 3–36 yield Reaction 3–31.

Ozone can act as a catalyst in autoxidation reactions, e.g., in the oxidation of sulfurous acid.

Ozonides

Ozone reacts with alkali hydroxides to form a colored product. This reaction was first observed by Schönbein (1844), and later investigated by Würz (1868), Von Bayer (1902), and others [41], but the structure and properties of the product were only recently established. Renewed interest in these compounds was aroused by the Russian investigators Kazarnovskii, Nikolski and Abletrova. [42] The ozonides are unstable red or brown ionic compounds of the composition MO_3, where M is a monovalent cation.

Preparation. Ozonides of Na^+, K^+, Rb^+, Cs^+, and $(CH_3)_4N^+$ are prepared by reaction of their dry hydroxides with ozone at low temperatures [42]:

$$3\,KOH + 2\,O_3 \xrightarrow{-15^\circ} 2\,KO_3 + KOH\cdot H_2O + \tfrac{1}{2}O_2 \qquad (3\text{–}37)$$

The product is extracted by liquid ammonia and isolated by evaporation of the solvent. An ammonium ozonide (NH_4O_3) was prepared by reaction of O_3 with NH_3 at $-100°$, but is unstable even at this temperature. [43] The formation of a lithium ozonide is doubted on thermodynamic grounds, but a tetra-ammoniated lithium ozonide $Li(NH_3)_4O_3$ was recently prepared. [44] Preparation of ozonides by reaction of O_3 with the superoxides of K and Cs was recently reported. [45]

Properties. Ozonides contain the O_3^- ion, which has a typical absorption spectrum in the visible region. [46] Of the 19 valence electrons that this ion possesses, one was expected to be unpaired, as was confirmed by its magnetic moment (1.67 BM). [42] An X-ray powder photographic examination was claimed to establish the linear structure of O_3^- [47], but an alternative interpretation of these data attributed a "bent" structure to this ion. [48] The "bent" structure is further supported by esr measurements [49] and by theoretical considerations [48] applying to all similarly constituted triatomic molecules having 19 valence electrons (e.g., ClO_2). The 19th electron is in an orbital that is spread over the whole ion. [49] According to the valence bond approach, the ozonide is described as a resonance hybrid between structures containing single and 3-electron bonds [50]:

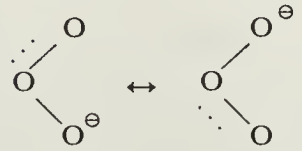

VII VIII

The ozonides are soluble in liquid ammonia. They decompose spontaneously to superoxides and oxygen:

$$2\ KO_3 \rightarrow 2\ KO_2 + O_2 \qquad (3\text{-}38)$$

Their stability depends largely on the lattice energy, and increases with the radius of the cation: NaO_3 is completely decomposed within 53 hours at room temperature, but KO_3 [51] takes 11 days to decompose. For this reason LiO_3 was not prepared. Water decomposes ozonides in a vigorous reaction:

$$4\ MO_3 + 2\ H_2O \rightarrow 4\ MOH + 5\ O_2 \qquad (3\text{-}39)$$

The ozonide ion and its conjugated acid HO_3 may take part in numerous inorganic reactions in solution, such as the decomposition of H_2O_2 by NaOH [49], and the exchange reaction between water and oxygen. [52]

The well-known reactions of ozone with organic compounds, such as the cracking of stressed rubber, the formation of ozonides by addition to the C = C double bond, oxidation, and catalysis of autoxidation, will not be described. The reader is referred to recent investigations in this field. [53, 54, 55]

3-5 USES

Ozone is an ideal oxidizing agent for many purposes—such as the purification of water. [53] Lower production costs due to recently improved methods of production and handling may result in the replacement of chlorine by ozone in bleaching processes. Ozone is already used in the organic chemical industry, e.g., in the production of azelaic and pelargonic acids by ozonization of oleic acid, and the future may see a great expansion in this area.

REFERENCES

1. E. Warburg, *Z. El. Chem.*, **26**, 56 (1920); *ibid.*, **27**, 133 (1921).
2. W. E. Waugham and A. Noyes, *Rev. Mod. Phys.*, **5**, 280 (1933).
3. E. Briner, *Ozone Chemistry and Technology*, p. 1, Am. Chem. Soc. (1959).
4. For an extensive survey, see Gmelin's *Handbuch der anorg. Chemie*, System No. 3, Lieferung 4, pp. 1092–1099 (1960).
5. See, e.g., Taube and Bray's criticism of the work of Weiss, *J. Am. Chem. Soc.*, **62**, 3357 (1940).
6. W. K. Wilmarth, *J. Phys. Chem.*, **63**, 358 (1959).
7. R. H. Hughes, *J. Chem. Phys.*, **21**, 959 (1953). R. Trambarulo, N. S. Ghosh, C. A. Burrus and W. Gordy, *J. Chem. Phys.*, **21**, 851 (1953).
8. L. Pierce, *J. Chem. Phys.*, **24**, 139 (1956).
9. R. H. Hughes, *J. Chem. Phys.*,**24**, 131 (1956).
10. W. Shand and R. A. Spurr, *J. Am. Chem. Soc.*, **65**, 179 (1943).
11. G. M. Phillips, J. S. Hunter and L. E. Sutton, *J. Chem. Soc.*, (1945), p. 161.
12. I. Fischer, Hjalmars, *Arkiv. Fysik*, **11**, 529 (1957).
13. A. C. Jenkins *et al.*, *J. Chem. Phys.*, **20**, 1158 (1952).
14. A. C. Jenkins *et al.*, *J. Chem. Phys.*, **25**, 296 (1956); C. Brown *et al.*, *J. Chem. Phys.*, **22**, 1151 (1954).
15. R. I. Brabets *et al.*, *J. Chem. Phys.*, **28**, 1212 (1958).
16. A. C. Jenkins *et al.*, *J. Chem. Phys.*, **23**, 441 (1955).
17. *N. B. S. Circular*, No. 500 (1952).
18. A. C. Jenkins *et al.*, *J. Chem. Phys.*, **23**, 2049 (1955).
19. E. Briner *et al.*, *Helv. Chim. Acta*, **22**, 397 (1939).
20. G. M. Epprecht, *Z. ang. Math. Phys.*, **1**, 138 (1950).
21. C. K. Hersh *et al.*, *J. Phys. Chem.*, **63**, 1968 (1959).

21a. E. E. Muschlitz *et al.*, *J. Phys. Chem.*, **60**, 681 (1956); J. T. Herron *et al.*, *J. Chem. Phys.*, **24**, 1266 (1956).
22. E. H. Riesenfeld and E. Wassmuth, *Z. Phys. Chem.*, **A143**, 397 (1929).
23. S. W. Benson and A. E. Axworthy, *J. Chem. Phys.*, **26**, 1718 (1957); J. A. Zaslowsky *et al.*, *J. Am. Chem. Soc.*, **82**, 2682 (1960).
24. E. H. Riesenfeld and E. Wassmuth, *Z. Phys. Chem.*, **B8**, 314, (1930).
25. H. J. Schumacher *et al.*, *Z. Phys. Chem.*, **B6**, 423 (1930); *ibid.*, **13**, 353 (1957).
26. L. S. Kassel, *The Kinetics of Homogeneous Gas Reactions* (1932).
27. G. M. Schwab and G. Hartman, *Z. Phys. Chem.*, **B56**, 72 (1956).
28. J. Weiss, *Advances in Catalysis*, **IV**, 343 (1952); E. Abel, *Monatsch.*, **86**, 44 (1955).
29. L. J. Heidt, *J. Am. Chem. Soc.*, **57**, 1710 (1935).
30. W. D. McGrath and R. G. W. Norrish, *Proc. Roy. Soc.*, **254**, 317 (1960).
31. G. Kistiakowsky, *Z. Phys. Chem.*, **117**, 348 (1925).
32. L. J. Heidt and G. S. Forbes, *J. Am. Chem. Soc.*, **56**, 1671 (1934).
33. H. Taube, *Trans. Farad. Soc.*, **53**, 656 (1957).
34. W. N. Latimer, *Oxidation Potentials*, 2nd ed., Prentice-Hall, New York (1952).
35. *C. A.*, **49**, 12171*f*.
36. H. J. Schumacher *et al.*, *Z. Phys. Chem.*, **A138**, 462 (1928); *Z. anorg. allg. Chem.*, **298**, 1 (1959); A. Pelugmacher, *Z. anorg. allg. Chem.*, **279**, 313 (1955); *ibid.*, **298**, 9 (1959).
37. P. Hartek and S. Dondes, *J. Chem. Phys.*, **22**, 758 (1954). Criticism in *Chem. Ber.*, **90**, 987 (1957).
38. H. S. Johnston *et al.*, *J. Chem. Phys.*, **22**, 689 (1954); G. G. Goyer, *C. A.*, 5612 (1957).
39. S. Dondes, *C. A.*, **48**, 3160h (1954).
40. N. I. Kobozev *et al.*, *Zhur. Fiz. Khim.*, **30**, 2580 (1956); *ibid.*, **31**, 1843 (1957).
41. See: A. W. Petrocelli and R. V. Chiarenzelli, *J. Chem. Educ.*, **39**, 557 (1962)—historical survey.
42. I. A. Kazarnovskii, G. P. Nikolski and I. A. Abletrova, *Doklady Akad. Nauk, SSSR*, **64**, 69 (1949).
43. I. J. Solomon *et al.*, *J. Am. Chem. Soc.*, **84**, 34 (1962).
44. A. J. Kacmarek *et al.*, *J. Inorg. Chem.*, **1**, 659 (1962).
45. I. I. Volnov *et al.*, *Izv. Akad. Nauk SSSR*, 1127(1962).
46. I. J. Solomon *et al.*, *J. Phys. Chem.*, **64**, 168 (1960).
47. G. S. Zhdanov *et al.*, *Zhur. Fiz. Khim.*, **25**, 100 (1951).
48. A. D. Walsh, *J. Chem. Soc.*, 2266 (1953).
49. A. D. McLachlan *et al.*, *ibid.*, 952 (1959).
50. L. Pauling, *The Nature of the Chemical Bond*, 3rd ed., Cornell University Press, (1960) p. 354.
51. G.O. Nikolski *et al.*, *Doklady Akad. Nauk SSSR*, **77**, 69 (1951).
52. O. L. Forchheimer and H. Taube, *J. Am. Chem. Soc.*, **76**, 2099 (1954).
53. Ozone Chemistry and Technology, *Am. Chem. Soc.*, A. C. S., **18**, (1959).
54. P. S. Bailey, *Chem Rev.*, **58**, 926 (1958).
55. R. Criege, *Peroxide Reaction Mechanism*, Edwards, ed., Interscience, (1962), p. 29.

4

Hydrogen Peroxide

Hydrogen peroxide was discovered by Thenard (1818), who prepared it from barium peroxide and nitric acid. He first interpreted his results as formation of an "oxygenated nitric acid," but soon realized that the new compound was "oxidized water." The thorough investigations conducted by Thenard, after this discovery, resulted in the discovery of new methods of formation (from alkali metal peroxides), concentration (by evaporation of the solvent water) and decomposition by numerous reactions (catalytic as well as noncatalytic). In 1821, Thenard established the correct composition of hydrogen peroxide (twice as much oxygen as in pure water) by the gasometric determination of the oxygen evolved from what must have been pure, nearly 100% H_2O_2!

4-1 OCCURRENCE

The instability of H_2O_2 makes its occurrence in nature doubtful. Rain water and snow have been reported to contain

traces of hydrogen peroxide that might have been formed by ultraviolet solar radiation. The analytical methods used in these investigations were not specific for peroxides (oxidation of I^- to I_2 or Fe^{2+} to Fe^{3+}), and could easily mistake ozone or nitric oxides for H_2O_2.

4-2 FORMATION

From the Elements

The formation of hydrogen peroxide from the elements is favored thermodynamically at low temperatures. The reaction

$$H_2 + O_2 \rightarrow H_2O_2 \qquad (4\text{–}1)$$

is accompanied by a considerable decrease in free energy $\Delta F^\circ = -25.20$ kcal mole^{-1} at 25° C (log $K = 18.47$). Formation of H_2O_2 is, however, accompanied by formation of H_2O and usually the latter predominates. Furthermore, H_2O_2 is unstable with respect to decomposition into $H_2O + O_2$ (cf. Section 4–4) and, as a result, only low yields can be obtained by this method. The yield can be increased somewhat by using catalysts, such as palladium, which permit the use of lower temperatures, but it is still too low to make the use of this method practical on an industrial scale.

The mechanism proposed for the thermal chain reaction of oxygen with hydrogen (cf. Section 2–6) predicts the formation of H_2O_2 in Reactions 2–18 and 2–20 and its destruction by Steps 2–19 and 2–21. When the pressure is gradually increased, the yield of H_2O_2 will increase first, reach a maximum at approximately 40 mm (near the second explosion limit), and then fall off again. This was explained [1] by assuming that Reaction 2–17 could proceed without a three-body collision and produce an excited $HO_2^{\cdot *}$ radical

$$H + O_2 \rightarrow HO_2^{\cdot *} \qquad (4\text{–}2)$$

This very short-lived species could react with H_2 as in

$$HO_2^{\cdot *} + H_2 \rightarrow H_2O_2 + H \qquad (4\text{–}3)$$

However, two reactions will compete with Reaction 4–3: (1) decomposition of HO_2^* into OH· and O atom; this step predominates at low pressures because of the scarcity of collisions with H_2; (2) formation of normal HO_2 by Reaction 2–17 in preference to HO_2^* would occur at higher pressure. Above the second explosion limit most of the normal HO_2 radicals will be destroyed at the walls by Reaction 2–18, and only at much higher pressures will Reaction 2–20 become important, and an increase in the yield of H_2O_2 again be observed.

By substituting the thermal formation of free radicals by photochemical or electric discharge methods of free radical formation, higher yields of hydrogen peroxide are obtained: when hydrogen and oxygen are passed through an electric discharge, yields of up to 60 wt% were obtained. [2] Atoms of hydrogen and oxygen, formed by electron bombardment in the discharge tube, react with the oxygen and hydrogen molecules by the same mechanism as in the thermal reaction, producing OH· and HO_2 radicals and H_2O_2 molecules. Although more economical than the thermal method, this method is too expensive for large-scale production.

Hydrogen peroxide is formed by irradiating a mixture of the elements with ultraviolet light. When the mercury-lamp line of 2537 Å is used, a sensitizer must be added, to absorb the radiation efficiently. Mercury vapor is an efficient sensitizer, because the excited Hg* atoms can produce H atoms by collision with a hydrogen molecule—the excitation energy (112 kcal gram-atom^{-1}) is higher than the dissociation energy of H_2 (104 kcal mole^{-1}), but lower than the dissociation energy of O_2 (118 kcal mole^{-1}). A nonsensitized reaction occurs, when shorter ultraviolet wavelengths are used, that can be absorbed by the oxygen molecules, e.g., in the Schumann-Runge bands. Ozone will be formed as a by-product (cf. Section 3–2).

From Water

The enthalpy change of the reaction

$$H_2O + \tfrac{1}{2}\,O_2 \rightarrow H_2O_2 \qquad (4\text{–}4)$$

is ΔH° + 25.27 kcal mole^{-1} and ΔF° is + 29.42 kcal mole^{-1} at 25°C, hence a thermal formation of hydrogen peroxide from water is impossible at room temperature (log $K = -21.56$ at 25°C). High pressures and temperatures improve the yield only slightly: even at 1000 atm and 1500° K only $2 \cdot 10^{-4}$ mole will be formed from one mole H_2O and ½ mole O_2. H_2O_2 has been obtained from water vapor by an electric discharge [3] and by short-wave ultraviolet radiation [4] (around 1650 Å). Longer ultraviolet as well as visible light can form H_2O_2 in water (liquid) containing white pigments such as zinc oxide (sensitizers). Ozone reacts with water photochemically to form H_2O_2 and oxygen [5]:

$$H_2O + O_3 \xrightarrow{h\nu} H_2O_2 + O_2 \qquad (4\text{–}5)$$

Ultrasonic vibrations and ionizing radiation also produce hydrogen peroxide in aqueous solutions.

Molecular oxygen is reduced electrolytically in aqueous solutions when present at the cathode. Under suitable conditions, high yields of H_2O_2 can be obtained by this process. The yield depends on pH, current density, composition of electrolyte, temperature, etc. It will increase with increasing concentration of oxygen in the liquid phase (pressure) and by the use of highly absorbent cathodes (activated carbon). [6] It has been claimed that all the peroxidic oxygen originates in O_2, and none in the water. [7] A very high energy yield, 7.5 kwh per kg H_2O_2, has been reported [8], but this was obtained in alkaline solution, in which H_2O_2 is unstable and from which its extraction is expensive —these are the main obstacles to the practical application of this promising process.

By Autoxidation

The process of autoxidation of metals and organic compounds is often accompained by the intermediate formation of H_2O_2 or other peroxides (cf. Section 2–6). Traces of peroxide were detected during the corrosion of metals in the presence of moisture (e.g., Zn, Pb, Sn, Ca, Al, Mg, Fe) by exposing a photographic plate

to the vapors. Most autoxidation reactions of organic compounds proceed too slowly to be of practical use, and usually the peroxide is consumed by further reactions as fast as it is formed but, of the few notable exceptions, some have been utilized successfully for large-scale H_2O_2 production. Substituted anthraquinones have found wide application in these processes: 2-ethylanthraquinone, dissolved in an organic solvent, is hydrogenated catalytically to the corresponding anthrahydroquinol and then oxidized directly by air to reproduce the quinone and hydrogen peroxide:

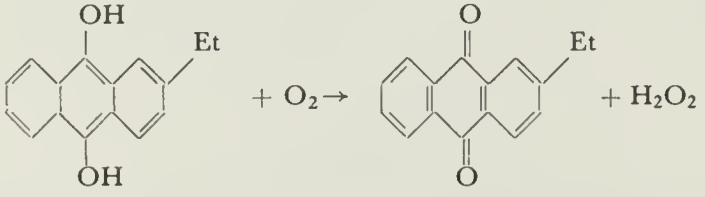

H_2O_2 is extracted with water and the quinone is re-used. A 20% H_2O_2 solution is obtained by this process.

H_2O_2 is also formed as an intermediate in combustion of organic compounds. When low temperatures are maintained and the products are rapidly cooled, H_2O_2 and other peroxides can be isolated. A recent industrial process uses the oxidation of isopropanol for production of H_2O_2 and acetone:

$$(CH_3)_2CHOH + O_2 \rightarrow (CH_3)_2CO + H_2O_2 \qquad (4\text{–}6)$$

From Peroxy Compounds

H_2O_2 can be formed indirectly from peroxy compounds, i.e., compounds containing the —O—O— group. The first industrial method of production was based on decomposition of barium peroxide by sulfuric acid. Barium oxide reacts with O_2 to form the peroxide at temperatures below 700° (at the partial oxygen pressure of 0.2 atm). The peroxide is decomposed by sulfuric or phosphoric acid.

$$BaO_2(s) + H^+ + HSO_4^- \rightarrow BaSO_4(s) + H_2O_2 \qquad (4\text{–}7)$$

Solutions containing 6% to 8% peroxide are obtained in prac-

tice—higher concentrations would create difficulties in handling the thick slurry and would accelerate decomposition. This method is seldom used today, as it cannot compete with the more economical peroxydisulfate process. Other peroxides, such as sodium peroxide (obtained by burning the metal in air) may serve as a source for H_2O_2: the Na^+ ion can be replaced with H^+ by, passing an aqueous solution through a cation-exchange column with the resin in the acid form, or by neutralizing the solution with an acid. However, the relatively high cost of Na_2O_2 limits the use of this method.

The use of peroxydisulfuric acid and its salts as a source of hydrogen peroxide opened the way for large-scale production of this chemical (1909). The process is based on the hydrolysis of $H_2S_2O_8$ to H_2O_2 and H_2SO_4:

$$H_2S_2O_8 + 2\,H_2O \rightarrow H_2O_2 + 2\,H_2SO_4 \qquad (4\text{–}8)$$

and the subsequent isolation of the former by distillation under reduced pressure. Peroxydisulfuric acid can also decompose into sulfuric acid and O_2

$$H_2S_2O_8 + H_2O \rightarrow 2\,H_2SO_4 + \tfrac{1}{2}\,O_2 \qquad (4\text{–}9)$$

but at high acid concentrations ($[H^+] = 2$ to 5) Reaction 4–8 predominates, and this acidity is used in practice. Reaction 4–8 does not proceed directly. $H_2S_2O_8$ is first decomposed by one water molecule to H_2SO_5 (Caro's acid) and the latter is hydrolyzed to hydrogen peroxide:

$$H_2S_2O_8 + H_2O \xrightarrow{k_{10}} H_2SO_4 + H_2SO_5 \qquad (4\text{–}10)$$

$$H_2SO_5 + H_2O \xrightarrow{k_{11}} H_2SO_4 + H_2O_2 \qquad (4\text{–}11)$$

Reaction 4–10 is much faster than 4–11 (k_{10} is approximately 40 times greater than k_{11} at 50° C), so that most of the peroxydisulfuric acid is decomposed before H_2O_2 is formed. Caro's acid can oxidize H_2O_2 and thereby lower its yield:

$$H_2SO_5 + H_2O_2 \rightarrow H_2SO_4 + H_2O + O_2 \qquad (4\text{–}12)$$

In order to minimize loss by Reaction 4–12 it is necessary to remove H_2O_2 as soon as it is formed. In practice, this is done by hydrolyzing the $H_2S_2O_8$ solution at moderate temperatures under reduced pressure, which causes the H_2O_2 to evaporate rapidly from the solution (together with water). The vapors are condensed to an aqueous solution containing approximately 30 wt % H_2O_2. The rapid removal of H_2O_2 from the liquid phase helps to suppress its catalytic decomposition by impurities that accumulate in solution. Peroxydisulfuric acid is produced by electrolytic oxidation of a sulfuric acid solution. The experimental observation, that less than one volume of oxygen is produced for two volumes of hydrogen when sulfuric acid solution is electrolyzed, was explained by Berthelot (1878), who found that $H_2S_2O_8$ formation accounts for the missing oxygen. The standard potentials of the reactions taking place in acid solution ($[H^+] = 1$) are as follows:

$$2H_2O \rightarrow O_2 + 4H^+ + 4e^- \qquad -1.229\ V \qquad (4\text{–}13)$$

$$2H_2O \rightarrow H_2O_2 + 2H^+ + 2e^- \qquad -1.76\ V \qquad (4\text{–}14)$$

$$2HSO_4^- \rightarrow S_2O_8^{2-} + 2H^+ + 2e^- \qquad -2.18\ V \qquad (4\text{–}15)$$

Under reversible conditions only Reaction 4–13 occurs, when a potential difference of 1.229 V is applied. A much higher potential difference is maintained in the electrolytic cell by departing from reversible conditions, i.e., by the use of high anodic current densities (~ 1 amp/cm^2). Under these conditions all three reactions can occur. Reaction 4–14 is relatively unimportant, which may be due to its slow rate or to the fast oxidation of H_2O_2 to oxygen at the anode:

$$H_2O_2 \rightarrow O_2 + 2H^+ + 2e^- \qquad -0.693\ V \qquad (4\text{–}16)$$

Reaction 4–15 will predominate at high anodic current densities because evolution of oxygen by Reaction 4–13 will be limited by

polarization due to oxygen bubbles, especially if the anode material has a high oxygen overvoltage (bright platinum). High cell temperatures will lower the yield of $H_2S_2O_8$ by accelerating its hydrolysis (Reactions 4–10 and 4–11), and subsequent loss of H_2O_2 by anodic oxidation. The solution is maintained at room temperature by circulating cooling water (e.g., through a hollow lead-coil cathode), but this becomes impractical when very high current densities are used, therefore anodic current density is limited to about 1 amp/cm^2. The corresponding cell voltage is 5 to 6 V. Under these conditions, current yields of up to 80% were obtained. The cathode is separated from the anode by an unglazed porcelain diaphragm, to avoid cathodic reduction of $H_2S_2O_8$. After hydrolysis of $H_2S_2O_8$ and distillation of H_2O_2, the sulfuric acid is returned to the electrolytic cell and reoxidized. Impurities accumulate in the process and must be removed periodically in order to minimize catalytic decomposition of H_2O_2 prior to distillation. In some processes a mixture of sulfuric acid and ammonium sulfate is used; as a result, higher current yields are obtained, but undesirable side reactions occur. A well-established practice is to separate the peroxydisulfate from solution by precipitation with potassium bisulfate, followed by hydrolysis of the salt

$$S_2O_8^{2-} + 2K^+ \rightarrow K_2S_2O_{8(s)} \qquad (4\text{–}17)$$

with sulfuric acid. The advantages of this method are (1) the elimination of impurities by the process of crystallization, (2) the smaller rate of hydrolysis caused by the low solubility of the salt: this decreases the steady state concentration of Caro's acid in solution and therefore lowers lossess of H_2O_2 by Reaction 4–12. The main advantages of the electrolytic method over the older barium peroxide process are its ability to supply directly a high concentration of H_2O_2 (30% to 35%), the possibility of continuous operation, and the low volume of raw materials required. The chief drawbacks are high power consumption (over 15 kwh kg^{-1}), as well as high capital investment, which are not expected to drop considerably with future improvements. Autoxidation processes are therefore expected to replace this method gradually.

Concentrated H_2O_2

The 30% to 35% solution obtained from electrolytic plants is suitable for most practical purposes, but higher concentrations are required for special uses such as rocket propellants and research. H_2O_2 solutions are concentrated by distilling off the water, which is much more volatile than the peroxide. The system H_2O—H_2O_2 has no vapor pressure minimum (cf. Section 4–3), and it is therefore possible, in principle, to obtain any desired concentration by fractional distillation. The difficulties lie in the instability of the peroxide: thermal decomposition increases rapidly with temperature and concentrated H_2O_2 vapor is explosive (above 110° C); therefore distillation is carried out under reduced pressure, inert construction materials are used, and stabilizers are added to the solution prior to distillation (e.g., $Na_4P_2O_7$ or 8-hydroxyquinoline). Vapors containing over 26 vol % are to be avoided (explosive limit). Ninety percent H_2O_2 is produced commercially, and shipped in aluminum drums. Higher concentrations are obtained from the above by fractional crystallization (freezing, cf. Section 4–3):

4-3 PHYSICAL PROPERTIES

The instability of pure hydrogen peroxide, especially at high temperatures, interferes with measurement of its physical properties by direct experimental methods. Early estimates were mostly based on extrapolation of data obtained for aqueous solutions of H_2O_2. During the last twenty years, improved methods of purification and handling have made possible the direct determination of a number of properties (heat of fusion and vaporization, electric conductivity, etc.) and further determinations are expected in future, but some properties, such as the normal boiling point or the critical temperature, will probably not be measured directly for a long time, perhaps never, owing to the high temperatures required.

Anhydrous H_2O_2

Some of the more important physical properties of anhydrous H_2O_2 are presented in Table 4–1, together with those of water.

Table 4–1[a] *Physical Properties of Hydrogen Peroxide and Water (values are for 25 °C and 1 atm unless otherwise noted).*

Property	H_2O_2	H_2O
Molecular weight	34.016	18.016
Density of solid, fp, g/cm^3	1.71	0.917
Density of liquid, 20 °C, g/cm^3	1.450	0.998
Viscosity of liquid, 20 °C, centipoises	1.245	1.002
Surface tension, 20 °C, dyn cm^{-1}	80.4	72.75
Heat of sublimation, fp, kcal mole^{-1}	15.58	12.17
Melting point, °C	− 0.43	0
Heat of fusion, mp., kcal mole^{-1}	2.987	1.436
Boiling point, °C	150.2	100.0
Heat of vaporization, kcal mole^{-1}	12.33	10.51
Critical temperature, °C	457	374.2
Critical pressure, atm	214	218.2
Heat capacity of solid, fp, cal gram^{-1} °C	0.39	0.50
Heat capacity of liquid, cal gram^{-1} °C	0.628	0.998
Heat capacity of vapor, cal mole^{-1} °C	10.22	8.025
Heat of formation in vapor, kcal mole^{-1}	− 32.53	− 57.80
Free energy of formation in vapor, kcal mole^{-1}	− 25.20	− 54.64
Dielectric constant, 20 °C	73.1	80.4
Magnetic susceptibility, 10^6 cgs emu/g	− 0.50	− 0.720
Refractive index	1.4067	1.3325
Specific conductivity, 10^{-7} ohm^{-1} cm^{-1}	3.9	

[a]* These data are taken from Ref. (8), p. 302, with certain small corrections made as a result of recent investigations.

A glance at this table reveals the close resemblance of H_2O_2 and water. In the gaseous state, the behavior of H_2O_2 is near ideal at low pressures: no evidence for association was found at 92° C and 35 mm Hg. [9] In the liquid state, extensive association and polymerization occur. The large dipole moment contributes to association, but the major portion of the intermolecular attraction is due to hydrogen bonding. The high boiling point and the large value of the latent heat of vaporization are a direct consequence of association, as is the large value of Trouton's constant—26.6 cal mole^{-1} (compare with 21 cal mole^{-1} for unassociated liquids). H_2O_2 is a good solvent for polar molecules and electrolytes—some salts, such as KNO_3, are more soluble than in water.

The crystal structure of solid H_2O_2 has been determined

by X-ray diffraction. [10] The tetragonal crystal has the following dimensions: a = b = 4.06 ± 0.02 Å, c = 8.00 ± 0.02 Å, space group D_4^4–$P4_12_1$ (enantiomorphous with D_4^8–$P4_32_1$), four molecules per unit cell, volume of unit cell 131.9 $Å^3$. The packing of the crystal is quite dense and therefore a normal decrease of density is observed upon melting (in contrast to water).

The System H_2O_2—H_2O

Hydrogen peroxide is miscible with water in all proportions. The process of mixing of the pure components is accompanied by evolution of heat—the integral heat of solution is always negative to the extent of several hundred calories per mole—e.g., for a 50 wt % solution at 25° C ΔH equals 636 cal per mole H_2O_2. This property illustrates the nonideal behavior of the liquid system H_2O—H_2O_2 (in ideal solution, the free energy change that accompanies mixing is made up solely of entropy changes, and the enthalpy change is zero). The process of mixing is also accompanied by a change in volume—the specific volume is not a linear function of the molar fraction of H_2O_2 (as in ideal solutions) but is concave upwards, i.e., the volume shrinks (1.7% for a 50% solution at 0° C).

Irregular behavior is also revealed in the change of viscosity with concentration: upon dilution of anhydrous H_2O_2 it first rises to a maximum before dropping to that of pure water (at infinite dilution). A similar change is observed in the dielectric constant, which has a maximum value at about 55% H_2O_2 (at 0° C) and in the specific conductance (which increases by a factor of 10 in a 50% solution).

The vapor pressure of aqueous solution is less than the vapor pressure of an ideal solution. Because of this negative deviation from Raoult's law, the total vapor pressure is not a linear function of the mole fraction, but is concave upwards. In spite of these negative deviations, there is no minimum in the vapor pressure-composition curve, because of the difference in volatility of the pure components. As a result, no azeotropes exist, and the components can be separated by fractional distillation (Fig. 4–1). The deviations of the physical properties mentioned above from

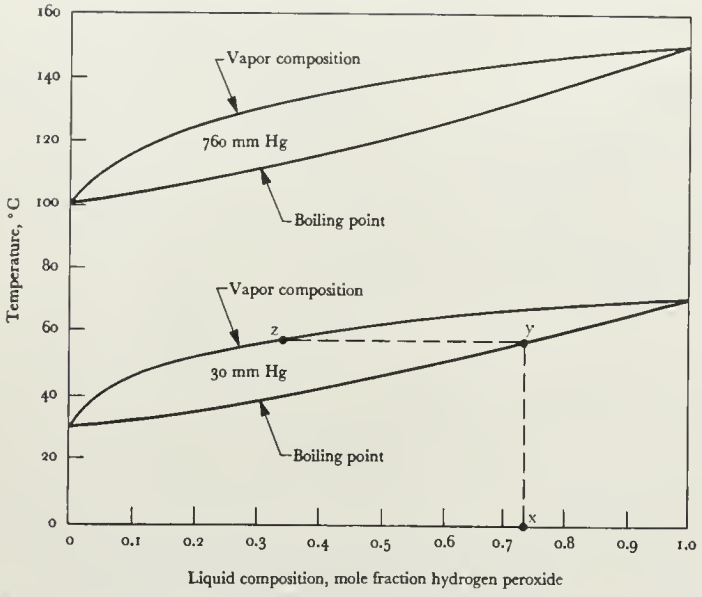

Figure 4-1 *Boiling points of, and vapor composition over, hydrogen peroxide-water mixtures at* 30 *and* 760 *mm* Hg *total pressure.*

those of ideal solutions point in the same direction: the solvent-solute interaction is greater than the molecular interaction in the pure components. The attractive forces consist mainly of hydrogen bonds, and it therefore seems that the hydrogen bonds between H_2O and H_2O_2 are more stable or more numerous than in the pure components.

The solid-liquid phase diagram of the system H_2O—H_2O_2 is shown in Fig. 4–2. In dilute H_2O_2 solutions, near ideal behavior is observed (deviations of the freezing point are less than 0.1° at concentrations below 5%); the same holds for highly concentrated solutions (i.e., dilute H_2O solution in H_2O_2). There are two eutectic points, one at 45.2% H_2O_2 (− 52.2° C), and the other, at 61.2% (− 56.1° C). Between them, two solid phases are in equilibrium with the solution: one is the dihydrate $H_2O_2 \cdot 2H_2O$, and the other is ice (below 48.6%) or anhydrous solid H_2O_2 (above 48.6%). In the range 0 to 45.2% H_2O_2, ice (H_2O) is the only stable solid phase, and in the range 61.2—100% anhydrous H_2O_2 is in equilibrium with the solution. The structure of the crystalline dihydrate was determined by X-ray diffraction. [11] The H_2O_2 molecule is strongly distorted in the lattice; it is therefore not surprising that the dihydrate does not persist in the liquid

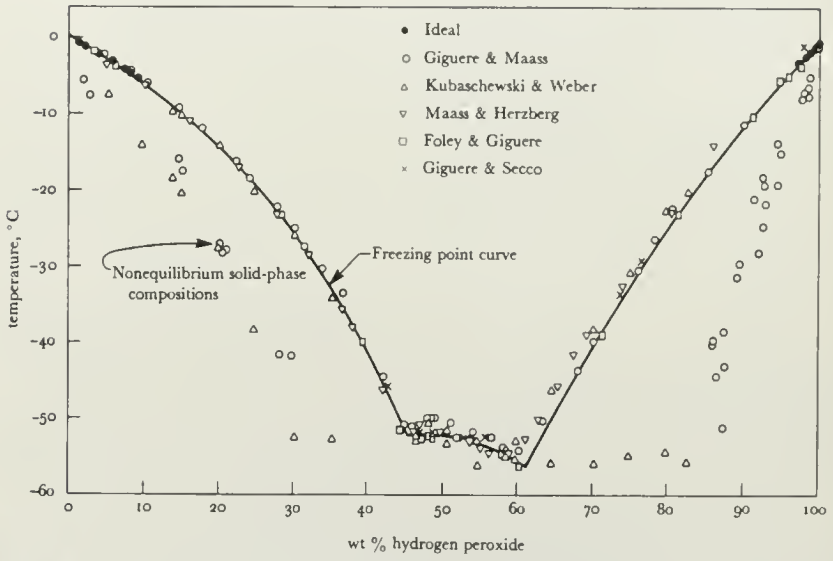

Figure 4-2 *Solid-liquid phase diagram for the system hydrogen peroxide-water.*

phase, as can be seen from the very flat maximum at the congruent boiling point of − 52.0° C. Mother liquor is tenaciously occluded in the solid phase at all compositions of the solution—the stable solid phases are not precipitated in pure form. This phenomenon led early investigators to suggest the existence of solid solutions, but this assumption was disproved experimentally. [12, 13]

The occlusion of mother liquor lowers the efficiency of H_2O_2 concentration by fractional crystallization. This method is used only for precipitation of anhydrous H_2O_2 from very concentrated solutions: in this concentration range it is preferred to fractional distillation, which causes considerable decomposition.

Absorption Spectra

H_2O_2 is colorless—no absorption occurs in the visible region. A high absorption band in the ultraviolet starts below 4010 Å ($\varepsilon = 0.001$) and rises continuously to the limit of the investigated region ($\varepsilon = 140$ at 2000 Å). This absorption effects splitting of H_2O_2 into OH· radicals (cf. Section 4–4).

The absorption in the infrared region, arising from the vibrations of the H_2O_2 molecule, are composed of 6 fundamental vibrations [14, 15]: $\nu_1 = 3599\ cm^{-1}$; $\nu_2 = 1380\ cm^{-1}$; $\nu_3 = 880$

cm^{-1}; $\nu_4 = 317$ cm^{-1}; $\nu_5 = 3608$ cm^{-1}; $\nu_6 = 1260$ cm^{-1}, which enter many combinations ($\nu_2 + \nu_5$, $\nu_1 + \nu_6$, etc.), and give rise to the numerous bands observed in this region. The study of these bands and their rotational fine structure is most valuable in determining the configuration of the molecule, as are the Raman and microwave spectra (see next section).

The Structure of the Molecule

The molecular weight of hydrogen peroxide, 34, corresponding to the molecular formula H_2O_2, was established in the gas phase (Victor Meyer method) and in dilute aqueous solution (depression of the freezing point). The two hydrogen atoms are bound through a peroxide bridge H—O—O—H. Some authors proposed a trigonal structure [8] (Fig. 4–3) which could be either

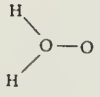

Figure 4-3

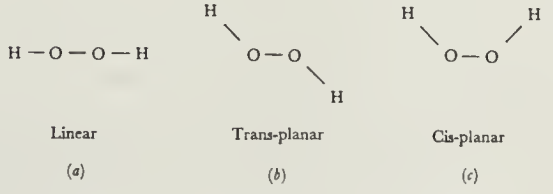

Figure 4-4 *(A) Linear; (B) trans-planar; (C) cis-planar.*

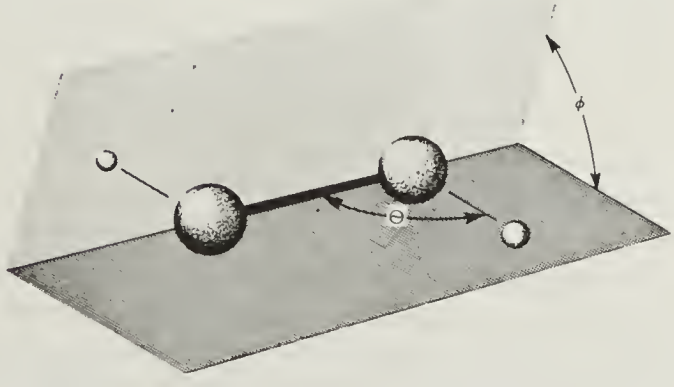

Figure 4-5 *Skew chain structure of hydrogen peroxide molecule.*

planar or pyramidal, but numerous physical data (spectra, bond energies, etc.) as well as theoretical considerations are incompatible with this structure. Even before these data became available, the trigonal structure was rejected by many chemists on purely chemical grounds: dialkyl peroxides (formed from H_2O_2) are reduced to alcohols and not to ethers, as implied by this structure.

Hydrogen peroxide is a polar molecule. The dipole moment of $2.26 \cdot 10^{-18}$ esu was determined by the Stark effect in the microwave spectrum [16], and agrees with earlier data based on the dielectric constant of dilute H_2O_2 solutions. [17] The polarity rules out a linear or *trans*-planar configuration (Fig. 4–4, a and b). The two remaining alternatives are *cis*-planar (Fig. 4–4 c), and the three-dimensional skew chain (Fig. 4–5) (both possess a dipole moment). Preference for the skew chain resulted from theoretical considerations (1934). This structure was later confirmed experimentally by infrared and X-ray diffraction measurements. [18, 19]

The $2p$ electrons of the O atom are the main contributors to the chemical bonds in H_2O_2 (although some sp hybridization takes place). One of the $2p$ electrons of each O atom forms the O—O σ bond and another will combine with the $1s$ of hydrogen to form another σ bond. This leaves the third p orbital occupied by a lone electron pair in each O atom. These bonds are expected to favor an O—O—H angle (θ) of about 90° (not considering repulsive forces or sp hybridization). The relative position of the two O—H bonds, defined by the dihedral angle ϕ, is also expected to be about 90°, thereby minimizing repulsion between the lone electron pairs. [8] Penney and Sutherland [20] used the valence bond method to estimate the change of the potential energy of the molecule with variation of ϕ from 0 to 360° and found a minimum value at approximately 100°. These calculations demonstrate that rotation of the hydrogens about the O—O axis is restricted by an energy barrier—a fact fully borne out by infrared and microwave data. This energy barrier is estimated to be 2.5 kcal $mole^{-1}$. [15]

X-ray diffraction studies were carried out on three crystalline compounds of H_2O_2: (1) urea-hydrogen peroxide addition compound [18] $CO(NH_2)_2 \cdot H_2O_2$, (2) solid pure H_2O_2 [10], and (3) the dihydrate $H_2O_2 \cdot 2H_2O$. [14] They confirm the skew

chain structure. H atoms cannot be "seen" by X rays, and are assumed to lie on the connecting lines between neighboring O_2 groups. The angles θ and ϕ differ in each case, because the free H_2O_2 molecule is always distorted by the neighboring groups in the crystal $\theta_{(1)}$ is 101.5°, $\theta_{(2)}$ 96° 52′, and $\theta_{(3)}$ 98°. The dihedral angles are $\phi_{(1)}$ 106°; $\phi_{(2)}$ 93° 51′, and $\phi_{(3)}$ 130°. Evidence for the skew chain structure of the free H_2O_2 molecule (in the gas phase) is obtained from infrared and Raman spectra. The H_2O_2 molecules possess 12 degrees of freedom, 3 of which are translational, 3 rotational, and 6 vibrational. The 6 vibrational motions are shown in Fig. 4–6. In a skew chain model having a twofold

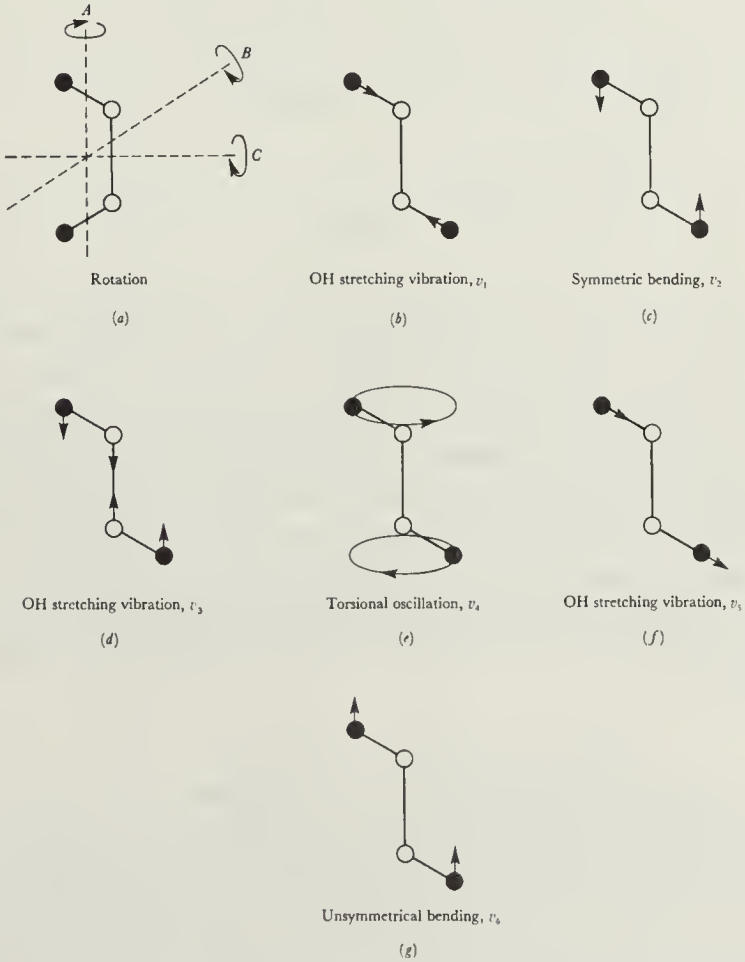

Figure 4-6 *Modes of rotational and vibrational motion for the hydrogen peroxide molecule.*

axis of symmetry (C_2 point group), all 6 will be active in the infrared becuse they will be accompanied by a dipole moment change, and will give rise to 6 fundamental frequencies.

More symmetrical structures will have fewer active vibrations (5 in the case of the *cis*-planar configurations). The 6 fundamentals found in infrared spectra support the skew chain configuration. Analysis of data obtained by high resolution of infrared bands furnished the following values for the structural parameters of the free molecule [14]: O—O bond 1.475 Å, O—H bond 0.950 Å, $\theta = 94.8°$, $\phi = 119.8°$.

4-4 CHEMICAL PROPERTIES

H_2O_2 is stable with respect to dissociation into the elements ($\Delta F°$ of formation is -25.20 kcal mole^{-1} at 25° C), but it is highly unstable with respect to decomposition into oxygen and water: the reaction

$$H_2O_2 \rightarrow H_2O + \tfrac{1}{2} O_2 \qquad (4\text{–}18)$$

is accompanied by a free energy change of -29.42 kcal mole^{-1} at 25° C ($\Delta H° = -25.27$ kcal mole^{-1} at 25° C), and consequently the equilibrium is entirely shifted towards the products (log $K = 21.56$). Absolutely pure H_2O_2 kept in inert containers does not decompose at ordinary temperatures because of the high activation energy of this reaction. It was estimated [21] that even at 100° C the half-life of the reaction was of the order of 10^7 years. The notable decomposition of H_2O_2 in the gas and liquid phases at room temperatures is due to catalysis. Catalysts may be heterogeneous (surface of containers) or homogeneous (dissolved impurities).

Thermal Decomposition in the Gas Phase

The difficulty in investigating this reaction is caused by the accompanying heterogeneous reaction taking place on the surface of the reaction vessel. The existence of this heterogeneous reaction becomes evident through the noted dependence of the rate constant on the surface to volume ratio. Using specially treated glassware,

this heterogeneous reaction could be made slow enough to make possible an investigation of the homogeneous reaction, above 420° C [22] (where the latter predominates). The initial step of the reaction probably consists of the splitting of H_2O_2 into two OH· radicals:

$$H_2O_2 \rightarrow 2\ OH\cdot \qquad (4\text{–}19)$$

The estimated dissociation energy of the O—O bond (48.5 kcal) equals the experimentally determined activation energy. [21]

The following (fast) steps take place after Reaction 4–19:

$$OH\cdot + H_2O_2 \rightarrow H_2O + HO_2^{\cdot} \qquad (4\text{–}20)$$

$$2\ HO_2^{\cdot} \rightarrow H_2O_2 + O_2 \qquad (4\text{–}21)$$

A chain mechanism was proposed for this reaction, which was initiated by Reaction 4–19 and propagated by Reactions 4–20 and 4–22:

$$HO_2^{\cdot} + H_2O_2 \rightarrow OH\cdot + H_2O + O_2 \qquad (4\text{–}22)$$

but this mechanism was discarded by recent investigations. [22] The reaction is of the first order with respect to H_2O_2. The first order rate constant is, however, pressure-dependent, as expected for a unimolecular decomposition in its low-pressure second-order region (Lindeman's mechanism for unimolecular reactions). This dependence becomes evident when we remember that Reaction 4–19 is preceded by

$$H_2O_2 + H_2O_2 \rightarrow H_2O_2^{*} + H_2O_2 \qquad (4\text{–}23)$$

The activation of H_2O_2 may be achieved by collision with a different gas molecule M, such as H_2O or O_2 (formed during decomposition), or an inert gas such as N_2 or He. In this case, Reaction 4–23 becomes

$$H_2O_2 + M \rightarrow H_2O_2^{*} + M \qquad (4\text{–}23a)$$

Reaction 4–23a is usually less efficient than 4–23, but if M is in a large excess over H_2O_2, the over-all order of the reaction becomes two. [22]

Decomposition by Light

Photodecomposition of gasous H_2O_2 by uv radiation proceeds similarly to the thermal reaction: the initial step

$$H_2O_2 + h\nu = 2\ OH\cdot \qquad (4\text{–}24)$$

is followed by reactions 4–20 and 4–21. This mechanism would lead to a maximum quantum yield of 2 at high radiation intensities, and this yield was indeed observed.[23] At low intensities of radiation, much higher quantum yields were observed, due to a chain mechanism propagated by Reaction 4–22, which becomes important at a low HO_2 concentration.

In aqueous solution the decomposition by light is complicated by participation of the solvent. Reactions such as Reaction (4–24) or

$$H_2O_2^* \rightarrow H_2O + O \qquad (4\text{–}25)$$

are followed by diffusion of the radicals through the hydration shell, or by recombination (thermal deactivation) within this shell. [24, 25]

Acid Properties of H_2O_2

H_2O_2 is a slightly stronger acid than H_2O. The dissociation constant of

$$H_2O_2 \rightleftharpoons H^+ + HO_2^- \qquad (4\text{–}26)$$

is $1.78 \cdot 10^{-12}$ at 20° C. The acid salts of this acid, such as NaOOH, are less stable in the solid state than the dibasic salts containing the O_2^{2-} ion (e.g., Na_2O_2). The acidic nature of H_2O_2 tends to decrease the dissociation of weak acids when it replaces water as a solvent, but this does not apply to dilute solutions of strong acids.

The ratio of the limiting conductance of $HClO_4$ to $KClO_4$, $\alpha = \Lambda^\circ HClO_4/\Lambda^\circ KClO_4$, decreases gradually as water ($\alpha \sim 3$) is replaced by H_2O_2 ($\alpha \sim 1$ in 99% H_2O_2) [26]. This decrease is probably not due to a smaller dissociation of this strong acid in H_2O_2, but to a change in the conductive mechanism. The abnormally high H^+ conductance in water, caused by a proton transfer mechanism, is gradually eliminated as water is replaced by H_2O_2, making its equivalent conductance approach that of other univalent cations. Because of the stronger acidity of H_2O_2, the HO_2^- ion will be found in higher concentration than OH^- in acid solutions, a fact that tends to favor ion pair formation with heavy metal cations such as $FeOOH^{2+}$, along with hydrolysis products such as $FeOH^{2+}$, in weakly acidic solutions.

Redox Reactions in Solution

The intermediate oxidation number of oxygen in H_2O_2 (-1) makes it an oxidizing agent as well as a reducing agent. The powerful oxidizing property is evident from the potential of Reaction 4–27:

$$H_2O_2 + 2H^+ + 2e^- \rightarrow 2H_2O \qquad (4\text{–}27)$$

$E^\circ = +1.76$ volts in acid solution ($\alpha_{H^+} = 1$)

$E^\circ = +0.87$ volt in basic solution ($\alpha_{OH^-} = 1$)

As a reducing agent H_2O_2 is moderate: the potential E° of Reaction 4–28

$$H_2O_2 \rightarrow 2H^+ + O_2 + 2e^- \qquad (4\text{–}28)$$

is -0.693 volt in acid solution, and -0.084 volt in basic solution. The thermodynamic instability of H_2O_2 in aqueous solution is expressed by the sum of Reactions 4–27 and 4–28:

$$2H_2O_2 \rightarrow O_2 + 2H_2O + 1.07\ V \qquad (4\text{–}29)$$

Many redox reactions of H_2O_2 are well known from general and analytical chemistry. One should, however, keep in mind that many reactions which are thermodynamically favored do not take place (e.g., oxidation of Cr^{III} to Cr^{VI} in acid solution), and many others are quite slow, because of a high activation energy barrier. The investigation of these relatively slow reactions was one of the earliest objects of kinetic measurements in the 19th century. Although hundreds of papers have been published on some of these reactions, their mechanisms are still not known with certainty. Considerable advance has been made in this field in the last twenty years, especially through O^{18} tracer experiments. The uncertainty regarding mechanism involves not only minor points (e.g., as to whether HO_2^- or O_2^{2-} takes part in a certain step), but much more fundamental questions, such as whether the reactions proceed by a 1- or a 2-electron mechanism. Reactions 4–27 and 4–28 involve a net transfer of 2 electrons. These electrons could be transferred in one step, i.e., by a 2-electron mechanism, or in consecutive 1-electron steps. The transfer does not necessarily involve free electrons; an O atom transfer, for example, will be equivalent to an abstraction of 2 electrons, and an OH· radical transfer is equivalent to a 1-electron transfer in the opposite direction.

The view that all redox reactions proceed by consecutive 1-electron steps, developed in the case of H_2O_2 by Haber and Willstatter [27], is an oversimplification. In those cases where a 2-electron change in the reactant yields a stable oxidation state, e.g., $S^{IV} \rightarrow S^{VI} + 2e$, a direct 2-electron transfer should not be excluded *a priori*. There is strong evidence that some reactions do indeed proceed by such a mechanism. Such is probably the case of quadrivalent ruthenium, which is reduced by H_2O_2 to the divalent state without intermediate formation of Ru^{III}. [28] When 2-electron changes are improbable in the reactant, e.g., in the reaction $Ti^{3+} \rightarrow Ti^{4+} + e^-$ or $Ce^{4+} + e^- \rightarrow Ce^{3+}$, the operation of a 1-electron mechanism is almost certain (much too high energy would be required in formation of Ti^{5+} by removal of a $2p$ electron). In these cases the reaction proceeds by a radical mechanism involving the radicals $OH\cdot$ or $HO_2\cdot$. In the reduction of quadrivalent cerium the following mechanism was suggested [29]:

$$Ce^{4+} + H_2O_2 \rightleftharpoons Ce^{3+} + HO_2^{\cdot} + H^+ \qquad (4\text{–}30)$$

$$Ce^{4+} + HO_2^{\cdot} \rightarrow Ce^{3+} + H^+ + O_2 \qquad (4\text{–}31)$$

It was demonstrated experimentally by epr measurements [30] that $HO_2^{\cdot}$ radicals are formed in solution. Similarly the oxidation of Ti^{3+} to Ti^{4+} proceeds by

$$Ti^{3+} + H_2O_2 \rightarrow Ti^{4+} + OH\cdot + OH^- \qquad (4\text{–}32)$$

$$Ti^{3+} + OH\cdot \rightarrow Ti^{4+} + OH^- \qquad (4\text{–}33)$$

Here the formation of $OH\cdot$ radicals was demonstrated. [31] In systems where 2-electron steps might operate, the mechanism is less certain. In the oxidation of Fe^{2+} by H_2O_2 to Fe^{3+}:

$$2Fe^{2+} + H_2O_2 \rightarrow 2Fe^{3+} + 2OH^- \qquad (4\text{–}34)$$

one could assume an exactly analogous mechanism to that of Ti^{3+} (Reactions 4–32, 4–33), but a 2-electron mechanism could also operate:

$$Fe^{2+} + H_2O_2 \rightarrow Fe^{4+} + 2OH^- \qquad (4\text{–}35)$$

$$Fe^{4+} + Fe^{2+} \rightarrow 2Fe^{3+} \qquad (4\text{–}36)$$

Some insight into the mechanism of these reactions is obtained by using O^{18} tracer experiments (H_2O^{18} does not exchange its oxygen with $H_2O_2^{16}$). Upon oxidation of H_2O_2 by many oxidizing agents (Ce^{IV}, MnO_4^-, Cl_2, HClO, $Cr_2O_7^{2-}$) all of the O_2 is derived from a single peroxide molecule, and none from H_2O. [32, 33] This proves that the O—O bond in H_2O_2 is not broken during the reaction. These facts cannot distinguish between a 1-electron and a 2-electron mechanism. Similar results were obtained for catalytic decomposition of H_2O_2 by Fe^{3+}, $I^- - I_2$, $Br^- - Br_2$, MnO_2, etc. [32, 33] When $H_2O_2^{16}$, in H_2O^{18} solution, is reduced to water, isotope fractionation occurs, i.e., the proportions of the 2 isotopes change, upon going from the reactant (H_2O_2) to the

product (H_2O). The fractionation factor (fr) is approximately 0.94 for Fe^{2+}, Sn^{2+}, Cr^{2+}, and Cu^{+} but almost 1 for Ti^{3+} (fr = 0.994. [32] Ti^{3+} is the only reducing agent in this group for which a 2-electron path must be excluded and the difference in fr is attributed to a difference in mechanism. In all the other cases, a mechanism analogous to Reactions 4–35, and 4–36 might operate. On the other hand, there is strong evidence favoring the reaction

$$Fe^{2+} + H_2O_2 \rightarrow Fe^{3+} + OH\cdot + OH^- \qquad (4\text{–}37)$$

This mixture (Fenton's reagent) can initiate polymerization of many monomers (e.g., styrene) which require free radicals for reaction initiation.

Catalytic decomposition

In neutral or acid aqueous solutions, H_2O_2 would probably not decompose at all if all catalysts were removed. In basic solution a homogeneous decomposition takes place (OH^- catalysis). The observed rate law for this reaction is

$$-\frac{d[H_2O_2]}{dt} = k[H_2O_2]\,[HO_2^-]$$

and to account for it, the following mechanism was proposed [34]:

$$H_2O_2 + OH^- \rightleftharpoons HO_2^- + H_2O \qquad (4\text{–}38)$$

$$H_2O_2 + HO_2^- \rightarrow H_2O + O_2 + OH^- \qquad (4\text{–}39)$$

Hundreds of catalysts of decomposition are known, among them the majority of the investigated chemical elements (or their compounds). Some are simple ions such as Fe^{3+}, while others have the complex structure of an enzyme, such as catalase, which is the most efficient catalyst known for any reaction. They are conveniently divided into (1) homogeneous, and (2) heterogeneous catalysts. Although hundreds of papers dealing with these

reactions have been published, little is known *with certainty* about the mechanism of catalysis in the first group, and still less about the second group. The numerous kinetic investigations conducted on these reactions demonstrate the truism that rate measurements may be very useful for disproving certain reaction paths which disagree with the rate law, but can rarely supply a conclusive proof for a single mechanism by eliminating *all* other conceivable reaction paths.

Homogeneous Catalysis. An explanation of catalysis was offered by the assumption that intermediate peroxy compounds of the catalyst are formed which decompose into the products. Another approach was made by assuming that the catalyst is oxidized by one H_2O_2 molecule and reduced by another molecule [8]:

$$\text{Reduced catalyst} + H_2O_2 \rightarrow \text{oxidized catalyst} + H_2O \quad (4\text{–}40)$$

$$\text{Oxidized catalyst} + H_2O_2 \rightarrow \text{reduced catalyst} + O_2 \quad (4\text{–}41)$$

These schemes are not mutually exclusive, because intermediate peroxides may take part in Reactions 4–40 and 4–41. A more useful classification would be into 1-electron and 2-electron redox catalysts. If an element exists in two oxidation states having a suitable redox potential, so that the lower oxidation state can be oxidized by H_2O_2 and the higher state can be reduced by it, and if both reactions proceed at a mesurable rate, this element will act as a catalyst for H_2O_2 decomposition.* Such a system will reach a steady state, in which the concentration of both forms of catalyst will be constant and Reactions 4–40 and 4–41 will proceed at equal rates, with the net result of Reaction 4–29. This is the case of catalytic decomposition by halogens. [35] The stoichiometric reactions responsible for catalysis are

$$H_2O_2 + 2I^- + 2H^+ \rightarrow I_2 + 2H_2O \quad (4\text{–}42)$$

$$I_2 + H_2O_2 \rightarrow 2I^- + 2H^+ + O_2 \quad (4\text{–}43)$$

* Such a system will not necessarily react by Reactions 4–40 and 4–41, because an alternative path may exist by which a much faster decomposition occurs.

The rate laws of Reactions 4–42 and 4–43 were determined separately. The steady state concentrations of I_2 and I^- were calculated from these rate data, and are in agreement with the experimental data of catalysis: between pH 4 and 8 the rate law for the catalytic Reaction 4–29 is

$$-\frac{dH_2O_2}{dt} = k_{29}\,[H_2O_2]\,[I^-]$$

Reactions 4–42 and 4–43 are acid-dependent, but in the above-mentioned pH range this dependence is negligible. The rate laws for these reactions are

$$\frac{d[I_2]}{dt} = k_{42}[H_2O_2]\,[I^-]; \quad -\frac{d[I_2]}{dt} = k_{43}[H_2O_2]\,[I_2]$$

at the steady state $d[I_2]/dt = 0$, hence $[I_2]/[I^-] = k_{42}/k_{43}$. This concentration ratio agrees with the experimental data. Furthermore, since oxidation and reduction proceed at equal rates, the rate constant of catalytic decomposition (k_{29}) should be numerically twice the value of k_{42}, $k_{29} = 2k_{42}$, and this too was confirmed experimentally. The mechanism of I_2 catalysis is resolved, to the extent that it involves Reactions 4–42 and 4–43, but the mechanism of each of these reactions is not determined by the above-mentioned data: it is possible to conceive a 2-electron mechanism for these reactions involving the I^+ oxidation state (hypoiodite), or a 1-electron mechanism involving $OH\cdot$ and $HO_2^{\cdot}$ radicals, as in Reactions 4–30 to 4–33.

The catalytic action of Fe^{3+} in moderately acidic solutions was the object of numerous investigations. [8] Haber and Weiss [36] assumed a mechanism involving reduction of Fe^{III} to Fe^{II} followed by reoxidation to Fe^{III} in 1-electron steps. This scheme, as modified by Barb, Baxendale, George, and Hargrave [37], consists of a chain reaction with the following steps:

Initiation $Fe^{3+} + HO_2^- \rightarrow Fe^{2+} + HO_2^{\cdot}$ (4–44)

Propagation

$Fe^{2+} + H_2O_2 \rightarrow Fe^{3+} + OH\cdot + OH^-$ (4–37)

$OH\cdot + H_2O_2 \rightarrow HO_2^{\cdot} + H_2O$ (4–45)

$Fe^{3+} + HO_2^{\cdot} \rightarrow Fe^{2+} + H^+ + O_2$ (4–46)

Termination

$Fe^{2+} + OH\cdot \rightarrow Fe^{3+} + OH^-$ (4–47)

$Fe^{2+} + HO_2^{\cdot} \rightarrow Fe^{3+} + HO_2^-$ (4–48)

The oxidation of Fe^{2+} by H_2O_2 is included in this scheme (Reactions 4–37 and 4–47). The scheme accounts for the observed rate law at high H_2O_2 concentrations, but fails at low H_2O_2 concentrations. An alternative mechanism, based on parallel titrimetric and spectrophotometric measurements was suggested recently [38]:

$$Fe^{3+} + HO_2^- \rightarrow FeHO_2^{2+} \quad (4\text{–}49)$$

$$FeHO_2^{2+} \rightarrow FeO^{3+} + OH^- \quad (4\text{–}50)$$

$$FeO^{3+} + HO_2^- \rightarrow Fe^{3+} + OH^- + O_2 \quad (4\text{–}51)$$

This scheme involves 2-electron steps, and the catalyst is assumed to be in the + 3 and + 5 oxidation states. A similar mechanism was proposed for catalase. [39]

Many complexes of transition elements are catalytically active, e. g., the cupric ammonia complexes [40] or the triethylenetetramine complex of Fe^{III}. [41] The activity of ferric complexes is of special interest, since they may serve as a model for enzymes, such as catalase which is composed of four ferric protoporphyrin complex ions bound to a protein molecule.

Heterogeneous catalysis. A great number of heterogeneous catalysts for hydrogen peroxide decomposition are known. Slight catalytic activity has been observed even in usually inert substances such as glass, especially colored glasses containing heavy

metals. Among the active catalysts are metals such as platinum, silver, and lead, oxides, hydroxides, and salts. The mechanism of their activity is only partly understood; all inherent difficulties mentioned in homogeneous catalysis are encountered here, as well as problems specific to heterogeneous reactions. A redox mechanism consisting of Steps 4–40 and 4–41 has been proposed for heterogeneous catalysis, and probably operates in many catalysts. Many redox systems, such as $Ce^{3+} \rightleftharpoons Ce^{4+} + e$, are inactive in the homogeneous state (solution), although they are favored thermodynamically, because of slow reaction rates. Some of these couples become active as soon as transition to a heterogeneous system is observed (precipitation), i.e., the redox reaction is catalyzed by the solid phase. Such is the case of the Mn^{II}–Mn^{IV} couple: Mn^{2+} ion is inactive in solution but, when a manganous solution containing peroxide is made basic by titration with NaOH, catalysis commences at a certain pH. This pH [42] is identical with that needed for overcoming the solubility product $[Mn^{2+}]\,[OH^-]^2 = 10^{-14}$. When the solubility product is exceeded, decomposition proceeds by the redox couple $Mn(OH)_2$–MnO_2. Similar behavior is observed in argentous ion which becomes active in basic solution when the solubility product, $[Ag^+]\,[OOH^-] = K$, is exceeded. [43] Similarly, Pb^{2+} is inactive, but in basic solution a violent reaction takes place through the $Pb(OH)_2$–Pb_3O_4 couple.

The dependence of activity on surface area was demonstrated for MnO_2 [44]—an increase of activity with surface area was found—as expected for heterogeneous catalysts. Some metals, such as gold, show pronounced activity only in the finely dispersed form of a colloidal sol, while other metals are active also in macroparticles. The activity of a single silver crystal was measured [45]: at high H_2O_2 concentrations (1.8 M) the kinetics were of zero order, indicating that the surface was saturated with reactive species. Formation of an oxide film was also observed, and no catalytic activity was found in acid solutions where the formation of the oxide was prevented. Catalytic activity of platinum and iridium in acid solutions was observed only when the metals were covered with an oxide film, and stopped when this film was removed by adding chloride ions (complex formation). [46]

4-5 USES

Hydrogen peroxide is mainly used as bleaching agent. Its milder oxidizing action makes it superior to hypochlorite in the bleaching of textiles. Its expensiveness at the beginning of the century limited its use to wool and hair bleaching, but improved production methods and lower costs made possible its intensive application in cotton cloth and chemical pulp bleaching. Other uses are (1) source of energy and oxygen, either alone or in combination with a fuel; it has been used in rocketry since introduction by the Germans in their V-2 rockets in the second World War; (2) source of free radicals for initiation of polymerization; (3) a gas-forming agent in the manufacture of porous substances, such as foam rubber or porous concrete.

4-6 HYDROGEN SUPEROXIDES

The synthesis of a superoxide of hydrogen H_2O_n ($n > 2$) was attempted by many investigators, beginning with Berthelot (1880). The existence of the analogous sulfanes H_2S_n is well known, and many of them have been isolated in pure form (for preparation of H_2S_n, where n is 3, 4, 5, 6, 7, 8, cf. Ref. 47). Early reports on the existence of a hydrogen superoxide were shown to be erroneous: they were based on inaccurate experimental results or on a false interpretation of the experimental data (for a review cf. Ref. 48). Renewed interest in hydrogen superoxides was aroused by the Russian group of Nekrasov, Kobosev, and coworkers who, in a series of papers [49], described the properties of a glassy product obtained by the action of hydrogen atoms (generated by an electric discharge in H_2) on a thin film of liquid ozone at $-196°$ C. When this product is warmed to $-115°$, it decomposes into H_2O_2 and oxygen. The molar ratio of these products is, in some cases, equal to 1 and the authors use this ratio as evidence that their glassy product is H_2O_4:

$$(H—O—O—O—O—H)$$

(It is not $HO_2^{\cdot}$, as this radical is paramagnetic and the glassy product is diamagnetic.) This compound is supposed to be

formed by the combination of two $HO_2^{\cdot}$ radicals (the initial product):

$$HO_2^{\cdot} + HO_2^{\cdot} \rightarrow H_2O_4 \qquad (4\text{–}52)$$

and to decompose at $-115°$ by

$$H_2O_4 \rightarrow H_2O_2 + O_2 \qquad (4\text{–}53)$$

These conclusions were rejected by Giguère [48], who points out that the ratio of the evolved oxygen to the remaining hydrogen peroxide is variable and depends on the experimental conditions. Furthermore, he rejects the existence of *any* superoxide in the glassy product and tries to explain all its properties by assuming that it consists of vitreous hydrogen peroxide contaminated by very active heterogeneous catalysts of decomposition. The existence of H_2O_4 was questioned on theoretical grounds by Benson [50] who estimated its heat of formation at $+18.1$ kcal mole^{-1}. This would make it unstable with respect to decomposition into two $HO_2^{\cdot}$ radicals ($\Delta H_{f_{HO_2}} = 2$ kcal mole^{-1}). Furthermore, this decomposition is believed to occur without activation energy, so that the synthesis of H_2O_4 by the reverse reaction 4–52 is improbable. The hypothetical H_2O_3, on the other hand, has an estimated heat of formation of -7 kcal mole^{-1} [50], and is stable with respect to disproportionation into the radicals $OH\cdot + HO_2^{\cdot}$. This compound could be formed by

$$OH\cdot + HO_2^{\cdot} \rightarrow H_2O_3 \qquad (4\text{–}54)$$

A recent kinetic investigation [51] of the rapid reaction of $HO_2^{\cdot}$ radicals in aqueous solution (into which they were introduced, in high concentration, by irradiating O_2-saturated water with a powerful electron beam) revealed that a relatively stable superoxide is formed in the solution, with a half-life of up to 2 seconds at room temperature. The data rule out the composition $H_2O_{n\geq 4}$ and the suggested composition is H_2O_3. New evidence supporting the existence of a superoxide in the glassy product obtained from

ozone and atomic hydrogen has recently been published. [52] The infrared spectrum of this product does not conform to that of H_2O_2 at $-196°$, and only when it decomposes at higher temperatures do the characteristic H_2O_2 lines appear.

4-7 IONIC PEROXIDES AND SUPEROXIDES

Peroxides are derivatives of H—O—O—H, in which hydrogen is replaced by atoms of another element. If replaced by a polyatomic radical, the product is a peroxo compound of some other class (e.g., peroxo acids). In peroxo compounds of nonmetals and some transition metals, the bonds between the peroxidic oxygens and the other element are covalent. The peroxides of metals of the Ia and IIa groups are ionic—Li_2O_2, Na_2O_2, K_2O_2, Rb_2O_2, Cs_2O_2, MgO_2, CaO_2, SrO_2, BaO_2. The arrangement of the O_2^{2-} and metal ions in the crystal lattice depends on their radii. The structure of Na_2O_2 is shown in Fig. 4–7.

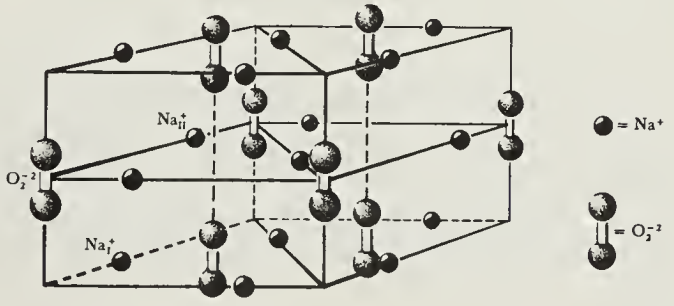

Figure 4-7 *The sodium peroxide structure.*

The peroxides of barium, strontium, and calcium have the structure of calcium carbide (Fig. 4–8). The O—O interatomic distance in O_2^{2-} is nearly the same as in hydrogen peroxide and covalent peroxo compounds ($\sim$ 1.48 Å). The ionic peroxides are diamagnetic and usually colorless. They are powerful oxidizing agents. Carbon dioxide converts them to carbonates and oxygen:

$$2\ CO_2 + 2\ Na_2O_2 \rightarrow 2\ Na_2CO_3 + O_2 \qquad (4\text{–}55)$$

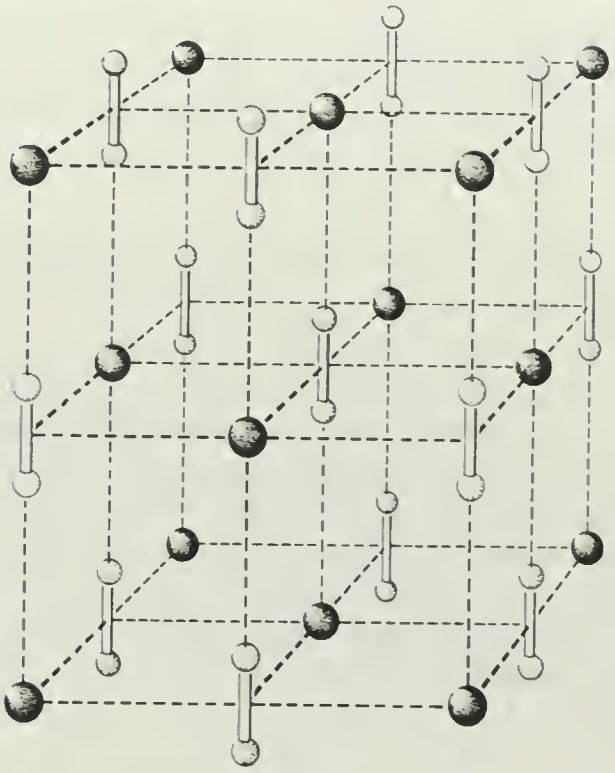

Figure 4-8 *Calcium carbide structure.*

Addition of H_2O_2 to the cold solution of hydroxides of groups Ia and IIa precipitates peroxide hydrates ($CaO_2 \cdot 8H_2O$), peroxide-hydroperoxidates ($K_2O_2 \cdot 2H_2O_2$), or mixed hydrate-hydroperoxidates ($Li_2O_2 \cdot H_2O_2 \cdot 2H_2O$). All ionic peroxides are decomposed in aqueous solution to yield hydrogen peroxide or its anion HO_2^-:

$$O_2^{2-} + H_2O \rightarrow HO_2^- + OH^- \qquad (4\text{–}56)$$

This reaction is very rapid, in contrast to the hydrolysis of stable covalent peroxo compounds which proceeds slowly (e.g., hydrolysis of $H_2S_2O_8$). The "Riesenfeld test" was claimed to distinguish between true peroxides and salt hydroperoxidates such as $Na_2SO_4 \cdot H_2O_2 \cdot 9H_2O$: the former were expected to oxidize a neutral potassium iodide solution to free iodine without evolution of oxygen, while the latter liberated oxygen in this solution (catalytic decomposition). This test is misleading as only

stable covalent peroxo compounds behave as expected (e. g., persulfates), whereas easily hydrolyzed peroxo compounds and all ionic peroxides behave like hydrogen peroxide and its addition compounds.

Superoxides are derivatives of $HO_2^{\cdot}$. Superoxides of most elements in groups Ia and IIa are known, but some of them have not been prepared in pure form. Their color is yellow-orange. Potassium superoxide was discovered by Harcourt [53], who formulated it as K_2O_4. The superoxides were first believed to contain the $[O—O—O—O]^{2-}$ ion, in analogy to the tetrasulfide ion S_4^{2-}, but this structure was ruled out by their *paramagnetism*. The paramagnetic moment of about 2 Bohr magnetons is consistent with the existence of one unpaired electron in every pair of oxygen atoms. The structure O_2^- proposed by Pauling [54] was supported by the magnetic data, and was finally confirmed by the elucidation of the crystal structure of KO_2. [55] The lattice of KO_2 (and of RbO_2, CsO_2) has the calcium carbide structure (Fig. 4–8) and the crystal of NaO_2 has a disordered pyrite structure. The O—O bond length is ~ 1.3 Å, as expected for a bond order of $1\frac{1}{2}$. The superoxides are powerful oxidizing agents. They react with water to form peroxides and oxygen

$$2\ MO_2(s) + H_2O \rightarrow 2\ M^+ + OH^- + HO_2^- + O_2(g) \quad (4\text{–}57)$$

and with carbon dioxide to from carbonates and oxygen.

Formation

Ionic peroxides and superoxides are formed by (1) action of oxygen on the metals or their oxides at elevated temperature; (2) decomposition of peroxide hydrates and hydroperoxidates; (3) oxidation of metal ammonia solutions with O_2. The first method is used to produce Na_2O_2* and BaO_2. Potassium, rubidium, and cesium yield the respective superoxides

* Commercial Na_2O_2 (formed by burning sodium metal in oxygen) contains some superoxide detected by its paramagnetism. [56] The yellow color may also be due to this superoxide.

by this method. The elevated temperatures used in these reactions (up to 500° C) accelerate the establishment of equilibrium in the metal-oxygen system, therefore only the stable oxide is formed. The stability of the higher oxides depends on the stability of their ionic lattices, which in turn depends on the radius of the cation: the large ions of potassium, rubidium, and cesium can accomodate the superoxide ion in a stable lattice; smaller ions favor the peroxide lattices (Na_2O_2), and the smallest (lithium) form no higher oxide by high temperature oxidation (cf. Table 4–2).

Table 4-2 *Stable Forms of Alkali Metal Oxides Produced by Direct Combustion of the Metals in an Excess of Oxygen* [57]

Metal	Oxide Formed	Ionic Radius (Å)
Li	Li_2O	0.60
Na	Na_2O_2	0.95
K	KO_2	1.33
Rb	RbO_2	1.48
Cs	CsO_2	1.69

The combination of a peroxide with oxygen to form the superoxide, and the reverse reaction, are at equilibrium when the dissociation oxygen pressure of the superoxide is maintained. In stable superoxides this pressure is very low (estimated at 1.6 mm Hg at 300° C for K_2O_2). [58] The reaction

$$2\ KO_2 \rightarrow K_2O_2 + O_2 \qquad (4\text{–}58)$$

can be carried out by heating the superoxide in vacuum at 400°. Unstable superoxides such as NaO_2 may be formed from the peroxide by heating in oxygen under high pressure (150 atm at 450° for Na_2O_2). The equilibrium pressure of NaO_2 has been estimated (from thermodynamic data of the reagents) to be 4 atm at 298° K and 40 ± 20 atm at 600° K (experimentally, a value of 30 atm was obtained at 600° K). The formation of BaO_2 from BaO has been previously mentioned (Section 4–2). SrO_2 is prepared in a similar fashion, but under higher pressure (200–250 atm at 350–400° C).

The second method of formation—dehydration of peroxide hydrates or hydroperoxidates may often yield pure anhydrous peroxides unobtainable by the first method: calcium peroxide octahydrate yields CaO_2, and $Li_2O_2 \cdot H_2O_2 \cdot 2H_2O$ yields Li_2O_2. Some peroxide-hydroperoxidates undergo disproportionation to superoxides and hydroxides [59]:

$$K_2O_2 \cdot 2H_2O_2 \rightarrow 2\ KO_2 + 2\ H_2O \qquad (4\text{–}59)$$

A similar reaction occurs in hydroperoxidates of sodium, calcium, and barium, but with a low yield of superoxide.

The formation of peroxides and superoxides by passing oxygen through the metal-ammonia solution proceeds stepwise: the peroxide is produced first and is converted to the superoxide by additional oxygen. In the case of stable superoxides, this conversion is complete, but with Na and Li smaller yields of the superoxide are obtained. Lithium superoxide could not be isolated without decomposition, but was shown to exist in solution by its absorption spectrum, which is similar to that of other superoxides. [60]

REFERENCES

1. A. C. Egerton and G. J. Minkoff, *Proc. Roy. Soc.*, **A 191**, 145 (1947).
2. K. Morinaga, *Bull. Chem. Soc. Japan*, **35**, 345 (1962).
3. R. A. Ruehrwein *et al.*, *J. Phys. Chem.*, **64**, 1317 (1960).
4. M. C. Chen and H. A. Taylor, *J. Chem. Phys.*, **27**, 857 (1957).
5. H. Taube, *Trans. Faraday Soc.*, **53**, 656 (1957).
6. W. G. Berl, *Trans. Electrochem. Soc.*, **76**, 359 (1939).
7. T. M. Abramova *et al.*, *Dopovidi Akad. Nauk Ukr. R.S.R.*, 974 (1958); *C. A.*, **53**, 6837i (1959).
8. W. C. Schumb, C. N. Satterfield and R. L. Wentworth, *Hydrogen Peroxide*, A. C. S. Monograph 128, Reinhold (1955).
9. G. L. Matheson and O. Maass, *J. Am. Chem. Soc.*, **51**, 674 (1929).
10. S. C. Abrahams, *et al.*, *Acta Cryst.*, **4**, 15 (1951).
11. I. Orlovson and D. H. Templeton, *Acta Chem. Scand.*, **14**, 1325 (1960).
12. W. T. Foley and P. A. Giguère, *Can. J. Chem.*, **29**, 123 (1951).
13. P. A. Giguère *et al.*, *Can. J. Chem.*, **32**, 117 (1954).
14. R. L. Redington, W. B. Olson and P. C. Cross, *J. Chem. Phys.*, **36**, 1311 (1962).
15. D. Chin and P. A. Giguère, *J. Chem. Phys.*, **34**, 690 (1961).

16. J. T. Massey and D. R. Bianko, *J. Chem. Phys.*, **22**, 442 (1954).
17. E. P. Linton and O. Maass, *Can. J. Res.*, **7**, 81 (1932).
18. C. S. Lu, E. W. Hughes and P. A. Giguère, *J. Am. Chem. Soc.*, **63**, 1507 (1941).
19. P. A. Giguère, *Can. J. Res.*, **28B**, 485 (1950).
20. W. G. Penney and G. B. B. M. Sutherland, *Trans. Faraday Soc.*, **30**, 898 (1934); *J. Chem. Phys.*, **2**, 492 (1934).
21. P. A. Giguère and I. D. Liu, *Can. J. Chem.*, **35**, 283 (1957).
22. D. E. Hoare, J. B. Protheroe and A. D. Walsh, *Trans. Faraday Soc.*, **55**, 548 (1959).
23. D. H. Volman, *J. Chem. Phys.*, **17**, 947 (1949).
24. J. P. Hunt and H. Taube, *J. Am. Chem. Soc.*, **74**, 5999 (1952).
25. J. H. Baxendale and J. A. Wilson, *Trans. Faraday Soc.*, **53**, 344, (1957); M. Anbar, *Trans. Faraday Soc.*, **57**, 971 (1961).
26. M. Kilpatrick, *Can. J. Chem.*, **37**, 163 (1959).
27. F. Haber and R. Willstatter, *Ber.*, **64**, 2844 (1931).
28. N. Keslo King and M. E. Winfield, *Austr. J. Chem.*, **12**, 47, 138, 147 (1959).
29. S. Baer and G. Stein, *J. Chem. Soc.*, 3176 (1953); P. B. Siegler and B. J. Masters, *J. Am. Chem. Soc.*, **79**, 6353 (1957).
30. E Saito and B. H. J. Bielski, *J. Am. Chem. Soc.*, **83**, 4467 (1961); G. Czapski, B. H. J. Bielski and N. Sutin, *J. Phys. Chem.*, **67**, 201 (1963).
31. Dixon and Norman, *Nature*, **196**, 891 (1962).
32. A. E. Cahill and H. Taube, *J. Am. Chem. Soc.*, **74**, 2312 (1952).
33. M. Anbar, *J. Am. Chem. Soc.*, **83**, 2031 (1961).
34. F. R. Duke and T. W. Haas, *J. Phys. Chem.*, **65**, 304 (1961).
35. J. H. Baxendale, *Advances in Catalysis*, **4**, 31, Academic Press (1952).
36. F. Haber and J. Weiss, *Proc. Roy. Soc.*, **147A**, 332 (1934).
37. W. G. Barb, J. H. Baxendale, P. George and K. R. Hargrave, *Trans. Faraday Soc.*, **47**, 462, 591 (1951).
38. M. L. Kremer, *Trans. Faraday Soc.*, **58**, 702 (1962).
39. P. Jones and W. F. K. Wynne-Jonne, *Trans. Faraday Soc.*, **58**, 1148 (1962).
40. B. Kirson, *Bull. Soc. chim. France*, 957 (1952); *ibid.*, 404 (1953); *ibid.*, 157, 950 (1954).
41. J. H. Wang, *J. Am. Chem. Soc.*, **77**, 822, 4715 (1955).
42. D. B. Broughton and R. L. Wentworth, *J. Am. Chem. Soc.*, **69**, 741 (1947).
43. F. T. Maggsand and D. Sutton, *Trans. Faraday Soc.*, **54**, 1861 (1958).
44. W. M. Wright and K. E. Rideal, *Trans. Faraday Soc.*, **24**, 530 (1928).
45. J. Bagg, *Austral. J. Chem.*, **15**, 201 (1962).
46. G. Bianchy, F. Mazza and T. Mussini, *Electrochem. Acta*, **7**, 457 (1962).
47. F. Feliér *et al.*, *Z. Anorg. Chem.*, **288**, 113, 123 (1956).
48. P. A. Giguère, *I. C. S. U. Review*, **4**, 172 (1962)
49. L. I. Nekrasov, N. I. Kobosev *et al.*, *Zh. Fiz. Khim.*, **30**, 2580 (1956); *ibid.*, **31**, 515 (1957); *ibid.*, **33**, 300 (1959); *ibid.*, **35**, 14, 691 (1961); *ibid.*, **36**, 274 (1962).
50. S. W. Benson, *J. Chem. Phys.*, **33**, 306 (1960).

51. G. Czapski and B. H. J. Bielski, *J. Phys. Chem.*, **67**, 2180 (1963).
52. J. A. Wojtovicz, F. Martinez and J. A. Zaslowsky, *J. Phys. Chem.*, **67**, 849 (1963).
53. A. V. Harcourt, *J. Chem. Soc.*, **14**, 267 (1862).
54. L. Pauling, *J. Am. Chem. Soc.*, **53**, 3225 (1931).
55. V. Kassatochkin and V. Kotov, *J. Chem. Phys.*, **4**, 458 (1936).
56. P. George, *J. Chem. Soc.*, 2367 (1955).
57. A. W. Petrocelli and D. L. Kraus, *J. Chem. Educ.*, **40**, 146 (1963).
58. I. A. Kazarnovskii : nd S. I. Reichtein, *Zh. Fiz. Khim.*, **21**, 245 (1947).
59. I. A. Kazarnovskii and A. B. Neiding, *Doklady Akad. Nauk SSSR*, **86**, 717 (19 2).
60. J. K. Thompson and J. Kleinberg, *J. Am. Chem. Soc.*, **73**, 1243 (1951).

Index

Acid dissociation constant of H_2O_2, 86
Atmospheric bands, 3, 33
Atomic weight, 3
Autoxidation, 42, 71
  of anthrahydroquinol, 72
  chain mechanism, 45
  of Fe^{2+}, 44
  of sulfite, 45
  of Ti^{3+}, 43
  peroxide mechanism, 44

Bond angles, in hydrogen peroxide, 83
  in oxides, 10, 11
  in ozone, 55

Caro's acid, 73
  decomposition rate, 73
Catalytic decomposition of H_2O_2 by Fe^{2+}, 92
  by I_2, 91
  by $Mn(OH)_2$, 94
  by single silver crystal, 94
Coordination number, 10
Crystal structure of calcium carbide, 98
  hydrogen peroxide, 77
  potassium superoxide, 99
  sodium peroxide, 97
  sodium superoxide, 99

Discovery of hydrogen peroxide, 68
  the element, 1, 2
  ozone, 48
  superoxides, 99
Dissociation energy of O_2, 34, 35

Electric conductivity of oxides, 12
Electric dipole moment of hydrogen peroxide, 82
  ozone, 55
Electrolysis of water, 25
  energy, 25, 26
  under pressure, 26
Electrolytic reduction of O_2, 71

Electron affinity, 9
Energy levels of the oxygen atom, 7, 8
Eutectic points in $H_2O_2 - H_2O$ system, 79
Explosion limits of hydrogen-oxygen mixtures, 38
Explosion mechanism of ozone, 58

Fenton's reagent, 90
Free oxygen atoms, analytical determination, 15, 16
formation, 14, 17
occurrence, 13
reactions, 15, 17
recombination, 14–17
Fundamental vibrations of hydrogen peroxide, 80, 81, 83

Ground state of O_2 molecule, 31

Herzberg bands, 34
High purity oxygen from $KMnO_4$, 20
Hydrates of O_2, 29

Infrared absorption of hydrogen peroxide, 80
ozone, 57
Interatomic distances in H_2O_2, 84
in O_2, 35
in O_3, 55
in peroxides, 97
in superoxides, 99
Ionic oxides, 11–13
Ionization potential of the atom, 8, 9
of O_2, 35
of ozone, 57
Isotopes, discovery, 3
fractionation in reduction of H_2O_2, 89
radioactive, 7
ratio, 3, 4
separation, 5, 6
separation factor, 5

Liquefaction of air, Claude's process, 21
Linde's process, 20, 21

Magnetic moment of O_2, 29, 30
ozonides, 65
superoxides, 99
Melting point of ozone, 56
Microwave absorption of hydrogen peroxide, 82
of O_2, 35
of ozone, 54

Oxygen carrying chelates, 45

Paleotemperature scale, 5
Peroxide hydrates, 98
Peroxydisulfuric acid, 73–75
decomposition rate, 73
Photochemical decomposition of ozone, 60

Restricted rotation in hydrogen peroxide, 82
Reversible O_2 electrode, 42, 43
Riesenfeld test, 98

Schumann-Runge bands, 33, 41
Separation of O_2 from air, biochemical, 25
Brin process, 24
electrochemical, 26
fractional distillation, 20, 22, 23
minimum energy of, 20
Siemens' ozonizer, 52
Solid modifications of O_2, 27, 28
Solubility of O_2, 29
ozone, 57
Specific conductance of H_2O_2–H_2O system, 78

Warm layer of ozone, 49
World production of oxygen, 27

Date Due

APR 26 1972

JAN 11 1973

MAR 28 1973

OCT 28 1975

NOV 17 1978

NOV 10 1978

NOV 20 1993

APR 11 1977

OCT 5 1978

NOV 10 1982

OCT 06 1993

bdy

CAT. NO. 23 233

PRINTED IN U.S.A.

QD 181 .O1 A73
Ardon, Michael, 1928-
Oxygen: elementary forms and h
010101 000
0 1163 0059299 9
TRENT UNIVERSITY

DATE DUE

NOV 2 3 1993		APR 1 6	2002
FEB 0 2 1994			
JAN 3 1 1994			
MAR 2 2 1994			
MAR 1 2 1994			
NOV 2 3 1994			
NOV 1 4 1994			
JAN 2 8 1995			
JAN 2 6 1995			

62106

QD
181
.O1A73

Ardon, Michael
Oxygen

Trent
University